

Oncology and Translational Medicine

Volume 5 • Number 5 • October 2019

Estimation of the effect of target and normal tissue sparing based on equivalent uniform dose-based optimization in hypofractionated radiotherapy for lung cancer

Ying Shao, Fuli Zhang, Shi Wang, Weidong Xu, Jing Jiang 197

Correlation between miR-564, TGF- β 1, and radiation-induced lung injury

Yunzhang Ge, Tao Xie, Bin Yang, Qianxia Li, Qingrong Ren, Xiaoyi Zhou, Desheng Hu, Zhongshu Tu 204

Clinical significance of S100A7 protein in predicting recurrence of breast cancer in patients undergoing breast-conserving surgery with radiotherapy

Chao Zhang, Changyou Li, Gaoyang Lin, Yao Qi, Zhenfeng Li, Jing Xu, Tianhui Su, Xin Liu, Xiao Zou 211

Application of pegylated recombinant human granulocyte colony-stimulating factor (PEG-rhG-CSF) for the prevention of neutropenia in triple negative breast cancer patients older than 65 years during adjuvant chemotherapy

Shuxian Qu, Jianing Qiu, Yidan Zhang, Yongming Liu, Zhendong Zheng 218

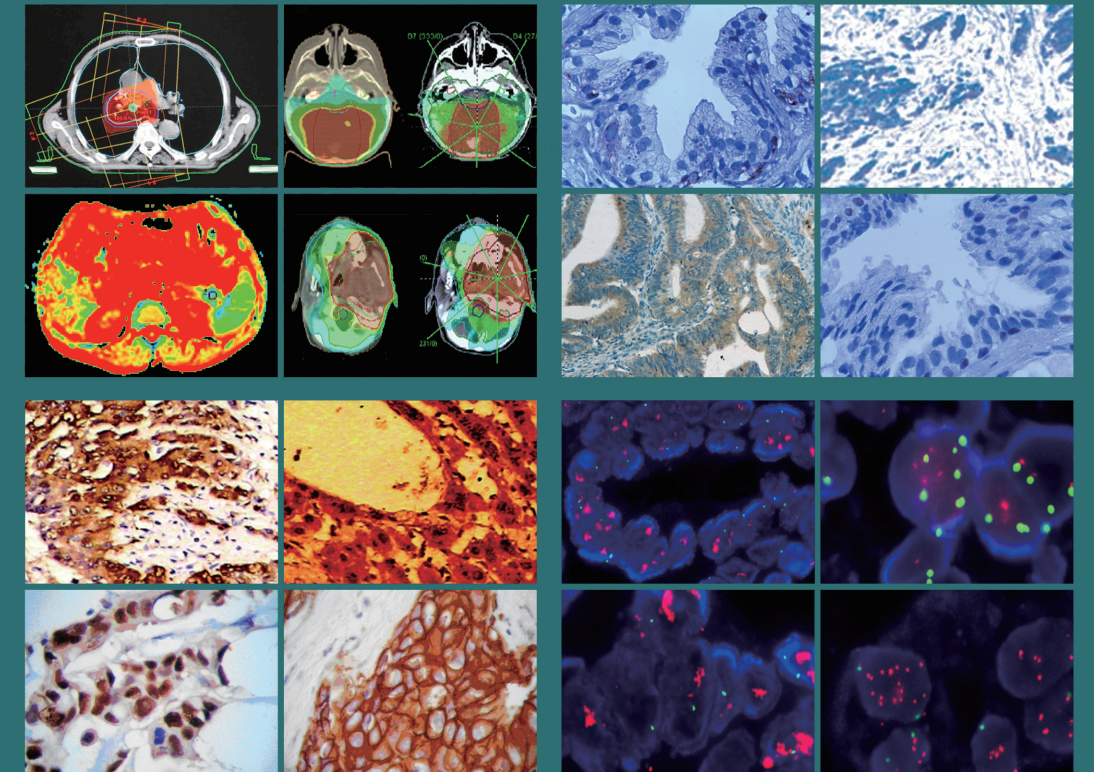
Oncology and Translational Medicine

Volume 5 • Number 5 • October 2019

pp 197-248

Oncology and Translational Medicine

ISSN 2095-9621
CN 42-1865/R



Online First
Immediately Online

otm.tjh.com.cn

Faster
publication!

邮发代号: 38-121

ISSN 2095-9621



GENERAL INFORMATION
» otm.tjh.com.cn

Volume 5
Number 5
October 2019





Honorary Editors-in-Chief

W.-W. Höpker (Germany)
Mengchao Wu (China)
Yan Sun (China)

Editors-in-Chief

Anmin Chen (China)
Shiying Yu (China)

Associate Editors

Yilong Wu (China)
Shukui Qin (China)
Xiaoping Chen (China)
Ding Ma (China)
Hanxiang An (China)
Yuan Chen (China)

Editorial Board

A. R. Hanauske (Germany)
Adolf Grünert (Germany)
Andrei Iagaru (USA)
Arnulf H. Hölscher (Germany)
Baoming Yu (China)
Bing Wang (USA)
Binghe Xu (China)
Bruce A. Chabner (USA)
Caicun Zhou (China)
Ch. Herfarth (Germany)
Changshu Ke (China)
Charles S. Cleeland (USA)
Chi-Kong Li (China)
Chris Albanese (USA)
Christof von Kalle (Germany)
D Kerr (United Kingdom)
Daoyu Hu (China)
Dean Tian (China)
Di Chen (USA)
Dian Wang (USA)
Dieter Hoelzer (Germany)
Dolores J. Schendel (Germany)
Dongfeng Tan (USA)
Dongmin Wang (China)
Ednin Hamzah (Malaysia)
Ewerbeck Volker (Germany)
Feng Li (China)
Frank Elsner (Germany)
Gang Wu (China)
Gary A. Levy (Canada)
Gen Sheng Wu (USA)
Gerhard Ehninger (Germany)
Guang Peng (USA)
Guangying Zhu (China)
Gunther Bastert (Germany)
Guoan Chen (USA)

Guojun Li (USA)
Guoliang Jiang (China)
Guoping Wang (China)
H. J. Biersack (Germany)
Helmut K. Seitz (Germany)
Hongbing Ma (China)
Hongtao Yu (USA)
Hongyang Wang (China)
Hua Lu (USA)
Huaqing Wang (China)
Hubert E. Blum (Germany)
J. R. Siewert (Germany)
Ji Wang (USA)
Jiafu Ji (China)
Jianfeng Zhou (China)
Jianjie Ma (USA)
Jianping Gong (China)
Jihong Wang (USA)
Jilin Yi (China)
Jin Li (China)
Jingyi Zhang (Canada)
Jingzhi Ma (China)
Jinyi Lang (China)
Joachim W. Dudenhausen (Germany)
Joe Y. Chang (USA)
Jörg-Walter Bartsch (Germany)
Jörg F. Debatin (Germany)
JP Armand (France)
Jun Ma (China)
Karl-Walter Jauch (Germany)
Katherine A. Siminovitch (Canada)
Kongming Wu (China)
Lei Li (USA)
Lei Zheng (USA)
Li Zhang (China)
Lichun Lu (USA)
Lili Tang (China)
Lin Shen (China)
Lin Zhang (China)
Lingying Wu (China)
Luhua Wang (China)
Marco Antonio Velasco-Velázquez (Mexico)
Markus W. Büchler (Germany)
Martin J. Murphy, Jr (USA)
Mathew Casimiro (USA)
Matthias W. Beckmann (Germany)
Meilin Liao (China)
Michael Buchfelder (Germany)
Norbert Arnold (Germany)
Peter Neumeister (Austria)
Qing Zhong (USA)
Qinghua Zhou (China)

Qingyi Wei (USA)
Qun Hu (China)
Reg Gorczynski (Canada)
Renyi Qin (China)
Richard Fielding (China)
Rongcheng Luo (China)
Shenjiang Li (China)
Shenqiu Li (China)
Shimosaka (Japan)
Shixuan Wang (China)
Shun Lu (China)
Sridhar Mani (USA)
Ting Lei (China)
Ulrich Sure (Germany)
Ulrich T. Hopt (Germany)
Ursula E. Seidler (Germany)
Uwe Kraeuter (Germany)
W. Hohenberger (Germany)
Wei Hu (USA)
Wei Liu (China)
Wei Wang (China)
Weijian Feng (China)
Weiping Zou (USA)
Wenzhen Zhu (China)
Xianglin Yuan (China)
Xiaodong Xie (China)
Xiaohua Zhu (China)
Xiaohui Niu (China)
Xiaolong Fu (China)
Xiaoyuan Zhang (USA)
Xiaoyuan (Shawn) Chen (USA)
Xichun Hu (China)
Ximing Xu (China)
Xin Shelley Wang (USA)
Xishan Hao (China)
Xiuyi Zhi (China)
Ying Cheng (China)
Ying Yuan (China)
Yixin Zeng (China)
Yongjian Xu (China)
You Lu (China)
Youbin Deng (China)
Yuankai Shi (China)
Yuguang He (USA)
Yuke Tian (China)
Yunfeng Zhou (China)
Yunyi Liu (China)
Yuquan Wei (China)
Zaide Wu (China)
Zefei Jiang (China)
Zhangqun Ye (China)
Zhishui Chen (China)
Zhongxing Liao (USA)

Oncology and Translational Medicine

October 2019 Volume 5 Number 5

Contents

Estimation of the effect of target and normal tissue sparing based on equivalent uniform dose-based optimization in hypofractionated radiotherapy for lung cancer

Ying Shao, Fuli Zhang, Shi Wang, Weidong Xu, Jing Jiang 197

Correlation between miR-564, TGF- β 1, and radiation-induced lung injury

Yunzhang Ge, Tao Xie, Bin Yang, Qianxia Li, Qingrong Ren, Xiaoyi Zhou, Desheng Hu, Zhongshu Tu 204

Clinical significance of S100A7 protein in predicting recurrence of breast cancer in patients undergoing breast-conserving surgery with radiotherapy

Chao Zhang, Changyou Li, Gaoyang Lin, Yao Qi, Zhenfeng Li, Jing Xu, Tianhui Su, Xin Liu, Xiao Zou 211

Application of pegylated recombinant human granulocyte colony-stimulating factor (PEG-rhG-CSF) for the prevention of neutropenia in triple negative breast cancer patients older than 65 years during adjuvant chemotherapy

Shuxian Qu, Jianing Qiu, Yidan Zhang, Yongming Liu, Zhendong Zheng 218

Determining the efficacy of vitamin B12 mixed oral liquid in the treatment of radiation-induced esophagitis

Yindi Tian, Ya Guo, Yue Ke, Yuyan Guo, Pengtao Yang, Hongbing Ma, Baofeng Wang 223

Treatment results of childhood extracranial malignant germ cell tumors and the salvage approach for recurrent and refractory cases: a single-center report

Kejun He, Xiaojun Yuan, Zhen Tan 229

Efficacy and safety of combined decitabine and ruxolitinib in the treatment of chronic myelomonocytic leukemia

Jiaming Li, Sujiang Zhang, Yubao Chen, Zeying Yan, Ying Wang, Zhiyin Liu, Haimin Sun, Yu Chen 237

Expression of HERG in musculoskeletal tumors with different degrees of malignancy

Lu Gan, Mo Li (Co-first author), Tongtao Yang (Co-first author), Jin Wu, Junjie Du, Zhuojing Luo, Yong Zhou 242

Oncology and Translational Medicine

Aims & Scope

Oncology and Translational Medicine is an international professional academic periodical. The Journal is designed to report progress in research and the latest findings in domestic and international oncology and translational medicine, to facilitate international academic exchanges, and to promote research in oncology and translational medicine as well as levels of service in clinical practice. The entire journal is published in English for a domestic and international readership.

Copyright

Submission of a manuscript implies: that the work described has not been published before (except in form of an abstract or as part of a published lecture, review or thesis); that it is not under consideration for publication elsewhere; that its publication has been approved by all co-authors, if any, as well as – tacitly or explicitly – by the responsible authorities at the institution where the work was carried out.

The author warrants that his/her contribution is original and that he/she has full power to make this grant. The author signs for and accepts responsibility for releasing this material on behalf of any and all co-authors. Transfer of copyright to Huazhong University of Science and Technology becomes effective if and when the article is accepted for publication. After submission of the Copyright Transfer Statement signed by the corresponding author, changes of authorship or in the order of the authors listed will not be accepted by Huazhong University of Science and Technology. The copyright covers

the exclusive right and license (for U.S. government employees: to the extent transferable) to reproduce, publish, distribute and archive the article in all forms and media of expression now known or developed in the future, including reprints, translations, photographic reproductions, microform, electronic form (offline, online) or any other reproductions of similar nature.

Supervised by

Ministry of Education of the People's Republic of China.

Administered by

Tongji Medical College, Huazhong University of Science and Technology.

Submission information

Manuscripts should be submitted to:
<http://otm.tjh.com.cn>
dmedizin@sina.com

Subscription information

ISSN edition: 2095-9621
CN: 42-1865/R

■ Subscription rates

Subscription may begin at any time. Remittances made by check, draft or express money order should be made payable to this journal. The price for 2017 is as follows: US \$ 30 per issue; RMB ¥ 28.00 per issue.

Database

Oncology and Translational Medicine is abstracted and indexed in EM-BASE, Index Copernicus, Chinese Science and Technology Paper Citation Database (CSTPCD), Chinese Core Journals Database, Chinese Journal Full-text Database (CJFD), Wanfang

Data; Weipu Data; Chinese Academic Journal Comprehensive Evaluation Database.

Business correspondence

All matters relating to orders, subscriptions, back issues, offprints, advertisement booking and general enquiries should be addressed to the editorial office.

Mailing address

Editorial office of
Oncology and Translational Medicine
Tongji Hospital
Tongji Medical College
Huazhong University of Science and Technology
Jie Fang Da Dao 1095
430030 Wuhan, China
Tel.: +86-27-69378388
Email: dmedizin@sina.com

Printer

Changjiang Spatial Information Technology Engineering Co., Ltd. (Wuhan)
Hangce Information Cartography Printing Filial, Wuhan, China
Printed in People's Republic of China

Managing director

Jun Xia

Executive editors

Yening Wang
Jun Xia
Jing Chen
Qiang Wu

Estimation of the effect of target and normal tissue sparing based on equivalent uniform dose-based optimization in hypofractionated radiotherapy for lung cancer*

Ying Shao¹, Fuli Zhang² (✉), Shi Wang³, Weidong Xu², Jing Jiang¹

¹ Department of Radiotherapy, The Seventh Medical Center, PLA General Hospital/Beijing Tsinghua Changgeng Hospital affiliated to Tsinghua University, Beijing 102218, China

² Department of Radiotherapy, The Seventh Medical Center, PLA General Hospital, Beijing 100700, China

³ Department of Engineering Physics, Tsinghua University, Beijing 100084, China

Abstract

Objective This study aims to investigate the dosimetric differences among four planning methods of physical and biological optimization in hypofractionated radiation therapy for non-small cell lung cancer (NSCLC).

Methods Ten NSCLC patients receiving radiation therapy were chosen for this retrospective study. Volumetric modulated arc treatment plans for each patient were remade with dose-volume (DV) functions, biological-physical functions, and biological functions, using the same constraint parameters during optimization. The dosimetric differences between the four types of plans were calculated and analyzed.

Results For the target, equivalent uniform dose (EUD) of the EUD and EUD + DV groups was approximately 2.8%–3.6% and 3.2%–3.7% higher than those of the DV and DV + EUD groups, respectively. The average tumor control probability (TCP) of the EUD and EUD + DV groups was also significantly higher than those of the other two groups ($P < 0.05$). The difference in heterogeneity index (H_I) among the four groups was also statistically significant ($P < 0.05$), while the difference of conformity index (C_I) was not significant ($P > 0.05$). For the organs at risk, the differences of EUD, V_5 , V_{10} , V_{20} , V_{30} of normal lung tissues were not statistically significant ($P > 0.05$); however, the mean lung dose of the EUD and EUD + DV groups was slightly lower than those of the other two groups.

Conclusion The biological optimization method has obvious advantages of improving EUD and TCP of the target, while decreasing the exposed dose of normal lung. This result is meaningful in choosing plan optimization methods in routine work.

Key words: non-small cell lung cancer (NSCLC); equivalent uniform dose (EUD); hypofractionated radiotherapy; plan optimization

Received: 14 June 2019

Revised: 27 August 2019

Accepted: 20 September 2019

Currently, several commercial treatment planning systems (TPS) including Eclipse, Pinnacle, Monaco, and Raystation can perform accurate dose optimization and calculations in radiation therapy of various cancers. However, most of the TPSs only use the dose-volume (DV)-based physical functions when optimizing the inverse intensity modulated radiotherapy (IMRT) treatment plans. The main drawback of this optimization is that it does not represent the nonlinear response of the tumor

and normal tissue to the irradiation. Furthermore, when calculating the dose, they all act on a certain point on the dose curve through the preset physical function^[1], which has certain limitations and cannot regulate the overall dose distribution of the target or organs at risk (OAR). The biological function based on equivalent uniform dose (EUD), which involves the biological parameters of the interaction between irradiation and tissues, may compensate for the limitation of simple physical function

✉ Correspondence to: Fuli Zhang. Email: radiozfl@163.com

* Supported by a grant from the Project of Beijing Municipal Science & Technology Commission (No. Z181100001718011).

© 2019 Huazhong University of Science and Technology

optimization to some extent. This study intends to compare the results of different planning optimization methods based on physical function, physical function and biological function, and biological function, as well as the impacts of the different biological parameters on the target EUD and tumor control probability (TCP). The differences between the four different optimization methods in the stereotactic radiotherapy plan for lung cancer were evaluated to provide a dosimetric reference for clinical applications.

Materials and methods

Methods

EUD is a biological dose concept related to tissue biological characteristics proposed by Niemierko *et al.* It is defined as follows: for an anatomical structure exposed to nonuniform doses, the resulting radiobiological effects can be equivalent to a uniform dose distribution. This uniform dose is called EUD [2-3] for uneven dose distribution. EUD is a concept linking physical dose with TCP and normal tissue complication probability (NTCP) [3]. The formula for the EUD model is as follows:

$$EUD = \left(\frac{1}{N} \sum_{i=1}^N D_i^a \right)^{\frac{1}{a}} \quad (1)$$

The formula applies to both tumor and normal tissues. Here, N is the number of voxels in the region of interest (ROI), D_i is the dose of the i voxel in the ROI, and a is a biological characteristic parameter describing the dose-volume effect of the tumor or normal tissue. It was found that when $a \rightarrow +\infty$, the EUD converged to the maximum dose D_{max} in the ROI region. From a clinical point of view, when a is given a large value, the high dose point in the ROI can be reflected by the EUD. When $a \rightarrow -\infty$, the EUD converges to the minimum dose D_{min} of the ROI region. When EUD is used to evaluate the absorbed dose in the target region, a negative a -value is given. The cold spot of the absorbed dose is clearly reflected by the EUD. Similarly, when $a \rightarrow 1$, EUD is equivalent to the arithmetic average dose, and when $a \rightarrow 0$, the EUD converges to the geometric mean of the entire calculated volume dose. For tumor tissues, a is usually taken as a negative value with a large absolute value; for serial OAR, a is usually taken as a positive value with a large absolute value, while for parallel OAR, a is usually taken as a positive value with a small absolute value [4-8]. In this experiment, in order to show the relationship between the value of a and the dose-response of the target and lung tissues, the value of a for the target was selected to be in the range of -100 to -10 , with intervals of 10; for lung tissue, the value of a was selected to be in the range of 0.1 to 1.0, and the interval were 0.1.

The widely used TCP calculation formula is as follows:

$$TCP = \frac{1}{1 + \left(\frac{TCD_{50}}{EUD} \right)^{4\gamma_{50}}} \quad (2)$$

Here, TCD_{50} is the dose required for a tumor control rate of 50%, and γ_{50} is the slope of the S-shaped dose-response curve of tumor tissue. TCD_{50} and γ_{50} are obtained from published clinical data. In this study, five groups of TCD_{50} and γ_{50} values in the literature were selected [9]; the calculated TCP results for each group were compared and analyzed.

The NTCP model is based on the TCP model assuming that there is no volume effect between the voxels of normal tissues [10]. NTCP calculation formula is similar to TCP:

$$NTCP = \frac{1}{1 + \left(\frac{TD_{50}}{EUD} \right)^{4\gamma_{50}}} \quad (3)$$

In the formula, TD_{50} is the dose at which the probability of normal tissue complications reaches 50%, and γ_{50} is the slope of the S-shaped dose-response curve of normal tissue, which can be replaced by $\frac{1}{m\sqrt{2\pi}}$, where m is

derived from the LKB model and parameters related to the slope of the dose-response curve were also obtained from reported clinical data [11].

Treatment plan design

The CT images of 10 patients with non-small cell lung cancer (NSCLC) who had undergone radiation therapy were selected. The volumetric arc intensity therapy (VMAT) plan was designed using the Monaco system (version 5.11, ElektaAB, Stockholm, Sweden). The Monaco system can provide constraints based on both physical and biological functions. Four groups of plans were designed for each case: physical function constrained group (DV group) for both target and OAR, physical function for target and biological function for OAR constrained group (DV + EUD group), biological function for target and physical function for OAR constrained group (EUD + DV group), and biological function constrained group (EUD group) for both target and OAR. The prescription dose was 60 Gy/10 f [12], and it was ensured that the prescribed dose could enclose at least 95% of the target volume. The beginning angle of the gantry was set to 180°; one partial arc was 200°, two arcs per plan; the control point number was set as 120; the minimum calculation grid was 0.2 cm; and the calculation uncertainty was set to 1%. When the four groups of plans were optimized, they were consistent in terms of calculation parameters, dose-volume constraints for target, and OAR.

Calculation and statistical analysis

The Matlab software (version 2015a, MathWorks, US) was used to calculate the following values based on the treatment plan: (1) target EUD for each group of plans, taking *a* in the range of -100 to -10 with an interval of 10; (2) target TCP for each group under different target TCD_{50}/γ_{50} combinations [9]; (3) NTCP of normal lung (lung-GTV) tissue, taking *a* in the range of 0.1–1.0 with an interval of 0.1. In addition, the homogeneity index (*HI*), conformity index (*CI*) of the target and the dose-volume parameters of the OAR were compared.

The calculation formula for the target *HI* was:

$$HI = \frac{D_{2\%} - D_{98\%}}{D_{50\%}} \times 100\% \quad (4)$$

$D_{2\%}$ represents the maximum dose in the target, $D_{98\%}$ represents the minimum dose in the target, and $D_{50\%}$ is the median dose in the target [13]; the calculation formula for the target *CI* was:

$$CI = \frac{V_{T, Pi}}{V_T} \times \frac{V_{T, Pi}}{V_{Pi}} \quad (5)$$

Where $V_{T, Pi}$ represents the target volume enclosed by the prescription dose, V_T represents the volume of the target, and V_{Pi} represents the volume enclosed by the prescription dose. Statistical analyses were conducted using SPSS 20.0 for one-way analysis of variance. When $P < 0.05$, the difference was considered statistically significant.

Results

Tumor target

Table 1 shows the results of the PTV in the four groups of plans, where V_{60} is the percentage of the volume of

the PTV wrapped by the prescription dose. It was found that $D_{2\%}$ and $D_{50\%}$ were higher in the EUD group and EUD + DV group than in the DV group and the DV + EUD group ($P < 0.05$), while the V_{60} and $D_{98\%}$ showed no significant difference ($P > 0.05$). Because the EUD function has a more powerful effect on the cold spot dose when performing target dose calculation [3], the result was closely related to the optimization characteristics of the EUD function.

Table 2 shows the EUD values of the target areas for the four groups of plans obtained when a different *a*-value was selected. It could be found that the EUD values of the EUD group and the EUD + DV group were significantly higher than those of the DV group and the DV + EUD group by 2.8%–3.6% and 3.2%–3.7%, respectively ($P < 0.05$). As the value of *a* decreases, the mean EUD of the four groups of plans also tended to decrease slightly, which specifically reflected the relationship between the *a*-value and EUD. The target TCP results for the four groups of plans are listed in Tables 3a–3d. It was found that the difference among the groups was statistically significant ($P < 0.05$) when the target area TCP values under different TCD_{50}/γ_{50} combinations in the four optimization methods were compared, showing that the value of TCD_{50}/γ_{50} had a greater impact on TCP. The statistical analysis results of *HI* and *CI* in the four groups are listed in Table 4. Through comparison and analysis, *HI* and *CI* were better in the DV + EUD group, and the difference in *HI* between the four groups was statistically significant ($P < 0.05$), whereas the difference in *CI* was not ($P > 0.05$).

In addition, regardless of the value of *a* and TCD_{50}/γ_{50} , the average TCP values of the EUD and EUD + DV groups

Table 1 Comparison of PTV parameters in four groups of plans

	DV group	DV + EUD group	EUD group	EUD + DV group	<i>P</i> value
V_{60} (%)	97.75 ± 1.02	98.45 ± 1.40	98.21 ± 1.72	98.04 ± 1.79	0.770
$D_{2\%}$ (Gy)	63.64 ± 0.38	63.66 ± 0.33	64.84 ± 0.62	65.05 ± 0.13	0.000
$D_{98\%}$ (Gy)	59.98 ± 0.22	60.18 ± 0.35	60.28 ± 0.96	60.20 ± 0.86	0.781
$D_{50\%}$ (Gy)	61.88 ± 0.13	61.94 ± 0.18	63.94 ± 0.61	63.26 ± 0.29	0.000

Table 2 EUD calculations results for four plan optimization methods with different *a*-values

<i>a</i> value	DV group (Gy)	DV + EUD group (Gy)	EUD group (Gy)	EUD + DV group (Gy)	<i>P</i> value
-10	89.56 ± 0.549	89.69 ± 0.334	92.47 ± 1.431	92.85 ± 0.616	0.000
-20	89.40 ± 0.518	89.55 ± 0.329	92.30 ± 1.433	92.68 ± 0.658	0.000
-30	89.24 ± 0.492	89.42 ± 0.327	92.13 ± 1.434	92.50 ± 0.700	0.000
-40	89.08 ± 0.471	89.29 ± 0.327	91.97 ± 1.435	92.33 ± 0.740	0.000
-50	88.93 ± 0.455	89.16 ± 0.328	91.80 ± 1.435	92.16 ± 0.779	0.000
-60	88.77 ± 0.447	89.03 ± 0.331	91.64 ± 1.434	92.00 ± 0.817	0.000
-70	88.62 ± 0.446	88.91 ± 0.334	91.48 ± 1.434	91.84 ± 0.853	0.000
-80	88.47 ± 0.454	88.79 ± 0.339	91.33 ± 1.434	91.68 ± 0.888	0.000
-90	88.32 ± 0.471	88.67 ± 0.344	91.17 ± 1.435	91.53 ± 0.921	0.000
-100	88.18 ± 0.496	88.55 ± 0.349	91.03 ± 1.437	91.39 ± 0.952	0.000

Table 3a TCP comparison of DV group with different TCD_{50}/γ_{50} values

a value	$TCD_{50}/\gamma_{50} = 36.50/0.72$	$TCD_{50}/\gamma_{50} = 54.92/2.04$	$TCD_{50}/\gamma_{50} = 51.87/2.17$	$TCD_{50}/\gamma_{50} = 51.97/1.81$	$TCD_{50}/\gamma_{50} = 49.12/1.25$	P value
-10	92.988 ± 0.115	98.182 ± 0.089	99.133 ± 0.046	98.091 ± 0.083	95.269 ± 0.138	0.000
-20	92.955 ± 0.109	98.156 ± 0.086	99.120 ± 0.044	98.067 ± 0.080	95.229 ± 0.132	0.000
-30	92.921 ± 0.104	98.130 ± 0.082	99.106 ± 0.042	98.042 ± 0.076	95.189 ± 0.126	0.000
-40	92.888 ± 0.100	98.104 ± 0.080	99.093 ± 0.041	98.018 ± 0.074	95.149 ± 0.122	0.000
-50	92.855 ± 0.097	98.077 ± 0.078	99.079 ± 0.040	97.993 ± 0.072	95.108 ± 0.118	0.000
-60	92.822 ± 0.096	98.051 ± 0.078	99.065 ± 0.040	97.969 ± 0.072	95.068 ± 0.117	0.000
-70	92.789 ± 0.097	98.023 ± 0.079	99.052 ± 0.041	97.944 ± 0.073	95.028 ± 0.118	0.000
-80	92.756 ± 0.099	97.996 ± 0.082	99.037 ± 0.042	97.919 ± 0.075	94.987 ± 0.122	0.000
-90	92.723 ± 0.104	97.969 ± 0.086	99.023 ± 0.045	97.894 ± 0.079	94.947 ± 0.128	0.000
-100	92.690 ± 0.110	97.941 ± 0.093	99.009 ± 0.048	97.868 ± 0.086	94.906 ± 0.136	0.000

Table 3b TCP comparison of DV + EUD group with different TCD_{50}/γ_{50} values

a value	$TCD_{50}/\gamma_{50} = 36.50/0.72$	$TCD_{50}/\gamma_{50} = 54.92/2.04$	$TCD_{50}/\gamma_{50} = 51.87/2.17$	$TCD_{50}/\gamma_{50} = 51.97/1.81$	$TCD_{50}/\gamma_{50} = 49.12/1.25$	P value
-10	93.016 ± 0.070	98.204 ± 0.054	99.144 ± 0.028	98.111 ± 0.050	95.303 ± 0.084	0.000
-20	92.987 ± 0.069	98.183 ± 0.054	99.133 ± 0.028	98.091 ± 0.050	95.269 ± 0.083	0.000
-30	92.959 ± 0.069	98.161 ± 0.054	99.122 ± 0.028	98.071 ± 0.050	95.236 ± 0.083	0.000
-40	92.932 ± 0.069	98.139 ± 0.055	99.111 ± 0.028	98.051 ± 0.051	95.202 ± 0.083	0.000
-50	92.905 ± 0.070	98.118 ± 0.055	99.100 ± 0.028	98.031 ± 0.051	95.170 ± 0.085	0.000
-60	92.878 ± 0.071	98.096 ± 0.057	99.089 ± 0.029	98.011 ± 0.052	95.137 ± 0.086	0.000
-70	92.851 ± 0.072	98.075 ± 0.058	99.078 ± 0.030	97.991 ± 0.053	95.104 ± 0.087	0.000
-80	92.825 ± 0.073	98.053 ± 0.059	99.067 ± 0.031	97.971 ± 0.055	95.072 ± 0.089	0.000
-90	92.798 ± 0.074	98.032 ± 0.062	99.056 ± 0.031	97.951 ± 0.056	95.040 ± 0.091	0.000
-100	92.772 ± 0.076	98.010 ± 0.062	99.045 ± 0.032	97.932 ± 0.057	95.008 ± 0.093	0.000

Table 3c TCP comparison of EUD group with different TCD_{50}/γ_{50} values

a value	$TCD_{50}/\gamma_{50} = 36.50/0.72$	$TCD_{50}/\gamma_{50} = 54.92/2.04$	$TCD_{50}/\gamma_{50} = 51.87/2.17$	$TCD_{50}/\gamma_{50} = 51.97/1.81$	$TCD_{50}/\gamma_{50} = 49.12/1.25$	P value
-10	93.559 ± 0.273	98.584 ± 0.185	99.337 ± 0.093	98.471 ± 0.176	95.929 ± 0.311	0.000
-20	93.528 ± 0.275	98.563 ± 0.187	99.326 ± 0.094	98.451 ± 0.178	95.894 ± 0.314	0.000
-30	93.496 ± 0.277	98.542 ± 0.190	99.316 ± 0.096	98.431 ± 0.180	95.859 ± 0.316	0.000
-40	93.465 ± 0.278	98.521 ± 0.192	99.305 ± 0.097	98.411 ± 0.182	95.823 ± 0.319	0.000
-50	93.433 ± 0.279	98.499 ± 0.194	99.294 ± 0.098	98.390 ± 0.184	95.787 ± 0.321	0.000
-60	93.402 ± 0.281	98.478 ± 0.197	99.283 ± 0.100	98.370 ± 0.186	95.750 ± 0.324	0.000
-70	93.371 ± 0.282	98.456 ± 0.199	99.272 ± 0.101	98.350 ± 0.188	95.715 ± 0.326	0.000
-80	93.340 ± 0.284	98.435 ± 0.202	99.261 ± 0.102	98.329 ± 0.190	95.680 ± 0.329	0.000
-90	93.311 ± 0.285	98.414 ± 0.204	99.251 ± 0.104	98.310 ± 0.193	95.645 ± 0.322	0.000
-100	93.282 ± 0.287	98.394 ± 0.207	99.240 ± 0.105	98.290 ± 0.195	95.612 ± 0.334	0.000

Table 3d TCP comparison of EUD + DV group with different TCD_{50}/γ_{50} values

a value	$TCD_{50}/\gamma_{50} = 36.50/0.72$	$TCD_{50}/\gamma_{50} = 54.92/2.04$	$TCD_{50}/\gamma_{50} = 51.87/2.17$	$TCD_{50}/\gamma_{50} = 51.97/1.81$	$TCD_{50}/\gamma_{50} = 49.12/1.25$	P value
-10	93.64 ± 0.113	98.63 ± 0.072	99.36 ± 0.036	98.52 ± 0.070	96.02 ± 0.126	0.000
-20	93.60 ± 0.122	98.62 ± 0.078	99.35 ± 0.039	98.50 ± 0.070	95.98 ± 0.136	0.000
-30	93.57 ± 0.130	98.60 ± 0.084	99.34 ± 0.042	98.48 ± 0.081	95.95 ± 0.146	0.000
-40	93.54 ± 0.139	98.58 ± 0.090	99.33 ± 0.046	98.46 ± 0.087	95.91 ± 0.156	0.000
-50	93.51 ± 0.147	98.55 ± 0.097	99.32 ± 0.049	98.44 ± 0.093	95.87 ± 0.166	0.000
-60	93.48 ± 0.155	98.53 ± 0.103	99.31 ± 0.052	98.42 ± 0.099	95.84 ± 0.175	0.000
-70	93.44 ± 0.163	98.51 ± 0.109	99.30 ± 0.055	98.40 ± 0.104	95.80 ± 0.185	0.000
-80	93.41 ± 0.170	98.49 ± 0.115	99.29 ± 0.058	98.38 ± 0.110	95.77 ± 0.194	0.000
-90	93.38 ± 0.178	98.47 ± 0.121	99.27 ± 0.061	98.36 ± 0.115	95.73 ± 0.203	0.000
-100	93.36 ± 0.185	98.45 ± 0.127	99.26 ± 0.064	98.34 ± 0.121	95.70 ± 0.211	0.000

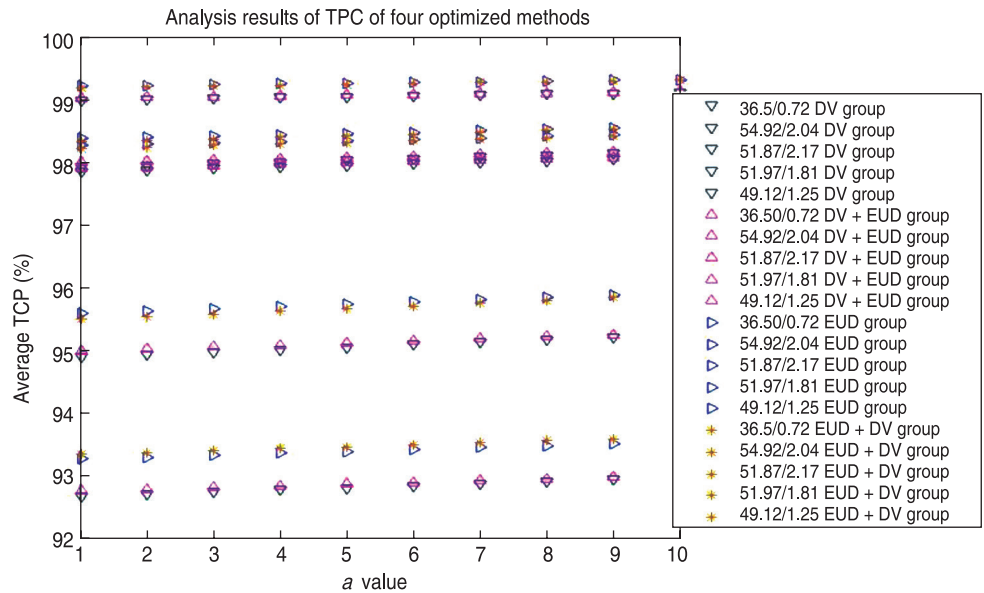


Fig. 1 Results of tumor control probability (TCP) for the four optimization methods

were always higher than those of DV and DV + EUD groups (Fig. 1). It could be seen that the EUD group had an absolute advantage in improving the TCP of the target area and was greatly affected by the value of TCD_{50}/γ_{50} .

Organs at risk

Table 5 shows the dose-volume parameters of OAR. There were no significant differences among the four groups ($P > 0.05$). As shown in Fig. 2, in the range of 0.1 to 1.0, the EUD of normal lung tissue tended to increase with the increase of the a -value in the four optimization methods. When the a -value was kept unchanged, the EUD mean values of lung tissue demonstrated no obvious difference, except for the EUD + DV group.

This study also compared the number of monitor units

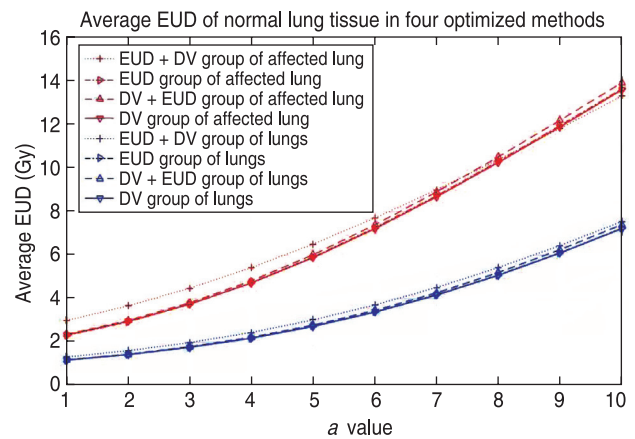


Fig. 2 EUD value of normal lung tissue of the four optimization methods

Table 4 HI/CI values for the four plan optimization methods

	DV group	DV + EUD group	EUD group	EUD + DV group	P value
HI	0.060 ± 0.008	0.057 ± 0.008	0.072 ± 0.014	0.077 ± 0.015	0.001
CI	0.730 ± 0.063	0.697 ± 0.095	0.703 ± 0.095	0.703 ± 0.088	0.957

Table 5 Dose-volume parameters of OAR under four optimization scenarios

	DV group	DV + EUD group	EUD group	EUD + DV group	P value
Lung Dmean (Gy)	5.90 ± 1.135	6.02 ± 1.211	5.91 ± 1.116	5.80 ± 1.036	0.966
Lung V ₅ (%)	33.26 ± 8.845	32.82 ± 8.679	34.26 ± 8.959	33.91 ± 8.789	0.983
Lung V ₁₀ (%)	21.54 ± 4.948	22.02 ± 5.235	21.46 ± 4.668	21.50 ± 5.020	0.994
Lung V ₂₀ (%)	13.07 ± 2.203	13.54 ± 1.842	13.14 ± 2.240	12.86 ± 2.072	0.908
Lung V ₃₀ (%)	10.19 ± 1.730	10.74 ± 1.673	10.51 ± 2.019	10.26 ± 2.069	0.908
Heart V ₃₀ (%)	3.97 ± 8.315	3.19 ± 8.974	3.75 ± 9.620	3.83 ± 9.736	0.998
Heart V ₄₀ (%)	1.80 ± 4.753	1.68 ± 5.078	1.36 ± 4.215	1.49 ± 4.477	0.997
Heart Dmean (Gy)	2.79 ± 3.068	2.74 ± 3.209	2.74 ± 3.112	2.90 ± 3.277	0.999
Cord Dmax (Gy)	9.23 ± 7.120	9.07 ± 6.682	9.33 ± 6.882	9.79 ± 7.530	0.996

Table 6 Comparison of the MU number and execution time for the four optimization methods

	DV group	DV + EUD group	EUD group	EUD + DV group	P value
MU	1808.97 ± 259.33	1799.67 ± 241.27	1387.12 ± 122.66	1450.96 ± 190.26	0.000
Delivery time (min)	3.08 ± 0.397	3.17 ± 0.359	2.45 ± 0.271	2.61 ± 0.341	0.000

(MUs) and plan-delivery time of the four optimization methods. As shown in Table 6, the MUs and delivery time of the EUD and EUD + DV groups were significantly lower than those of the other two groups ($P < 0.05$), showing that using the EUD function for the target area during the optimization was more efficient among the four optimization methods.

Discussion

Since physical optimization is more direct than biological optimization, the dose-volume objective function is more convenient to use in clinical practice [3]. However, the interaction between tissue and X-ray is a very complicated process. The EUD model and the TCP/NTCP model proposed by Niemierko *et al* [2-3, 9] have been considered to be related to the biological characteristics of tissues to some extent. The biological function optimization method based on the above model has some advantages in reflecting the biological response of the tissue to radiation compared to the physical function optimization method. The results of this study showed that the EUD, $D_{2\%}$, $D_{50\%}$, and $D_{98\%}$ of PTV in EUD and EUD + DV groups were higher than those in the other two groups. In other words, the target doses of both groups were generally improved. The authors believe these characteristics of the *a-value* that explain this result.

This study compared the results of four planning optimization methods for 10 patients with NSCLC and found that the EUD and TCP optimized using the biological function were significantly higher than those optimized by the physical function. At the same time, the mean dose of lung tissue was lower and there was a small difference in the dose of heart and spinal cord. This means that, given the same prescription dose and the same constraints, biological function optimization programs can ensure the target area achieves a higher biological effect without increasing the dose on normal tissue. In this way, the therapeutic gain ratio of treatment can be improved to a certain extent, and its advantages can be better reflected in hypofractionated radiotherapy. In addition, through this study, we found that biologically optimized plans are more efficient to implement. Studies have shown that [6], when the EUD function is used for the target area alone, the cold spot is overemphasized in the optimization process, and the constraints on the hotspot are weak. That is to say, in order to keep the dose

at each point not lower than the prescription dose, the overall dose in the target area has to be increased, thus the hotspot in the target area tends to be out of control; thus it is not recommended to apply the EUD function alone for the target area during the optimization. In this study, no uncontrollable situation occurred when only the EUD function was used for target area in the optimization. The reason may be that a global hot spot control structure "patient" is used. In this study, five groups of TCD_{50}/γ_{50} values were selected from the study of Okunieff *et al* [9]. In the four optimization methods, although the TCP values reached highest when $TCD_{50}/\gamma_{50} = 51.87/2.17$ is chosen, this combination is more suitable for adenocarcinoma, not for squamous carcinoma. In contrast, $TCD_{50}/\gamma_{50} = 51.97/1.81$ is applicable to all NSCLC cases [9], thus, the value of this combination is recommended for TCP calculations. However, to draw more convincing conclusions, we need to increase the sample size for further study.

In general, compared to the physical optimization, biological optimization has obvious advantages in improving the EUD of the target area and delivery efficiency. This makes the target area achieve a higher biological effect while the irradiated doses of the normal tissue do not increase as a result, being more advantageous in hypofractionated radiotherapy. Mihaylov *et al* [14] conducted a comparative study of physical and biological optimization for prostate cancer cases; it was found that biological optimization significantly increased the target dose while sparing more volumes of OAR. The reason why our results differed from those of some previous studies may be that the same constraints are applied to the same structure in the four optimizations, only the used functions are different, and the differences in the functions themselves may not have obvious influence. In addition, the planners' flexible application ability and experience of various physical and biological functions are also important in embodying the advantages of biological optimization. Nahum *et al* [15] believes that the two-dimensional dose-volume histogram (DVH) data used in the LKB model do not fully represent the dose distribution in three-dimensional space, while the Marsden TCP model also assumes that all clonal cells in each treatment have the same radio sensitivity. Therefore, the currently used biological optimization model only reflects the biological response of different tissues to X-rays to some extent, and there are still some defects and deficiencies. Nevertheless, with the development of technology and

the discovery of more biological optimization models, biological optimization will show more advantages in radiotherapy.

Conflicts of interest

The authors indicate no potential conflicts of interest.

References

- Senthilkumar K, Maria Das KJ, Balasubramanian K, *et al.* Estimation of the effects of normal tissue sparing using equivalent uniform dose-based optimization. *J Med Phys*, 2016, 41: 123–128.
- Niemierko A. Reporting and analyzing dose distributions: A concept of equivalent uniform dose. *Med Phys*, 1997, 24: 103–110.
- Thieke C, Bortfeld T, Niemierko A, *et al.* From physical dose constrains to equivalent uniform dose constrains in inverse radiotherapy planning. *Med Phys*, 2003, 30: 2332–2339.
- Luxton G, Keall PJ, King CR. A new formula for normal tissue complication probability (NTCP) as a function of equivalent uniform dose (EUD). *Phys Med Biol*, 2008, 53: 23–36.
- Bradley JD, Hope A, El Naqa I, *et al.* A nomogram to predict radiation pneumonitis, derived from a combined analysis of RTOG 9311 and institutional data. *Int J Radiat Oncol Biol Phys*, 2007, 69: 985–992.
- Wu Q, Mohan R, Niemierko A, *et al.* Optimization of intensity-modulated radiotherapy plans based on the equivalent uniform dose. *Int J Radiat Oncol Biol Phys*, 2002, 52: 224–235.
- Shaikh M, Burmeister J, Joiner M, *et al.* Biological effect of different IMRT delivery techniques: SMLC, DMLC, and helical tomotherapy. *Med Phys*, 2010, 37: 762–770.
- Gay HA, Niemierko A. A free program for calculating EUD-based NTCP and TCP in external beam radiotherapy. *Phys Med*, 2007, 23: 115–125.
- Okunieff P, Morgan D, Niemierko A, *et al.* Radiation dose-response of human tumors. *Int J Radiat Oncol Biol Phys*, 1995, 32: 1227–1237.
- Kim Y, Tomé W. Optimization of radiotherapy using biological parameters. *Cancer Treat Res*, 2008, 139: 257–278.
- Bentzen SM, Tucker SL. Quantifying the position and steepness of radiation dose-response curves. *Int J Radiat Biol*, 1997, 71: 531–542.
- Videtic GM, Hu C, Singh AK, *et al.* A randomized phase 2 study comparing 2 stereotactic body radiation therapy schedules for medically inoperable patients with stage I peripheral non-small cell lung cancer: NRG Oncology RTOG 0915 (NCCTG N0927). *Int J Radiat Oncol Biol Phys*, 2015, 93: 757–764.
- ICRU Report 83: prescribing, recording and reporting photon-beam intensity-modulated radiation therapy (IMRT). Oxford University Press, 2010.
- Mihaylov IB, Fatyga M, Bzdusek K, *et al.* Biological optimization in volumetric modulated arc radiotherapy for prostate carcinoma. *Int J Radiat Oncol Biol Phys*, 2012, 82: 1292–1298.
- Nahum AE, Uzan J. (Radio)biological optimization of external-beam radiotherapy. *Comput Math Methods Med*, 2012, 2012: 329214. doi: 10.1155/2012/329214. Epub 2012 Nov 6.

DOI 10.1007/s10330-019-0364-4

Cite this article as: Shao Y, Zhang FL, Wang S, *et al.* Estimation of the effect of target and normal tissue sparing based on equivalent uniform dose-based optimization in hypofractionated radiotherapy for lung cancer. *Oncol Transl Med*, 2019, 5: 197–203.

Correlation between miR-564, TGF- β 1, and radiation-induced lung injury*

Yunzhang Ge¹ (✉), Tao Xie², Bin Yang², Qianxia Li³, Qingrong Ren², Xiaoyi Zhou², Desheng Hu², Zhongshu Tu²

¹ Hubei Province Tongcheng County Hospital of Traditional Chinese Medicine, Xianning 437400, China

² Hubei Cancer Hospital, Tongji Medical College, Huazhong University of Science and Technology, HuBei Key Laboratory of Medical Information Analysis and Tumor Diagnosis & Treatment, Wuhan 430079, China

³ Tongji Hospital, Tongji Medical College, Huazhong University of Science and Technology, Wuhan 430030, China

Abstract

Objective Our study aimed to analyze the expression of miR-564 and TGF- β 1 in cancer tissues and the serum of patients with radiation-induced lung injury, and to investigate the relationship between them and radiation-induced lung injury.

Methods In situ hybridization and real-time fluorescence quantitative method were used to detect the expression of miR-564. Additionally, immunohistochemistry and enzyme-linked immunosorbent assay (ELISA) were performed to detect the expression of TGF- β 1.

Results The overall incidence of acute radiation pneumonia was 55.9% (100/179). The incidence of \geq grade 2 radioactive pneumonia was 24.0% (43/179) and that of grade 1 was 31.8% (57/179). The expression of miR-564 in grade \geq 2 was slightly higher than that in patients without or with grade 1, but there was no statistical difference ($P = 0.86$). The serum level and ratio of miR-564 in patients with grade \geq 2 were significantly higher than those without or with grade 1 ($P = 0.005$, $P = 0.025$, respectively). The expression of TGF- β 1 in grade \geq 2 was significantly higher than that of patients without or with grade 1 ($P = 0.017$). The serum levels of TGF- β 1 in grade \geq 2 were significantly higher than those in patients without or with grade 1 ($P = 0.038$). Although the ratio of TGF- β 1 in radiation pneumonia of grade \geq 2 was significantly higher than that of without or with grade 1, there was no significant difference ($P = 0.24$). Moreover, patients with higher expression of miR-564 and lower expression of TGF- β 1 had better prognosis.

Conclusion MiR-564 and TGF- β 1 are predictors of radiation-induced lung injury. Monitoring its changing trend can improve the accuracy of predicting radiation-induced lung injury. The levels and ratio of serum miR-564 and TGF- β 1 in patients with radiation-induced lung injury are related to the severity of radiation-induced lung injury.

Key words: radiation-induced lung injury; miR-564; TGF- β 1

Received: 23 October 2018

Revised: 13 June 2019

Accepted: 29 August 2019

Radiation-induced lung injury is the most common side effect of chest cancer radiotherapy. It includes early inflammatory reaction and late fibrosis, which seriously affect the quality of life of patients and become the bottleneck of increasing the dose of radiotherapy; however, its underlying mechanism is unclear [1–2].

Exploring the mechanism of radiation-induced lung injury

has become an interesting research topic at present. In recent years, studies have shown that radiation-induced lung injury results from the interaction of many kinds of cells, cytokines, and signaling pathways [3–4]. It has been proved that transforming growth factor- β 1 (TGF- β 1) is a predictor of radiation-induced lung injury, which can activate fibroblasts to differentiate into myofibroblasts,

✉ Correspondence to: Yunzhang Ge. Email: gezi432@163.com

* Supported by grants from the Fundamental Research for South-Central University for Nationalities (No. PJS140011604) and Chen Xiaoping Foundation Development of Science and Technology of Hubei (No. CXPJH11800004-015).

© 2019 Huazhong University of Science and Technology

promote matrix synthesis, produce large amounts of collagen, and mediate radiation-induced lung injury^[5]. Wang *et al*^[6] found that with increase in radiation dose, the plasma level of TGF- β 1 was consistently higher than the baseline level, and the level of TGF- β 1 was closely related to grade 2 radiation-induced lung injury. However, only a few studies have been conducted to evaluate the relationship between microRNA (miRNA) and radiation lung injury, and limited studies have explored the combination of miRNA and TGF- β 1 in radiation lung injury. It is not clear whether a correlation between them exists. This study is based on our previous findings that miR-564 serves as a negative regulatory gene in lung cancer^[7]. However, it is not clear whether miR-564 and TGF- β 1 are involved in the regulation of radiation-induced lung injury. In this study, we investigated the expression of miR-564 and TGF- β 1 in tumor tissues and the blood of patients with radiation pneumonitis, and we explored the relationship between their expression levels and radiation-induced lung injury.

Materials and methods

Participants

From November 2014 to December 2016, patients with pathologically confirmed non-small cell lung cancer (NSCLC), who received intensity-modulated radiotherapy (IMRT) at the Hubei Cancer Hospital, and were assessed to have a KPS score > 70 and expected survival time of more than 6 months were enrolled in this study. There were 100 male and 81 female patients with a median age of 59 years (27, 87 years). Among the patients, there were 121 smokers and 60 non-smokers, 87 adenocarcinoma, 73 squamous cell carcinoma, 21 adenosquamous carcinoma, 97 stage III A, and 84 stage III B lung cancer patients (according to the 8th stage of lung cancer). In addition, 94 cases were central type, 87 were peripheral type, 165 subjects received chemotherapy (74 subjects received concurrent chemotherapy), and 16 subjects did not receive chemotherapy. The general information for the patients is shown in Table 1.

Radiotherapy plan

All the patients were treated using Varian accelerator 23EX, with target dose of above 56 Gy, 1.8–2.0 Gy/F, administered once a day, and 5 times a week, and all patients were treated with intensity modulated radiotherapy (IMRT). To delineate the primary lung lesions at the pulmonary window (GTV) and the metastatic lymph nodes in the mediastinal fenestra (GTVnd), GTV exoduses 6 mm, 8 mm, and the corresponding regions of the metastatic lymph nodes CTV. CTV exoduses 3 mm as PTV; V20 \leq 28%, V5 \leq 60% in both lungs, D2 \leq 40 Gy in spinal cord, V30 \leq 40%, V40 \leq 30% in heart.

Table 1 The baseline characteristics of 181 patients with lung cancer

Clinical characteristics	No. of patients	%
Gender		
Male	100	55.2
Female	81	44.8
T staging		
T1	15	8.3
T2	38	21.0
T3	69	38.1
T4	59	32.6
N staging		
N0	8	4.4
N1	26	14.4
N2	66	36.5
N3	81	44.7
Pathological type		
Adenocarcinoma	87	48.1
Squamous cell carcinoma	73	40.3
Adenosquamous carcinoma	21	11.6
Clinical staging		
IIIA	97	53.6
IIIB	84	46.4
Gross type		
Central type	94	51.9
Peripheral type	87	48.1
Chemotherapy (yes/no)		
Yes	165	91.2
No	16	8.8
Curative effect evaluation		
CR	48	26.8
PR	107	59.8
SD	22	12.3
PD	2	1.1
Radiation pneumonia		
Grade 1	57	31.8
Grade 2 or above 2	43	24.0

Main reagent

The reagents used were RecoverALL Total Nucleic Acid Isolation Kit (Ambion) kit, Probe Mix (ABI Company), TaqMan probe (ABI), miScript SYBR Green PCR Kit (Qiagen Company), TGF- β 1 Antibody (Beijing Boosen Biotechnology Co., Ltd.), TGF- β 1 ELISA Kit (Xinbosheng Biotech Co., Ltd.), SP Kit (Beijing Zhongshan Jinqiao Biotechnology, Limited), and mirVanaTM PARISTM kit (American Applied Biosystem company product).

Serum collection

Before radiotherapy, 2 weeks, 4 weeks, 6 weeks, 2 weeks, 4 weeks, 6 weeks, 8 weeks, 5 mL, and 4 °C cold storage of cubital venous blood were collected. A 4 °C low temperature centrifugation of –80 °C supernatant at 1000 g for 10 min was performed within 12 h.

RNA extraction from paraffin samples and serum samples

Paraffin slices were dewaxed using xylene, and xylene was removed using ethanol and dried at room temperature, and 200 μL was added to digest buffer. Digestive enzyme of 4 μL was heated at 50 $^{\circ}\text{C}$ for 15 min, and then heated again at 80 $^{\circ}\text{C}$ for 15 min. Next, nucleic acid separation additive of 240 μL was added, centrifuged rinsed with Wash1 and Wash2 respectively, and then digested and purified using nuclease. Serum sample of 400 μL per copy was extracted using the method described in the instruction manual of mirVanaTM PARISTM kit, and the total RNA was stored in a refrigerator at -80°C for use.

Detection of miR-564 expression in cancer tissue by in situ hybridization

Paraffin sections were dry-heated in an oven at 68 $^{\circ}\text{C}$ for 30 min. Next, conventional xylene was dewaxed in water and the slices were treated with 0.5% H_2O_2 / methanol solution for 30 min, and inactivation of endogenous peroxidase occurred. Next, the slices were flushed with distilled water for 3 times. Pepsin was freshly diluted with 3% citric acid, digested at 37 $^{\circ}\text{C}$ for 25 min to expose miRNA fragments, and then flushed with 0.5 M PBS buffer for 3 times. Hybridization solution of 20 μL (probe concentration was 14 $\mu\text{g}/\text{mL}$) was added to each slice for overnight hybridization at 42 $^{\circ}\text{C}$ (about 16 h) each slice was then flushed with distilled water once for 5 min each time, and 20 μL hybridization solution (probe concentration 14 μmol) was added again to each slice for overnight hybridization (about 16 h). After hybridization, the slides were washed twice with $2 \times \text{SSC}$, preheated at 37 $^{\circ}\text{C}$ for 5 min each time, and then washed and sliced with $0.5 \times \text{SSC}$ and $0.2 \times \text{SSC}$ liquids, respectively. The slices were incubated at 37 $^{\circ}\text{C}$ for 30 min, then treated with biotinylated mouse anti-digoxin at 37 $^{\circ}\text{C}$ for 60 min, and washed with 0.5 M PBS for 3 times and 5 min each time. After incubating at SABC-POD, 37 $^{\circ}\text{C}$ for 30 min, the slices were washed with 0.5 M PBS for 4 times, 5 min each time, and the slides were incubated at 37 $^{\circ}\text{C}$ for 30 min with biotin peroxidase dripping, and then washed with 0.5 M PBS for 4 times, 5 min each time. Color with freshly prepared DAB solution, microscopically controlled coloration time, hematoxylin redyeing, 0.1% hydrochloric acid ethanol differentiation, distilled water turning blue, conventional alcohol gradient dehydration, dimethylbenzene transparent neutral gum sealing.

Real-time fluorescence quantitative PCR was used to detect the content of miR-564 in serum

The $2 \times$ All-in-OneTMqPCR Mix in miRNA-qRT-PCR Detection Kit was melted at room temperature, and then mixed gently upside down and centrifuged briefly. In the process of the preparation, PCR mix was

always stored in dark (operated on ice), and No Template Control (NTC), was designed as negative control of the experiment; therefore, other reagents of template cDNA, were replaced with water in the reaction. To determine whether the system was contaminated, PCR mix was quickly mixed and added to a 96-well plate. The 96-well plate was centrifuged briefly to ensure that all reaction fluids were at the bottom of the reaction hole. The standard three-step procedure was used for the PCR. After the PCR was performed, the following procedure was used to analyze the melting curve: iQ5 software and SPSS 17.0 were used for data analysis, the relative expression rate (Relative Expression, RQ) of the target gene hsa-miR-564 of the sample was calculated using the difference multiple method ($2^{-\text{Ct}}$), and the experiment was repeated three times.

The expression of TGF- β 1 was detected by immunohistochemistry

Paraffin sections of 4 μm in size were treated with xylene dewaxing, gradient ethanol (75%, 80%, 95%, and 100%) for dehydration, 3% H_2O_2 solution for incubation at 37 $^{\circ}\text{C}$ for 20 min, and PBS solution for washing thrice. The slices were placed in sodium citrate buffer at 100 $^{\circ}\text{C}$, heated for 15 min, naturally cooled, and washed with PBS solution for 3 times. Goat serum was sealed and incubated at 37 $^{\circ}\text{C}$ for 20 min and TGF- β 1 (1:100) antibody diluent was infused into the serum. The negative control was replaced with PBS and incubated at 4 $^{\circ}\text{C}$ overnight. IgG, 37 was incubated at 30 min with PBS for 3 times, enzyme / streptavidin complex was incubated at 37 $^{\circ}\text{C}$ for 30 min, with PBS and washed 3 times, DAB color was developed, hematoxylin was redyed, and normal dehydration and transparent sealing were performed.

Detection of serum TGF- β 1 content through enzyme-linked immunosorbent assay (ELISA)

Venous blood coagulated naturally at room temperature for 20 min, and it was centrifuged at 3000 rpm for 20 min. The supernatant was collected and repacked with 500 μL number, and was transferred to -80°C refrigerator for storage. The patients' serum TGF- β 1 content was detected using ELISA kit (Xinbosheng Biotech Co., Ltd) within 2 h after melting at room temperature. The procedure was performed in strict accordance with the manufacturer's instructions.

Result judgment

Considering the number of positive cells in a single visual field / the total number of tumor cells $\times 100\%$ as the evaluation criterion, according to the rate of positive cells in tumor cells, $\leq 1\%$ was (-), 1%–5% was (+), and 5%–15% was (2+), 15%–25% was (3+), and more than 25% was (4+). The positive cells were nucleoserous type (including

nucleoserous membrane, serosa, and membrane-positive) and karyotype (including nuclear and nucleocytoplasmic positive).

Assessment of radiation-induced lung injury

Acute radiation-induced lung injury was assessed weekly according to RTOG acute radiation-induced lung injury classification for a period of 3 months, from the beginning of radiotherapy to the end of radiotherapy [8].

Statistical analysis

SPSS 17.0 was used for statistical analysis, *t* test was used for mean comparison, and χ^2 and Fisher's precise probability method were used for rate comparison.

Results

Follow-up results

The shortest follow-up time was 7 months and the longest follow-up time was 31 months until June 30, 2017. The median follow-up period was 19 months and two cases were lost. The overall incidence of acute radiation pneumonitis was 55.9% (100 / 179), grade 2 and above (\geq grade 2) was 24.0% (43 / 179), and grade 1 was 31.8% (57 / 179). Efficacy evaluation: 48 cases of CR (26.8%), 107 cases of PR, 22 cases of SD (12.3%), 2 cases of PD (1.1%), Table 1.

Relationship between the expression of miR-564 in lung cancer tissues and the degree of radiation-induced lung injury

The expression of miR-564 in the cancer tissues of patients with \geq grade 2 radiation pneumonitis was slightly higher than that of patients without or with grade 1. However, there was no statistical difference ($P = 0.86$; Fig. 1).

Relationship between the level of serum miR-564 and the severity of radiation-induced lung injury

The level of miR-564 in the serum of patients with \geq grade 2 radiation pneumonitis increased gradually during radiotherapy, and reached the peak at the end of 4 weeks. Thereafter, it decreased gradually and was higher than that of patients without or with grade 1 radiation pneumonitis ($P = 0.005$) (Table 2). The ratio changes of miR-564 before and after radiotherapy were as follows: the ratio of patients with \geq grade 2 radiation pneumonitis increased gradually before and after radiotherapy. It reached the peak at the 4th week after radiotherapy, and then decreased gradually, but was higher than that of patients without or with grade 1 radiation pneumonitis ($P = 0.025$) (Table 3).

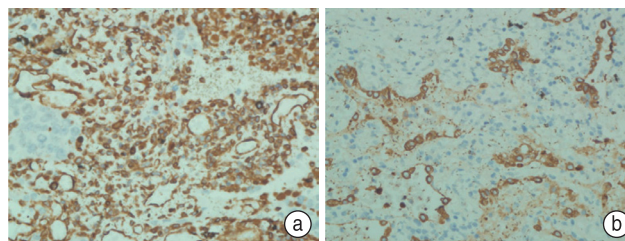


Fig. 1 Expression of miR-564 in cancer tissues of patients with different grades of radiation pneumonitis. (a) Grade 2 radiation pneumonitis patients; (b) Grade 1 radiation pneumonitis patients

Table 2 Relationship between serum miR-564 level and severity of radiation-induced lung injury in patients ($\bar{x} \pm s$, pg/mL)

Time	No or Grade 1 radiation pneumonia	Grade 2 or above 2 radiation pneumonia	<i>P</i>
Before radiotherapy	1.2 \pm 0.3	1.5 \pm 0.5	
2 weeks after radiotherapy	1.2 \pm 0.8	1.5 \pm 0.9	0.467
4 weeks after radiotherapy	1.1 \pm 1.0	2.5 \pm 1.0	0.005
6 weeks after radiotherapy	1.0 \pm 0.7	2.7 \pm 0.8	0.000
2 weeks end of radiotherapy	0.9 \pm 0.4	3.0 \pm 0.5	0.000
4 weeks end of radiotherapy	0.9 \pm 0.5	3.3 \pm 0.7	0.000
6 weeks end of radiotherapy	0.8 \pm 0.6	2.7 \pm 0.5	0.000
8 weeks end of radiotherapy	0.8 \pm 0.4	2.4 \pm 0.4	0.000

Table 3 Changes in miR-564 ratio before and after radiotherapy in two groups of patients

Time	No or Grade 1 radiation pneumonia	Grade 2 or above 2 radiation pneumonia
Before radiotherapy	1.2 \pm 0.3	1.5 \pm 0.5
2 weeks after radiotherapy	1.2 \pm 0.8	1.5 \pm 0.9
4 weeks after radiotherapy	1.1 \pm 1.0	2.5 \pm 1.0
6 weeks after radiotherapy	1.0 \pm 0.7	2.7 \pm 0.8
2 weeks end of radiotherapy	0.9 \pm 0.4	3.0 \pm 0.5
4 weeks end of radiotherapy	0.9 \pm 0.5	3.3 \pm 0.7
6 weeks end of radiotherapy	0.8 \pm 0.6	2.7 \pm 0.5
8 weeks end of radiotherapy	0.8 \pm 0.4	2.4 \pm 0.4

The relationship between the expression of TGF- β 1 in lung cancer tissues and the degree of radiation-induced lung injury

The expression of TGF- β 1 in the cancer tissues of patients with \geq grade 2 radiation pneumonitis was higher than that of patients without or with grade 1 radiation pneumonitis. The difference was statistically significant ($P = 0.017$) (Fig. 2).

Relationship between the level of TGF- β 1 in the serum and severity of radiation-induced lung injury

The level of TGF- β 1 in the serum of patients with \geq grade 2 radiation pneumonitis increased gradually

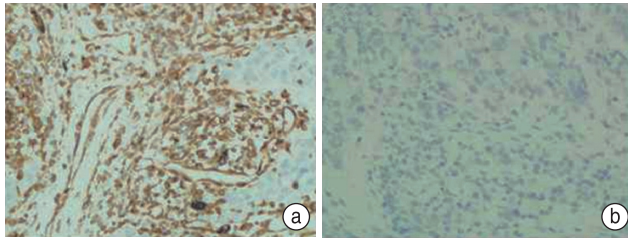


Fig. 2 Expression of TGF-β1 in cancer tissues of patients with different grades of radiation pneumonitis (a) Grade 2 radiation pneumonitis patients; (b) Grade 1 radiation pneumonitis patients

Table 4 Relationship between serum TGF-β1 level and severity of radiation-induced lung injury in patients ($\bar{x} \pm s$, pg/mL)

Time	No or Grade 1 radiation pneumonia	Grade 2 or above 2 radiation pneumonia	<i>P</i>
Before radiotherapy	2.4 ± 0.5	2.2 ± 0.3	
2 weeks after radiotherapy	2.4 ± 0.9	2.6 ± 0.5	0.087
4 weeks after radiotherapy	2.3 ± 1.0	2.9 ± 0.8	0.003
6 weeks after radiotherapy	2.5 ± 0.8	3.0 ± 0.9	0.000
2 weeks end of radiotherapy	2.4 ± 0.5	3.2 ± 1.0	0.000
4 weeks end of radiotherapy	2.2 ± 0.7	3.6 ± 0.7	0.000
6 weeks end of radiotherapy	2.4 ± 0.5	3.3 ± 0.8	0.000
8 weeks end of radiotherapy	2.2 ± 0.4	3.0 ± 0.6	0.000

during radiotherapy, and reached the peak at the end of 4 weeks. Thereafter, it decreased gradually and was higher than that in patients without or with grade 1 radiation pneumonitis ($P = 0.038$), and the rise of TGF-β1 was consistent with the rise of miR-564 (Table 4). The ratio of TGF-β1 in patients with ≥ grade 2 radiation pneumonitis increased gradually before and after radiotherapy, and then decreased, which was higher than that in patients without or with grade 1 radiation pneumonitis. However, there was no statistical difference ($P = 0.24$) (Table 5).

Relationship between miR-564, TGF-β1 expression, and patient prognosis

The prognosis of patients with high expression of miR-564 was better than that of patients with low expression of TGF-β1, while the prognosis of patients with low expression of TGF-β1 was better than that of patients with high expression of TGF-β1 (Fig. 3).

Discussion

miRNA is a group of 18-23 nucleotides long, endogenous non-coding single-stranded RNA, involved in a variety of important biological processes^[9]. To date, it has been reported that numerous miRNAs exist in animals, plants, fungi, viruses, and other organisms, and are widely involved in the development of the body, cell proliferation and apoptosis, tumor formation, and other

Table 5 Changes in TGF-β1 ratio before and after radiotherapy in two groups of patients

Time	No or Grade 1 radiation pneumonia	Grade 2 or above 2 radiation pneumonia
Before radiotherapy		
2 weeks after radiotherapy	1.0 ± 0.2	1.1 ± 0.2
4 weeks after radiotherapy	0.9 ± 0.3	1.3 ± 0.4
6 weeks after radiotherapy	1.0 ± 0.3	1.4 ± 0.1
2 weeks end of radiotherapy	1.0 ± 0.1	1.4 ± 0.5
4 weeks end of radiotherapy	0.9 ± 0.1	1.6 ± 0.2
6 weeks end of radiotherapy	1.0 ± 0.1	1.5 ± 0.2
8 weeks end of radiotherapy	0.9 ± 0.1	1.4 ± 0.3

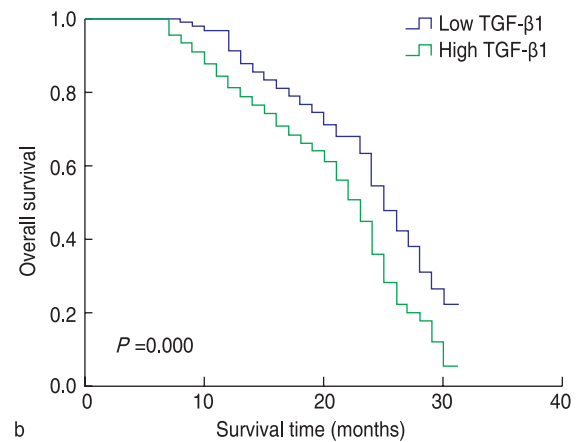
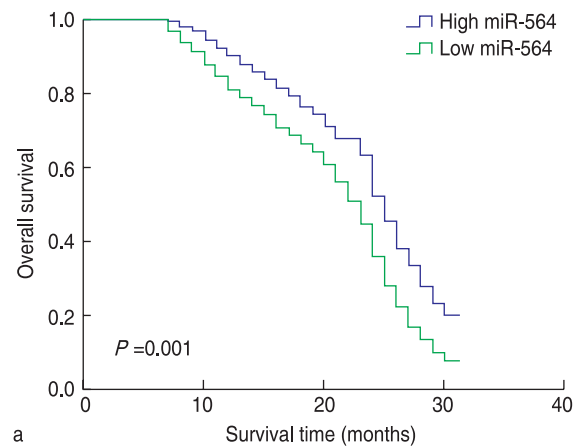


Fig. 3 (a) Relationship between the expression of miR-564 and prognosis; (b) Relationship between the expression of TGF-β1 and prognosis

physiological and pathological processes. In addition, it plays an important role in tumor angiogenesis^[10], miRNA spectra are their own characteristics in various tumors^[11]. Our previous study found that miR-564 could inhibit the proliferation, cell cycle progression, migration, and infiltration of lung adenocarcinoma A549 cells, and was

significantly higher in the paracancerous tissues of NSCLC than in the cancerous tissues. Moreover, patients with high expression of miR-564 in NSCLC have better prognosis than those with low expression; it is a negative regulatory gene in lung cancer^[7]. However, the relationship between miR-564 and radiation-induced lung injury has not been studied. We found that during radiotherapy, the serum levels of miR-564 in patients with \geq grade 2 radiation pneumonitis increased gradually with increase in dose from the 2nd week, reached the peak at the end of the 4th week after radiotherapy, and then decreased gradually; however, it was always higher than that in patients without or with grade 1 radiation pneumonitis. The serum levels of miR-564 for patients without or with grade 1 radiation pneumonitis was decreased gradually all long. Further studies showed that miR-564 ratio of patients with \geq grade 2 radiation pneumonia increased gradually after radiotherapy, reached the peak at the 4th week after radiotherapy, and then decreased gradually, while miR-564 ratio of patients without or with grade 1 radiation pneumonia decreased gradually after radiotherapy. It is suggested that patients with higher expression of miR-564 and ratio of serum miR-564 may have more severe radiation-induced lung injury, while patients with lower expression of miR-564 and ratio of serum miR-564 may have milder radiation-induced lung injury. It is suggested that the changes in miR-564 expressions miR-564 ratios are related to the occurrence of radiation-induced lung injury and provide a new idea for clinical prediction of radiation-induced lung injury. Studies have shown that miRNA affects apoptosis and autophagy by regulating TGF- β 1, suggesting that TGF- β 1 is a downstream gene of miRNA^[12]. However, whether miR-564 can also regulate TGF- β 1 is not clear; thus, we will continue to explore the relationship between the two in future studies.

TGF- β 1 is a member of TGF- β superfamily. It is a polypeptidase growth inhibitor with many biological functions. It is involved in the signal transduction pathway, inhibiting the proliferation and activity of T cells and macrophages, and regulating the expression of many kinds of target cell genes. It is an immunomodulatory factor and an apoptosis-promoting factor in embryonic growth and development, cell differentiation, and cell proliferation^[13]. TGF- β 1 is not only a predictor of radiotherapy^[14], but also an independent prognostic factor in non-small cell lung cancer^[15]. We also found that patients with high expression of TGF- β 1 in cancer tissues had poor prognosis. TGF- β 1 is not only associated with the prognosis of lung cancer, but also with radiation-induced lung injury. Stenmark *et al*^[16] found that the level of TGF- β 1 in the plasma was correlated with the degree of radiation pulmonary fibrosis, and TGF- β 1 could be used as an early predictor of radiation pulmonary fibrosis. Our study found that serum levels of TGF- β 1 in patients

with \geq grade 2 radiation pneumonia during radiotherapy increased gradually after 2 weeks of radiotherapy, reached the peak at the 4th week after radiotherapy, and then decreased gradually. However, the serum levels were higher than that of patients without or with grade 1 radiation pneumonitis. A similar trend was not observed in the serum levels of TGF- β 1 in patients without or with grade 1 radiation pneumonitis. It is suggested that monitoring the level of TGF- β 1 may help predict the occurrence of radiation-induced lung injury and the radiation dose can be adjusted appropriately.

In conclusion, our study found that miR-564 and TGF- β 1 were predictors of radiation-induced lung injury, and changes in miR-564 were observed early in radiation therapy. Therefore, monitoring their changing trends can improve the accuracy of radiation-induced lung injury prediction, and the levels and ratio of serum miR-564 in patients with radiation-induced lung injury are related to the severity of radiation-induced lung injury, which provides a new idea for clinical prediction of radiation-induced lung injury. Summarily, the factors affecting radiation-induced lung injury are complicated and need to be evaluated comprehensively to reduce the occurrence of radiation-induced lung injury and provide some guidance for clinical radiotherapy.

Conflicts of interest

The authors declare no potential conflicts of interest.

References

1. Love C, Palestro CJ. Radionuclide imaging of inflammation and infection in the acute care setting. *Semin Nucl Med*, 2013, 43: 102–113.
2. Xiong S, Pan X, Xu L, *et al*. Regulatory T cells promote β -catenin-mediated epithelium-to-mesenchyme transition during radiation-induced pulmonary fibrosis. *Int J Radiat Oncol Biol Phys*, 2015, 93: 425–435.
3. Ding NH, Li JJ, Sun LQ, *et al*. Molecular mechanisms and treatment of radiation-induced lung fibrosis. *Curr Drug Targets*, 2013, 14: 1347–1356.
4. Huang Y, Zhang W, Yu F, *et al*. The cellular and molecular mechanism of radiation-induced lung injury. *Med Sci Monit*, 2017, 23: 3446–3450.
5. Giridhar P, Mallick S, Rath GK, *et al*. Radiation induced lung injury: prediction, assessment and management. *Aaian Pac J Cancer Prev*, 2015, 16: 2613–2617.
6. Wang S, Campbell J, Stenmark MH, *et al*. Plasma levels of IL-8 and TGF- β 1 predict radiation-induced lung toxicity in non-small cell lung cancer: a validation study. *Int J Radiat Oncol Biol Phys*, 2017, 98: 615–621.
7. Yang B, Jia L, Qiaojuan Guo, *et al*. MiR-564 functions as a tumor suppressor in hum an lung cancer by targeting ZIC3. *Biochem Biophys Res Commun*, 2015, 467: 690–696.
8. Yin WB, Yu ZH, Zhen XG, *et al*. *Tumor radiotherapy*. Beijing: China Union Medical University Press. 2008. 652.
9. Bounds KR, Chiasson VL, Pan LJ, *et al*. MicroRNAs: new players in the pathobiology of preeclampsia. *Front Cardiovasc Med*, 2017,

- 4: 60.
10. Kuninty PR, Schnittert J, Storm G, *et al.* MicroRNA targeting to modulate tumor microenvironment. *Front Oncol*, 2016, 6: 3.
 11. Lu Jun, Getz Gad, Miska Eric A, *et al.* MicroRNA expression profiles classify human cancers. *Nature*, 2005, 435: 834–838.
 12. Wang J, Zhang Y, Song W, *et al.* microRNA-590-5p targets transforming growth factor β 1 to promote chondrocyte apoptosis and autophagy in response to mechanical pressure injury. *J Cell Biochem*, 2018, 119: 9931–9940.
 13. Chabicovsky M, Wastl U, Taper H, *et al.* Induction of apoptosis in mouse liver adenoma and carcinoma in vivo by transforming growth factor-beta1. *J Cancer Res Clin Oncol*, 2003, 129: 536–542.
 14. Gao F, Jia L, Han JJ, *et al.* Predictive value of serum levels of transforming growth factor beta 1 for the short-term effects of radiotherapy and chemotherapy in patients with esophageal cancer. *Oncol Transl Med*, 2018, 4: 1–5.
 15. Togashi Y, Masago K, Fujita S, *et al.* Association of the transforming growth factor β 1 promoter polymorphism, C-509T, with smoking status and survival in advanced non-small cell lung cancer. *Oncol Rep*, 2011, 25: 377–382.
 16. Stenmark MH, Cai XW, Shedden K, *et al.* Combining physical and biologic parameters to predict radiation-induced lung toxicity in patients with non-small-cell lung cancer treated with definitive radiation therapy. *Int J Radiat Oncol Biol Phys*, 2012, 84: e217–222.

DOI 10.1007/s10330-018-0311-1

Cite this article as: Ge YZ, Xie T, Yang B, *et al.* Correlation between miR-564, TGF- β 1, and radiation-induced lung injury. *Oncol Transl Med*, 2019, 5: 204–210.

Clinical significance of S100A7 protein in predicting recurrence of breast cancer in patients undergoing breast-conserving surgery with radiotherapy*

Chao Zhang¹, Changyou Li², Gaoyang Lin³, Yao Qi⁴, Zhenfeng Li⁵, Jing Xu⁴, Tianhui Su⁵, Xin Liu⁵, Xiao Zou⁵ (✉)

¹ Department of Medicine, Qingdao University, Qingdao 266003, China

² Biotherapy Center, The Second Affiliated Hospital of Qingdao University, Qingdao 266003, China

³ Department of Thoracic Surgery, The Affiliated Qingdao Hiser Medical Center of Qingdao University, Qingdao 266003, China

⁴ Department of Pathology, The Second Affiliated Hospital of Qingdao University, Qingdao 266003, China

⁵ Department of Breast Surgery, The Second Affiliated Hospital of Qingdao University, Qingdao 266003, China

Abstract

Objective To investigate the relationship between the expression of S100A7 protein and prediction of recurrence and prognosis of breast cancer in patients undergoing breast-conserving surgery combined with radiotherapy.

Methods 349 samples of carcinoma tissue wax blocks were selected from January 2011 to January 2014 in Qingdao Central Hospital. All the patients had undergone breast-conserving surgery. We analyzed S100A7 expression in tumor tissue by immunohistochemical staining. Using univariate and multivariate analyses, we evaluated the relationship between S100A7 and clinical results, to explore independent risk factors for local regional recurrence (LRR).

Results The positive expression of S100A7 in the recurrence group (66.7%) was significantly higher than in the non-recurrence group (38.4%), $P = 0.025$. A log-rank test showed that high S100A7 expression was significantly correlated with 5-year regional recurrence free survival rate (RFS) (94.9% vs 89.5%, $P = 0.0408$), distant metastasis free survival rate (DFS) (95.4% vs 83.5%, $P < 0.001$), and overall survival rate (OS) (99.0% vs 92.5%, $P = 0.0011$). Histological grade, vessel carcinoma embolus, lymph node metastasis, S100A7 expression, and tumor size were factors that influenced RFS. Multivariate analysis of the Cox proportional hazard model showed that high S100A7 expression was an independent risk factor that affected breast cancer RFS (HR = 6.864, 95 % CI: 1.575 - 29.915, $P = 0.01$). Thus, we concluded that high S100A7 expression is associated with increased risk of LRR and distant metastasis of breast cancer after breast-conserving surgery and postoperative radiotherapy. S100A7 can be used as a molecular marker to screen for patients with high recurrence risk after breast-conserving surgery.

Key words: S100A7, breast-conserving surgery, radiotherapy, locoregional recurrence, prognosis

Received: 13 August 2019

Revised: 29 September 2019

Accepted: 18 October 2019

The high incidence of breast cancer and the associated high death rates are major health problems globally. In 2018, an American Cancer Society study involving data from 185 countries and 36 types of cancer, showed that one of every 4 female patients with cancer had breast cancer, which was the first in both incidence and death

rate of female malignant tumors [1]. At present, the diversity of breast cancer treatment methods and the application of new technologies have made the breast-conserving surgery more popular, which can not only guarantee good therapeutic effect, but also does not reduce the quality of life. Breast-conserving surgery combined

✉ Correspondence to: Xiao Zou. Email: 18372704337@163.com

* Supported by a grant from The Medical Foundation of Wu Jieping (No.320.6750.16229).

© 2019 Huazhong University of Science and Technology

with radiotherapy has gradually become the standard treatment for patients with early stage breast cancer, and can significantly reduce the risk of local recurrence and distant metastasis^[2]. A study from the Chinese Academy of Medical Sciences also confirmed the above view. On the basis of standard treatment, breast-conserving surgery combined with postoperative radiotherapy can reduce the local regional recurrence rate by approximately 10 percent in 5 years^[3]. However, recurrence is an important cause of tumor advancement, metastasis, and treatment failure. Multiple studies have shown that local regional recurrence leads to poorer disease-free and overall survival^[4,5]. Therefore, to improve the therapeutic effect and reduce recurrence and metastasis rate, is a major research challenge in the field of breast cancer.

S100 proteins are a family of small acidic calcium ion-binding proteins and their abnormal expression is involved in the development of many tumors. At present, there are at least 20 known S100 protein family members in humans, and are abnormally expressed in many kinds of cancers, such as breast cancer, gastric cancer, skin cancer, and cervical cancer^[6]. S100A7 (S100 calcium-binding protein A7) was first implicated in psoriasis and it plays an important role in regulating various cellular functions such as calcium homeostasis, cell proliferation, differentiation, apoptosis, and cell invasion^[7]. S100A7 is believed to enhance the growth and invasiveness of breast cancer cells and plays an important role in the progression of breast cancer^[8]. The mechanism may be that the immunoglobulin transmembrane receptor family, also known as late glycation end product receptor (RAGE), acts like a cytokine^[9]. Many studies have confirmed that high S100A7 expression is closely related to a number of clinicopathological indicators, with differences in the expression of S100A7 in some special types of breast cancer, suggesting that it is a potential molecular marker for predicting the prognosis of recurrence and metastasis of different types of breast cancer^[10-11]. Tumor recurrence and metastasis are complex processes and involve many factors; specific mechanisms remain to be clarified. At present, there are only few studies on the relationship between S100A7 and breast cancer recurrence, and on the relationship between S100A7 and the reactivity of postoperative radiotherapy for breast cancer. This study retrospectively investigated the relationship between S100A7 expression levels after breast-conserving surgery and its relationship with radiotherapy reactivity, to find new molecular markers that can effectively predict breast cancer recurrence after breast-conserving surgery and thus, help to formulate rational treatment plans and improve patient prognosis.

Material and methods

Inclusion and exclusion criteria

The inclusion criteria for this study were: (1) Negative pathological cutting margin and invasive carcinoma after breast-conserving surgery, (2) Radiotherapy, neoadjuvant chemotherapy, and endocrine therapy were not performed before the surgery, (3) Availability of complete clinical data and pathological results, and (4) Standardized whole-breast radiotherapy performed postoperatively. Exclusion criteria were: (1) Non-primary breast cancer patients, (2) Bilateral cases, (3) Inflammatory breast cancer, (4) Patients with stage IV breast cancer with distant metastasis before surgery, (5) Patients with serious life-threatening diseases or other malignant tumors, and (6) Patients with incomplete medical records.

Radiotherapy regime and tumor classification

The samples were collected from January 2011 to January 2014 at The Second Affiliated Hospital of Qingdao University, China from 349 patients after breast-conserving surgery and preserved as wax blocks. After the surgery, the patients received standard whole-breast radiation treatment, and the average postoperative adjuvant radiotherapy dose for the whole breast and regional lymph nodes on the affected side was 50 Gy/25 times/5 weeks. During the study period, adjuvant systemic chemotherapy, endocrine therapy, and targeted therapy were also implemented according to the guidelines. All patients were female; the age of onset was determined by the time of definite diagnosis, and the tumor size was determined by the maximum diameter of tumor in the pathological report, referring to the TNM staging criteria published in the 8th edition by the AJCC^[12]. Histological grading was performed using the modified Scarff-Bloom-Richardson grading method, with grades 1–3. According to the expression of estrogen receptor ER, Progesterone receptor PR, human epidermal growth factor receptor-2 HER2, and proliferating cell related nuclear antigen (Ki67), the breast cancer was classified into the following types: Luminal A, Luminal B1, LuminalB2, and overexpression of HER2, TNBC type^[13].

Clinical outcomes after surgery and radiotherapy

The information on postoperative survival, recurrence and metastasis for all the patients was mainly obtained by consulting the information of hospitalization, case follow-up system, outpatient and imaging system examination, as well as regular emails and telephone calls, to understand and record the prognosis and survival information of patients. The local recurrence free survival (RFS), distant metastasis free survival (DFS) and overall survival (OS) were recorded after the surgery till the final follow-up or

the time of death.

Immunohistochemical staining

The sections (thickness 4 μm) were soaked with fresh xylene, dewaxed and hydrated with ethanol of different concentration gradients, and thoroughly rinsed with PBS. The well-matched EDTA antigen repair solution (Beijing Zhongshan Jinqiao Biotechnology Co. Ltd., China) was heated to boiling to fully expose the epitope (95 $^{\circ}\text{C}$, 6 min), cooled to room temperature, and then rinsed with PBS. The enzyme was removed by endogenous peroxidase inhibitors, incubated at room temperature for 10 min, and washed with PBS. Goat serum was used to avoid non-specific staining, incubated at room temperature for 15 min, and poured into the serum without washing. Primary antibody against S100A7 was added (dilution 1:200, Santa Cruz Biotechnology Co., Ltd., USA), and the antibody was replaced with PBS buffer in the negative control group, incubated at a constant temperature for 60 min (37 $^{\circ}\text{C}$), and fully washed with PBS. Goat anti-mouse/rabbit IgG (Beijing Zhongshan Jinqiao Biotechnology Co., Ltd., China) was added and incubated at room temperature for 15 min and rinsed completely with PBS. Horseradish-labeled streptomycin was added, incubated at room temperature for 15 min, and fully washed with PBS. Then the samples were incubated in 3,3'-diaminobenzidine tetrahydrochloride hydrate (DAB) (Beijing Solaibao co., Ltd., China) 5 min, and were re-dyed with hematoxylin. The film was sealed and observed under microscope.

Immunohistochemical results

Results were interpreted by two senior physicians from the Department of Pathology. Immunohistochemical results were analyzed and scored blindly. In case of controversy, multiple-head optical microscopy was used to observe and re-evaluate the results. Each slice was randomly evaluated by 10 high power microscopic field of view (400 \times). The S100A7 was mainly expressed in the nucleus or the cytoplasm^[14]. Immunohistochemical evaluation criteria used were based on a previous study^[15]. Positive expression of S100A7 was defined as expression

in more than 10% of stained cancer cells. ER was positive when there was more than 1% of the stained cells^[16]. Setting up Ki67 high expression group with (> 20%)^[17], HER2 immunohistochemistry was defined as 3+ positive, but further FISH test was needed for 2+ patients^[18].

Statistical analysis

SPSS 23.0 software was used for statistical analysis. Kaplan-Meier survival curve was drawn. Log-Rank method was used to compare the survival rates between two groups. Multivariate COX regression model was used to analyze the independent risk factors of recurrence. The risk ratio was calculated using HR and 95% confidence interval CI. The statistical significance was defined as $P < 0.05$.

Results

S100A7 staining results

The positive staining of S100A7 was mainly in the nucleus or cytoplasm, Under the microscope, it is brown or light yellow. The representative S100A7 immunostaining results are shown in Fig. 1.

Descriptive statistics

The median age of the patients in this study was 49 years old (ranged, 27–89 years), 117 patients (33.5%) were younger than 45 years old at the time of diagnosis, and 137 patients (39.3%) had postoperative pathological lymph node metastasis (lymph node ≥ 1). Seventy-three cases (20.9%) were luminal A type, 115 cases (33.0%) were luminal B1 type, 67 cases (19.2%) were luminal B2 type, 41 cases (11.7%) were overexpression of HER2, 39 cases (11.2%) were triple negative, and 14 cases were indeterminate type. Up to January 2019, the follow-up time was 27–93 months (median: 73 months), and the follow-up rate was 5.7% ($n = 20$).

S100A7 expression

Of the 349 samples, 141 samples showed positive S100A7 expression. S100A7 expression was found to be

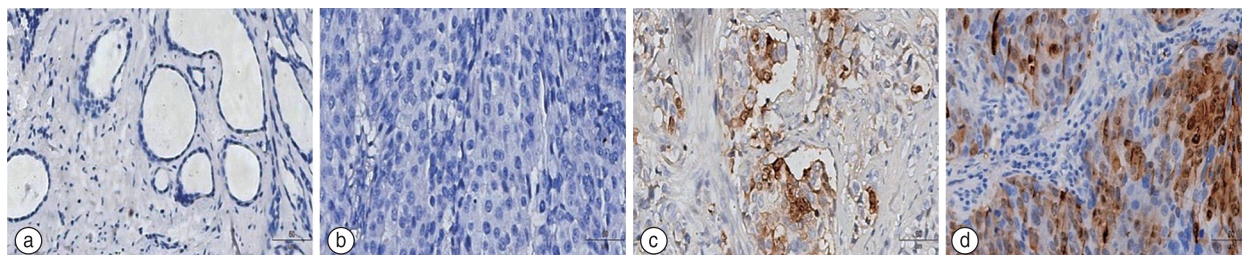


Fig. 1 Expression of S100A7 in breast cancer tissue (SP $\times 400$). (a) Negative expression in normal breast tissue; (b) Negative expression in breast cancer tissue; (c) Positive (predominantly cytoplasmic) expression in breast cancer tissue; (d) Positive (predominantly nuclear) expression in breast cancer tissue

closely correlated with tumor size, histological grade, axillary lymph node metastasis status, ER status, PR status, and breast cancer molecular classification, recurrence status, postoperative distant metastasis, survival status ($P < 0.05$), but had no significant correlation with other clinical data ($P > 0.05$) (Table 1).

Correlation between S100A7 and local regional recurrence and distant metastasis

The Log-rank 5-year survival analysis of the 329 patients showed that the expression of S100A7 protein was significantly correlated with the clinical outcomes of RFS (94.9% vs. 89.5% $P = 0.0408$), DFS (95.4% vs. 83.5% $P < 0.001$) and OS (99.0% vs. 92.5% $P = 0.0011$), as shown in Table 2. Kaplan-Meier survival curves are shown in Fig. 2.

Comparison of clinical characteristics between postoperative recurrence and

non-recurrence patients

Twenty patients could not be followed up. Of the remaining 329 patients, 24 (6.9%) had local regional recurrence, 31 (8.9%) had distant metastasis, and 12 (3.4%) died of breast cancer-related complications and secondary malignant tumors. The Log-rank test suggested that histological grade, intravascular thrombotic tumor, lymph node metastasis, S100A7 expression and tumor size were the factors influencing RFS ($P < 0.05$). COX analysis results showed that S100A7 expression (HR = 6.864, 95% CI: 1.575–29.915, $P = 0.01$), vessel carcinoma embolus (HR = 4.921, 95% CI: 1.072–22.599, $P = 0.04$), age (HR = 0.091, 95% CI: 0.015–0.556, $P = 0.009$), and molecular subtypes of cancer (HR = 0.615, 95% CI: 0.391–0.967 $P = 0.035$) are independent factors affecting local regional recurrence ($P < 0.05$) (Table 3).

Discussion

Breast cancer is the most common malignant tumor among women under 40 years [19]. Several studies have

Table 1 Correlation between clinical pathology features and S100A7 expression in 349 cases of Breast Cancer [n (%)]

Clinical pathology feature	n (%)	Expression of S100A7		P value	Clinical pathology feature	n (%)	Expression of S100A7		P value
		Negative	Positive				Negative	Positive	
Total	349	208	141		ER Status				0.002 ^a
Age (years)				0.528	Negative	84 (24.1)	38	46	
< 45	117 (33.5)	67	50		Positive	265 (75.9)	170	95	
≥ 45	232 (66.5)	139	93		PR Status				0.002 ^a
Menopausal				0.941	Negative	84 (24.1)	38	46	
Yes	184 (52.7)	110	74		Positive	265 (75.9)	170	95	
No	165 (47.3)	98	67		HER2 status				0.422
Tumor size (cm)				0.005 ^a	Negative	226 (64.8)	137	89	
≤ 2	207 (59.3)	136	71		Positive	109 (31.2)	65	44	
> 2	142 (40.7)	72	70		Unknown	14 (4.0)	6	8	
Location				0.316	Ki67 expression				0.102
Left	192 (55.0)	119	73		Low	142 (40.7)	92	50	
Right	157 (45.0)	89	68		High	207 (59.3)	116	91	
Histological grade				< 0.001 ^a	Pathologic types				0.069
I/II	255 (73.1)	168	87		Invasive ductal carcinoma	310 (88.8)	190	120	
III	94 (26.9)	40	54		The other types	39 (11.2)	18	21	
Vessel carcinoma embolus				0.001 ^a	Local recurrence				0.025 ^a
Negative	284 (81.4)	181	103		No	305 (87.4)	188	117	
Positive	65 (18.6)	27	38		Yes	24 (6.9)	8	16	
Lymph node metastasis				< 0.001 ^a	Lost to follow-up	20 (5.7)	12	8	
Negative	212 (60.7)	148	64		Postoperative distant metastasis				< 0.001 ^a
Positive	137 (39.3)	60	77		No	298 (85.4)	188	110	
Molecular Subtype				0.012 ^a	Yes	31 (8.9)	8	23	
Luminal A	73 (20.9)	47	26		Lost to follow-up	20 (5.7)	12	8	
Luminal B1	115 (33.0)	75	40		Survival status				0.001 ^a
Luminal B2	67 (19.2)	44	23		Alive	317 (90.8)	193	124	
HER2-overexpressed					Deceased	12 (3.4)	1	11	
TNBC	39 (11.2)	22	19		Lost to follow-up	20 (5.7)	12	8	
Unclassified	14 (4.0)	6	8						

^a $P < 0.05$

Table 2 Relationship between S100A7 expression and 5-year clinical outcome

Clinical outcome	S100A7 Expression (%)		P-Value
	Negative	Positive	
Local recurrence-free survival	94.9	89.5	0.0408
Distant metastasis-free survival	95.4	83.5	0.0001
Overall survival	99	92.5	0.0011

found that young female patients may have more aggressive tumor molecular characteristics and higher risk of distant and local recurrence than older patients^[19–20]. Breast-conserving surgery has the distinct advantages of less trauma, fewer complications, with less impact on women’s mental health. Breast-conserving surgery is now the first choice for young patients with early stage breast cancer. There is no statistical difference in the 5-year follow-up between adjuvant whole breast radiotherapy after breast-conserving surgery and modified radical mastectomy^[21]. Although breast-conserving surgery and postoperative radiotherapy are the recommended treatment methods for early breast cancer, there is still a high risk of recurrence. The effectiveness of radiotherapy is affected by the inherent biological resistance of the tumor as well as chemotherapy and endocrine therapy, so the recurrence of the tumor cannot be ignored. Studies have shown that some patients fail to benefit from radiotherapy after breast-conserving surgery due to the inherent radiation resistance of the tumor^[22]. It is probable that the radiotherapy causes DNA damage repair dysfunction of tumor cells from the ionizing radiation, and some signal transduction pathways affect the expression of one or more genes and proteins, leading to radiotherapy resistance, tumor recurrence, and metastasis. Recurrence is a well-known independent prognostic factor that affects breast cancer mortality^[23]. The presence of local recurrence causes patients to undergo reoperation, which increases the risk of distant metastasis even after

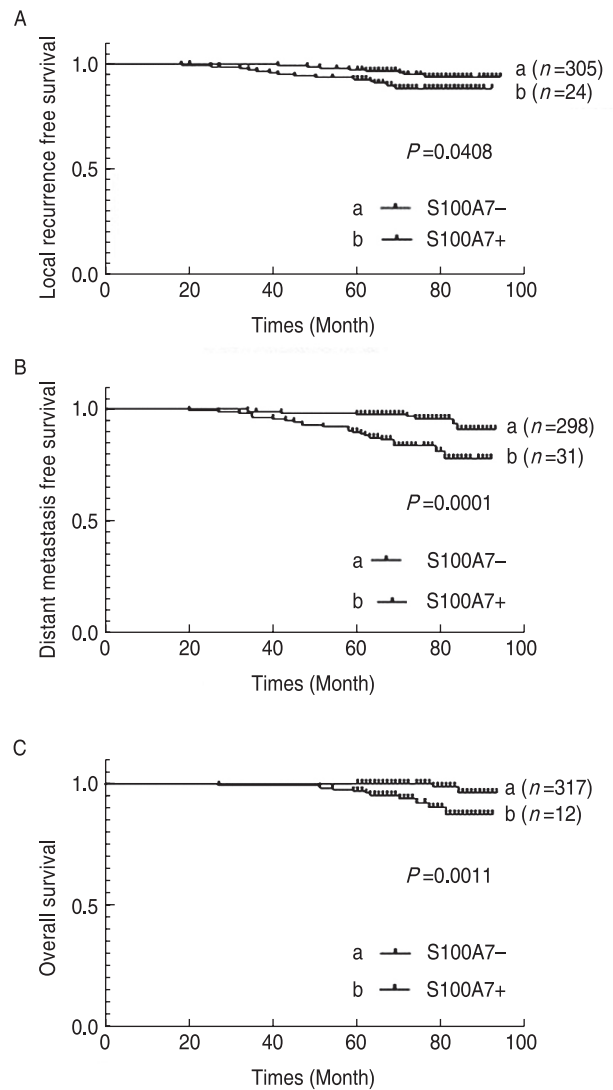


Fig. 2 Kaplan-Meier Survival Curves were drawn according to the expression of S100A7

Table 3 Factors influencing the recurrence free survival rate of Breast Cancer after breast-conserving surgery and postoperative radiotherapy were analyzed by single factor and multi-factor tests

Variable	S100A7 Expression (%)		Multivariate	
	P value	Relative risk (95% CI)	P value	Relative risk (95% CI)
Histological grade	0.0045 ^a	3.008 (1.193–7.582)	0.12	2.440 (0.794–7.499)
Vessel carcinoma embolus	0.012 ^a	2.754 (0.9695–7.821)	0.04 ^a	4.921 (1.072–22.599)
Lymph node metastasis	0.0043 ^a	3.123 (1.348–7.232)	0.099	0.368 (0.112–1.209)
S100A7 Expression	0.0408 ^a	2.276 (0.9985–5.188)	0.01 ^a	6.864 (1.575–29.915)
Tumor size	0.0053 ^a	3.137 (1.381–7.125)	0.139	0.389 (0.112–1.358)
HER2 status	0.0755		0.416	0.656 (0.237–1.812)
Age	0.669	1.211 (0.5181–2.831)	0.009 ^a	0.091 (0.015–0.556)
Molecular subtype	0.125		0.035 ^a	0.615 (0.391–0.967)
Ki67 expression	0.5612	1.285 (0.5661–2.917)	0.199	2.391 (0.632–9.048)

Univariate analysis was conducted by log-rank test, and multivariate statistical analysis was conducted by proportional hazard model (Cox). ^aP value < 0.05 was considered statistically significant; 95% CI, 95% confidence interval

the second operation, leading to poor prognosis for the patients. Therefore, it is of great significance to screen high-risk breast cancer recurrence patients for various molecular markers through comprehensive assessment of risk factors to improve the treatment plan, the treatment effect, and the prognosis.

Many clinical studies have confirmed many influencing factors for local regional recurrence after breast-conserving surgery, including, lymph node metastasis, tumor stage, histological grade, and ER state^[24-25]. In this study, the 5-year follow-up of 349 patients with breast conserving surgery and postoperative radiotherapy showed significant statistical differences between the relapsed group and the non-relapsed group in the indicators of histological grade, intravascular thrombotic tumor, lymph node metastasis, S100A7 expression, and tumor size. Multivariate COX regression model analysis showed that the age, the histological grade, and the abnormal expression of S100A7 were independent risk factors for postoperative local recurrence of breast cancer. The results of large sample size studies showed that the risk of local regional recurrence was also high after adjuvant radiotherapy after modified radical surgery, suggesting that operative method is not an absolute factor affecting postoperative recurrence, and comprehensive treatment of various schemes is crucial, among which radiotherapy resistance is one of the urgent problems to be solved.

In recent years, research has focused on S100A7 expression in different classification and its association with other proteins, genes, and the influence on distant metastasis and prognosis, more focused on the study of breast cancer recurrence in patients with breast cancer, modified radical is still much research directly confirmed S100A7 with breast cancer confirmed breast surgery acceptance criteria recurrence after radiotherapy, the relationship between the radiation sensitivity and the prognosis. There have been few studies on the mechanisms of S100A7 expression, breast cancer recurrence, and radiation sensitivity relationship. A Japanese study results showed that adipose stromal cells can produce paracrine cytokine by raising S100A7 expression in breast cancer cells to promote the growth of cancer cells and thus, affect the recurrence and metastasis. Kaplan-Meier survival analysis and multivariate analysis showed that S100A7 could be used as an independent risk factor for predicting recurrence of invasive breast cancer^[26]. However, this study did not further analyze the recurrence rate and risk factors of breast-conserving surgery. Further research has shown that the^[27] members of the family S100A, coded by Chromosome 1 q21.3, mainly S100A7, S100A8, S100A9 and IL-1 receptor kinase 1 (IRAK1) make a feedback loop that drives the ball tumor growth and since this feedback loop is an important part of a breast cancer recurrence, it can be used as biomarker for recurrence and can also

serve as a therapeutic target. At present, most research on the S100 protein family has focused on studying S100A4. In terms of radiotherapy sensitivity, some studies have confirmed that the up-regulation of S100A4 in breast cancer cells may increase the interaction with mutated p53 gene and enhance the resistance to radiation^[28]. As a member of S100A family, other members may share the same regulatory mechanism. The correlation between S100A2 and S100A7 and breast cancer recurrence and radiotherapy sensitivity warrants further research.

To conclude, in this study, the expression and prognosis analysis of S100A7 protein in the recurrence group after breast-conserving surgery and radiotherapy were preliminarily discussed. However, the relatively small sample size was a limitation, and thus, the use of S100A7 as a molecular marker for breast cancer recurrence needs to be verified by a larger sample size study and in vitro cell experiments, to provide stronger theoretical basis for the follow-up study on molecular mechanisms and signaling pathways.

Conflicts of interest

The authors indicated no potential conflicts of interest.

References

1. Bray F, Ferlay J, Soerjomataram I, *et al.* Global cancer statistics 2018: GLOBOCAN estimates of incidence and mortality worldwide for 36 cancers in 185 countries. *CA Cancer J Clin*, 2018, 68: 394–424.
2. Early Breast Cancer Trialists' Collaborative Group (EBCTCG), Darby S, McGale P, *et al.* Effect of radiotherapy after breast-conserving surgery on 10-year recurrence and 15-year breast cancer death: meta-analysis of individual patient data for 10,801 women in 17 randomised trials. *Lancet*, 2011, 378 (9804): 1707–1716.
3. Chen SY, Tang Y, Song YW, *et al.* Prognosis and risk factors of 1791 patients with breast cancer treated with breast-conserving surgery based on real-world data. *Chin J Oncol (Chinese)*, 2018, 40: 619–625.
4. Bollet MA, Sigal-Zafrani B, Mazeau V, *et al.* Age remains the first prognostic factor for loco-regional breast cancer recurrence in young (< 40 years) women treated with breast conserving surgery first. *Radiother Oncol*, 2007, 82: 272–280.
5. Wang X, Ma J, Mei X, *et al.* Outcomes following salvage radiation and systemic therapy for isolated locoregional recurrence of breast cancer after mastectomy: impact of constructed biologic subtype. *J Oncol*, 2018, 2018: 4736263.
6. Jia J, Duan Q, Guo J, *et al.* Psoriasis, a multifunctional player in different diseases. *Curr Protein Pept Sci*, 2014, 15: 836–842.
7. Madsen P, Rasmussen HH, Leffers H, *et al.* Molecular cloning, occurrence, and expression of a novel partially secreted protein "psoriasis" that is highly up-regulated in psoriatic skin. *J Invest Dermatol*, 1991, 97: 701–712.
8. Emberley ED, Murphy LC, Watson PH. S100A7 and the progression of breast cancer. *Breast Cancer Res*, 2004, 6: 153–159.
9. Nasser MW, Wani NA, Ahirwar DK, *et al.* RAGE mediates S100A7-induced breast cancer growth and metastasis by modulating the tumor microenvironment. *Cancer Res*, 2015, 75: 974–985.

10. Li J. Expression of S100A7, Cripto-1 and CD34 in basal cell-like breast cancer and their clinical significance. Chengde: Chengde Medical College. 2014.
11. Mayama A, Takagi K, Suzuki H, *et al.* OLFM4, LY6D and S100A7 as potent markers for distant metastasis in estrogen receptor-positive breast carcinoma. *Cancer Sci*, 2018, 109: 3350–3359.
12. Giuliano AE, Edge SB, Hortobagyi GN. Eighth Edition of the AJCC Cancer Staging Manual: Breast Cancer. *Ann Surg Oncol*, 2018, 25: 1783–1785.
13. Pata G, Guaineri A, Bianchi A, *et al.* Long-term outcomes of immunohistochemically defined subtypes of breast cancer less than or equal to 2 cm after breast-conserving surgery. *J Surg Res*, 2019, 236: 288–299.
14. Cancemi P, Di Cara G, Albanese NN, *et al.* Differential occurrence of S100A7 in breast cancer tissues: A proteomic-based investigation. *Proteomics Clin Appl*, 2012, 6: 364–373.
15. Mayama A, Takagi K, Suzuki H, *et al.* OLFM4, LY6D and S100A7 as potent markers for distant metastasis in estrogen receptor-positive breast carcinoma. *Cancer Sci*, 2018, 109: 3350–3359.
16. Hammond ME, Hayes DF, Dowsett M, *et al.* American Society of Clinical Oncology/College of American Pathologists guideline recommendations for immunohistochemical testing of estrogen and progesterone receptors in breast cancer (unabridged version). *Arch Pathol Lab Med*, 2010, 134: e48–72.
17. Maisonneuve P, Disalvatore D, Rotmensz N, *et al.* Proposed new clinicopathological surrogate definitions of luminal A and luminal B (HER2-negative) intrinsic breast cancer subtypes. *Breast Cancer Res*, 2014, 16: R65.
18. Lin L, Sirohi D, Coleman JF, *et al.* American Society of Clinical Oncology/College of American Pathologists 2018 Focused Update of Breast Cancer HER2 FISH Testing Guidelines Results From a National Reference Laboratory. *Am J Clin Pathol*, 2019, 152: 479–485.
19. Lambertini M, Pinto AC, Ameje L, *et al.* The prognostic performance of Adjuvant! Online and Nottingham Prognostic Index in young breast cancer patients. *Br J Cancer*, 2016, 115: 1471–1478.
20. Aalders KC, Postma EL, Strobbe LJ, *et al.* Contemporary locoregional recurrence rates in young patients with early-stage breast cancer. *J Clin Oncol*, 2016, 34: 2107–2114.
21. Fisher B, Bauer M, Margolese R, *et al.* Five-year results of a randomized clinical trial comparing total mastectomy and segmental mastectomy with or without radiation in the treatment of breast cancer. *N Engl J Med*, 1985, 312: 665–673.
22. Loganadane G, Xi Z, Xu HP, *et al.* Patterns of loco regional failure in women with breast cancer treated by Postmastectomy Conformal Electron Beam Radiation Therapy (PMERT): Large scale single center experience. *Clini Transl Radiat Oncol*, 2017, 4: 46–50.
23. Lê MG, Arriagada R, Spielmann M, *et al.* Prognostic factors for death after an isolated local recurrence in patients with early-stage breast carcinoma. *Cancer*, 2002, 94: 2813–2820.
24. Chung SR, Choi WJ, Cha JH, *et al.* Prognostic factors predicting recurrence in invasive breast cancer: An analysis of radiological and clinicopathological factors. *Asian J Surg*, 2019, 42: 613–620.
25. Song WJ, Kim KI, Park SH, *et al.* The risk factors influencing between the early and late recurrence in systemic recurrent breast cancer. *J Breast Cancer*, 2012, 15: 218–223.
26. Sakurai M, Miki Y, Takagi K, *et al.* Interaction with adipocyte stromal cells induces breast cancer malignancy via S100A7 upregulation in breast cancer microenvironment. *Breast Cancer Res*, 2017, 19: 70.
27. Goh JY, Feng M, Wang W, *et al.* Chromosome 1q21.3 amplification is a trackable biomarker and actionable target for breast cancer recurrence. *Nature Med*, 2017, 23: 1319–1330.
28. Hatoum D, Yagoub D, Ahadi A, *et al.* Annexin/S100A protein family regulation through p14ARF-p53 activation: a role in cell survival and predicting treatment outcomes in breast cancer. *PLoS One*, 2017, 12: e0169925.

DOI 10.1007/s10330-019-0373-3

Cite this article as: Zhang C, Li CY, Lin GY, *et al.* Clinical significance of S100A7 protein in predicting recurrence of breast cancer in patients undergoing breast-conserving surgery with radiotherapy. *Oncol Transl Med*, 2019, 5: 211–217.

Application of pegylated recombinant human granulocyte colony-stimulating factor (PEG-rhG-CSF) for the prevention of neutropenia in triple negative breast cancer patients older than 65 years during adjuvant chemotherapy

Shuxian Qu¹, Jianing Qiu¹, Yidan Zhang², Yongming Liu¹, Zhendong Zheng¹ (✉)

¹ Department of Oncology, The General Hospital of the Northern Theater of the Chinese people's Liberation Army, Shenyang 110000, China

² Department of Oncology of traditional Chinese and Western Medicine, Northeast international hospital, Shenyang 110000, China

Abstract

Objective The aim of this study was to compare the efficacy and safety of pegylated recombinant human granulocyte colony-stimulating factor (PEG-rhG-CSF) and recombinant human granulocyte colony-stimulating factor (rhG-CSF) for the prevention of neutropenia in elderly breast cancer patients during adjuvant chemotherapy.

Methods A total of 45 oncology inpatients with breast cancer, who received adjuvant chemotherapy and were older than 65 years from May 2017 to October 2018 in the General Hospital of the Northern Theater of the Chinese people's Liberation Army, were included. Epirubicin Cyclophosphamide-Docetaxel (EC-T) sequential adjuvant chemotherapy was chosen. Forty-five patients were randomly divided into two groups; 25 patients in the treatment group were treated with PEG-rhG-CSF and 20 patients in the control group were not treated with PEG-rhG-CSF, but only rhG-CSF. The experimental group was treated with the PEG-rhG-CSF at the end of chemotherapy for 24–48 h, with a 6 mg subcutaneous injection once per chemotherapy cycle. In the control group, rhG-CSF was administered after 48 h of chemotherapy, with a 100 µg subcutaneous injection, 1/d, d 1–7. The dosage could be increased step by step with the exacerbation of neutropenia. The primary aims of this study was to discover the incidence of leukopenia, neutropenia, neutrophilic fever, and adverse reactions in the two groups.

Results The incidence of neutropenia, neutrophilic fever and adverse reactions decreased in the treatment group compared to the control group, but no significant difference existed between two groups ($P > 0.05$). Patients in treatment group had a lower, but not statistically significant, incidence of adverse reactions ($P > 0.05$).

Conclusion Applying PEG-rhG-CSF could be effective in preventing neutropenia in elderly patients with postoperative adjuvant chemotherapy to treat breast cancer. It may effectively control the occurrence of neutropenia after chemotherapy and reduce the chance of infection. The incidence of side effects, such as fever and bone pain, was low. The adverse drug reactions were well tolerated by patients, which could ensure the smooth progress of chemotherapy.

Key words: elderly; breast cancer; neutropenia; pegylated recombinant human granulocyte colony-stimulating factor

Received: 29 May 2019

Revised: 15 June 2019

Accepted: 27 June 2019

Breast cancer is the most common malignant tumor in women and the leading cause of malignant tumors in women worldwide, which seriously threatens a woman's health. Chemotherapy is an important systemic adjuvant therapy and plays a role in the overall treatment of breast cancer. While improving overall survival and disease-free survival, chemotherapy drugs can also cause a series of adverse reactions. Neutropenia is considered the most severe hematological toxicity caused by chemotherapy and is the most common dose-limiting toxicity^[1]. Elderly women with triple-negative breast cancers, having a poor prognosis and high risk of recurrence, are faced with high-intensity and multi-cycle postoperative chemotherapy. This will cause their bone marrow reserve and hematopoietic function to decline, with increasing occurrence of chronic underlying diseases such as hypertension and coronary heart disease. There will be a significant increase in the risk of severe neutropenia and infection after chemotherapy, and an increase in the risk of death due to discontinuation of chemotherapy. Therefore, prevention of neutropenia is important to the smooth progress of chemotherapy. The use of recombinant human granulocyte colony-stimulating factor (rhG-CSF) is a significant milestone for chemotherapy of malignant tumors^[2]. It can stimulate the release of bone marrow to the peripheral blood, reduce the incidence of infection caused by the inhibition of hematopoiesis of bone marrow after chemotherapy, and ensure the completion of chemotherapy. Therefore, rhG-CSF is an effective drug for the prevention of neutropenia in tumor patients receiving chemotherapy and radiotherapy^[3-4]. RhG-CSF has been widely used in clinical practice^[5]. However, because plasma half-life is short, which leads to consecutive days in one chemotherapy period, rhG-CSF use causes inconvenience and suffering to patients^[5-6]. Pegylated recombinant human granulocyte colony-stimulating factor (PEG-rhG-CSF) is a long-acting rhG-CSF which acts on hemopoietic stem cells, stimulates the proliferation and differentiation of mononuclear granulocyte progenitor cells after binding to cell-specific surface receptors, and plays a role in simultaneously activating terminal cells. Additionally, its half-life is long and convenient for use, which increases the clinical application for the chemoprevention of neutropenia^[7]. This study was aimed at the prevention of neutropenia in elderly patients with breast cancer who needed intensive chemotherapy. Among them, 25 patients treated with PEG-rhG-CSF exhibited positive effects and safety in preventing neutropenia.

Materials and methods

Patients

A total of 45 breast cancer patients, all female, aged 65–77 years (67.8 ± 5.3 years), who were hospitalized in the

Department of Oncology of our hospital and underwent 4 cycles of CE followed by 4 cycles of T chemotherapy after breast cancer surgery, were used in this study.

Breast cancer was diagnosed by pathology. There were 36 cases of invasive ductal carcinoma, 6 cases of invasive lobular carcinoma, 2 cases of sarcomatoid carcinoma, and 2 cases of medullary carcinoma. All 45 cases underwent a modified radical mastectomy. Prior to chemotherapy, blood routine examination, liver and kidney function, myocardial enzyme spectrum, and electrocardiogram examination showed no obvious abnormality.

All patients had no history of severe cardiopulmonary disease, and no history of radiation or chemotherapy. After surgery, all patients were treated with CE then D regimen for adjuvant chemotherapy.

The 45 patients were divided into a treatment group (25 cases) and control group (20 cases). There was no statistical significance in age, course of disease, surgical method, chemotherapy, and disease condition between the two groups (all $P > 0.05$). Prior to chemotherapy, informed consent was obtained from every patient.

Treatment methods

The 45 patients underwent breast cancer surgery, 4 cycles CE, and 4 cycles of D chemotherapy (specifics: Epirubicin 70 mg/m^2 dL in combination with IV (intravenous) Cyclophosphamide 600 mg/m^2 IV dL 21 days/ cycle, for a total of four cycles; followed by Docetaxel 75 mg/m^2 IV dL 21 days/ cycle, for a total of four cycles). Patients were then divided into two groups according to the envelope method: treatment group (25 cases) and control group (20 cases).

Before chemotherapy, both groups were given 5 mg of IV Dexamethasone, 1 time/dL.

Before chemotherapy, Palonosetron was given at 0.25 mg, IV, dL.

On this basis, the treatment group was given PEG-rhG-CSF by subcutaneous injection at a dose of 6 mg/ time and once per chemotherapy cycle within 48 h after 24 h of chemotherapy^[1].

The control group received a subcutaneous injection of PEG-rhG-CSF at a dose of $100 \mu\text{g}$ for 48 h after chemotherapy, followed by a continuous 7 days of supportive treatment^[2]. The dosage could be gradually increased with the aggravation of leukopenia^[3]. Blood routine was regularly monitored during the application of PEG-rhG-CSF and rhG-CSF. Transient adverse reactions of PEG-rhG-CSF use were bone pain, allergic symptoms, and suspected allergic symptoms. Acetaminophen, nonsteroidal anti-inflammatory drugs, or other treatments may be used, including symptomatic treatment with opioids and antihistamines, or reduction of PEG-rhG-CSF dose^[8].

Table 1 Comparison of leukopenia, neutropenia, and neutropenia fever between the two groups (*n*)

Group	leukopenia		χ^2	<i>P</i>	neutropenia		χ^2	<i>P</i>	neutropenia fever		<i>P</i>	
	<i>n</i>	%			<i>n</i>	%			<i>n</i>	%		
Treatment group (25)	3	12	0.104	0.748	2	8	0.54	0.462	0	0	-	0.192
Control group (20)	4	20			4	20			2	10		

Observation indicators

Observation indexes: venous blood samples were collected on days 3, 7, 11, and 14 of the chemotherapy cycle for blood routine examination (leukopenia, neutropenia, and antibiotic use), and while blood cell (WBC) count, neutrophil count, granulocytic fever, and incidence of antibiotic use were compared between the two groups of PEG-rhG-CSF and rhG-CSF [4].

The incidence of various adverse reactions between the two groups was compared according to the World Health Organization (WHO) "classification criteria for common adverse reactions of anticancer drugs."

Statistical analysis

SPSS18.0 statistical software was used for data processing. The measurement data were expressed as $\bar{x} \pm s$, and a *t* test was used for comparison between groups. Chi-square test, continuous correction chi-square test, and Fisher's precise test were used for comparison between the counting data groups, and $P < 0.05$ was considered statistically significant.

Results

Main efficacy

The incidence of leukopenia, neutropenia, neutropenia fever and antibiotic use in the treatment group was 12%, 8%, 4% and 4% respectively, which was significantly lower than in the control group (20%, 20%, 10% and 10%) without statistical significance (all $P > 0.05$; Table 1).

In the treatment group, two cases appeared in the entire course of chemotherapy, one case 7 days after the 3rd cycle of chemotherapy, and one case after subcutaneous injection of PEG-rhG-CSF 11 days after the

6th cycle of chemotherapy. In the treatment group, there were no patients with granulocytic fever and antibiotic prophylaxis.

One patient in the control group developed granulocytic fever 7 days later and was treated with antibiotics. Chemotherapy was delayed for 1 week, and the completion of intensive chemotherapy was ensured for the rest of the control group.

The dynamic change of neutrophils

Two groups of granulocytes 24 h after blood tests in the drug treatment group were significantly higher than that of the treatment group (P values < 0.05). As more time passed, two groups of granulocytes showed no statistical difference ($P > 0.05$). However, 7, 11, and 14 days after chemotherapy, blood tests showed that the granulocytes in the treatment group were significantly higher than that of the treatment group ($P < 0.05$). All data are shown in Table 2.

Incidence of adverse reactions

The main adverse reactions in the experimental group and the control group were bone pain, pain at the injection site, fever, and fatigue, and a few patients had rashes, palpitations, and chest tightness. The number of adverse reactions in the application cycle of the experimental group was significantly lower than that in the control group, and the difference between the two groups was not statistically significant ($P > 0.5$; Table 3). All adverse reactions were I–II degrees, and patients exhibited symptomatic improvement after treatment.

Discussion

Neutropenia is considered the most severe hematologic toxicity caused by chemotherapy and the most common dose-limiting toxicity. In some patients, infection caused by neutropenia and reduction of chemotherapy dose may affect the therapeutic effect, and even increase the risk of death due to discontinuation of chemotherapy. Therefore, prevention and treatment of neutropenia has become important for the smooth progress of chemotherapy. The application of rhG-CSF is an important milestone in chemotherapy for malignant tumors [9]. The PubMed database has nearly 40 clinical studies on pegfilgrastim for breast cancer dose intensive chemotherapy, most of

Table 2 Dynamic changes of mean neutrophils after preventive use of PEG-rhG-CSF

Time (h)	PEG-rhG-CSF (<i>n</i> = 25)	rhG-CSF (<i>n</i> = 20)	<i>P</i>
D1 (24)	28.2 ± 0.77	14.6 ± 0.65	0.000
D4 (96)	16.4 ± 1.90	15.3 ± 1.80	0.055
D7 (168)	13.3 ± 1.20	13.9 ± 1.00	0.080
D11 (264)	12.8 ± 0.79	8.6 ± 0.98	0.000
D14 (336)	8.8 ± 2.1	6.8 ± 2.3	0.004

Table 3 Comparison of adverse reactions between PEG-rhG-CSF and rhG-CSF

Factors	PEG-rhG-CSF (n = 25) cycle		rhG-CSF (n = 20) cycle		χ^2	P
	n	%	n	%		
Bone pain	18	9	15	9.3	1.785	0.185
Pain in injection site	12	6	11	6.9	1.114	0.736
Fever	0	0	2	0.63	–	0.197
Palpitation	4	2	4	2.5	0.00	1.00
Rash	4	2	6	3.8	0.464	0.496
Fatigue and fatigue	24	12	28	17.5	2.176	0.140

which are single-center and single-arm studies^[10]. The application of rhG-CSF can stimulate the release of bone marrow to the peripheral blood, reduce the incidence of infection caused by the suppression of bone marrow function after chemotherapy, and ensure the smooth progress of chemotherapy^[11]. It is an effective drug for the prevention and treatment of neutropenia caused by chemotherapy and radiotherapy. However, due to its short half-life and frequent injection in clinical application, it brings inconvenience and pain to patients. In this study, 45 postoperative breast cancer patients who received CE followed by T-intensive adjuvant chemotherapy were divided into two groups. Among them, 25 patients in the treatment group were treated with PEG and 20 patients in the control group were treated with rhG-CSF. The incidence of neutropenia, granulocytic fever and antibiotic use in patients using PEG-rhG-CSF during non-chemotherapy was 12%, 6% and 6% lower than that of rhG-CSF, respectively. A study showed that early prophylactic administration of PEG-rhG-CSF can reduce the incidence of neutropenia by 94% and reduce the use of IV anti-infective drugs by 80%^[6]. A retrospective study showed that prophylactic use of PEG-rhG-CSF can reduce the risk of granulocytic fever in tumor patients after chemotherapy by 50%, without affecting the efficacy and overall survival^[12]. In order to avoid the pain for patients with venous blood every day, we have blood tests 1, 4, 7, 11, and 14 days after treatment. Blood tests 1 day (24 h) after drug blood granulocyte in the treatment group showed significantly higher granulocytes than that of the treatment group ($P < 0.05$), but after 4 and 7 days the two groups showed no statistical difference in granulocyte count ($P > 0.05$). After 7, 11 and 14 days, although average blood test were within the normal range, the granulocyte count in the treatment group was significantly higher than the control group ($P < 0.05$). This study showed that the experimental group maintained a higher granulocyte concentration than the control group. In this study, the main adverse reactions in the experimental group and the control group were bone pain, pain at the injection site, fever, and fatigue. Some patients exhibited rashes, palpitations, and chest tightness. The number of adverse reactions in

the application cycle in the experimental group was lower than in the control group, but the difference between the two groups was not statistically significant ($P > 0.05$). The adverse reactions of PEG-rhG-CSF were mainly bone pain, but these were generally transient. Paracetamol or non-steroidal anti-inflammatory drugs could reduce the pain symptoms. All patients improved after symptomatic treatment, and the incidence of adverse reactions was low. If allergic phenomenon occurred, symptomatic treatment and consideration of reduction of dosage was required. If it occurred repeatedly, the drug was discontinued. No allergic patients were found in this experiment.

Patients with tumor radiation and chemotherapy after granulocyte depletion are the most common adverse reactions. A lack of granulocytes can lead to infections in the respiratory tract, digestive tract, and urinary tract. It can also cause bacteremia, septic shock, and death. Granulocyte depletion can also cause fever, oral mucosa ulcer, and adverse reactions associated with peripherally inserted central catheter (PICC) removal. This will lead to the delay and reduction of chemotherapy, and affect the long-term effects of chemotherapy. In addition, it increases medical expenses, reduces quality of life and increases the risk of death. PEG-rhG-CSF has a significantly longer half-life (15–80 h) than traditional rhG-CSF. Therefore, the vast majority of patients with PEG-rhG-CSF can^[13]^[14]: be treated more conveniently, experience reduced the frequency of subcutaneous injection and venous blood pain, have improved compliance^[15], and safety, ensure treatment is completed on time according to the dose chemotherapy cycle, and improve the long-term effectiveness of chemotherapy. This will be especially useful for intensive therapy to increase the granulocyte count and the efficacy of chemotherapy, and reduce the risk of secondary infection. Therefore, using PEG-rhG-CSF can ensure the smooth progress of intensive therapy, maximize the curative effect and safety of the treatment, reduce the risk of granulocytopenia, relieve the suffering of frequent injections and blood tests, and reduce the use of antibiotics.

Conflicts of interest

The authors declare no conflict of interest.

References

1. Forouzanfar MH, Foreman KJ, Delossantos AM, *et al.* Breast and cervical cancer in 187 countries between 1980 and 2010: a systematic analysis. *Lancet*, 2011, 378:1461–1484.
2. Jiang BQ, Li ZD, Zhuang ZG. Studies on clinical safety of two docetaxel regimens in treatment of breast cancer. *Adverse Drug Reactions J*, 2009, 11:165–169.
3. Russell N, Mesters R, Schubert J, *et al.* A phase 2 pilot study of pegfilgrastim and filgrastim for mobilizing peripheral blood progenitor cells in patients with non-Hodgkin's lymphoma receiving chemotherapy. *Haematologica*, 2008, 93: 405–412.
4. National Comprehensive Cancer Network. NCCN Guidelines Myeloid Growth Factors. Version 1. 2013.
5. He XX, Jiao AM, Xia YQ, *et al.* Study on the effectiveness and the dosage of rhG-CSF given in accordance with the level of leukopenia after chemotherapy. *Chin J Clin Oncol Rehabil (Chinese)*, 2007, 14: 515.
6. Shi YK, Xu JP, Wu CP, *et al.* Multicenter postmarketing clinical study on using pegylated recombinant human granulocyte-colony stimulating factor to prevent chemotherapy-induced neutropenia. *Chin J Clin Oncol (Chinese)*, 2017, 44: 679–684.
7. Chinese Society of Clinical Oncology (CSCO). Chinese expert consensus on the clinical application of peg-rhG-CSF. *Chin J Clin Oncol (Chinese)*, 2016, 43: 271–274.
8. Hübel K, Engert A. Clinical applications of granulocyte colony-stimulating factor: an update and summary. *Ann Hematology*, 2003, 82: 207–213.
9. Ma J. Chinese expert consensus on the clinical application of polyethylene glycol recombinant human granulocyte-stimulating factor (PEG-rhG-CSF). *Chin Cancer Clin Oncol (Chinese)*, 2016, 43: 271–274.
10. Fernandes R, Mazzarello S, Stober C, *et al.* Optimal primary febrile neutropenia prophylaxis for patients receiving docetaxel-cyclophosphamide chemotherapy for breast cancer: a systematic review. *Breast Cancer Res Treat*, 2017, 161: 1–10.
11. Yang B, Kido A. Pharmacokinetics and pharmacodynamics of pegfilgrastim. *Clin Pharmacokinetic*, 2010, 50: 295–306.
12. Almenar D, Mayans J, Juan O, *et al.* Pegfilgrastim and daily granulocyte colony-stimulating factor: patterns of use and neutropenia-related outcomes in cancer patients in Spain- results of the LEARN Study. *Eur J Cancer Care*, 2009, 18: 280–286.
13. Molineux G. Pegylation: engineering improved pharmaceuticals for enhanced therapy. *Cancer Treat Rev*, 2002, 28 (Suppl A): 13–16.
14. Klastersky J, Awada A. Prevention of febrile neutropenia in chemotherapy-treated cancer patients: pegylated versus standard myeloid colony-stimulating factors. Do we have a choice? *Crit Rev Oncol Hematol*, 2011, 78: 17–23.
15. Ling MS, Xu XY, Shi FX, *et al.* Study of polyethylene glycol increasing renaturation efficiency of recombinant human granulocyte colony stimulating factor. *Pharm Biotechnol*, 1997, 4: 5–8.

DOI 10.1007/s10330-019-0350-0

Cite this article as: Qu SX, Qiu JN, Zhang YD, *et al.* Application of pegylated recombinant human granulocyte colony-stimulating factor (PEG-rhG-CSF) for the prevention of neutropenia in triple negative breast cancer patients older than 65 years during adjuvant chemotherapy. *Oncol Transl Med*, 2019, 5: 218–222.

Determining the efficacy of vitamin B12 mixed oral liquid in the treatment of radiation-induced esophagitis*

Yindi Tian¹, Ya Guo², Yue Ke², Yuyan Guo², Pengtao Yang², Hongbing Ma² (✉),
Baofeng Wang² (✉)

¹ Department of Infectious Diseases, The Second Affiliated Hospital of Medical College, Xi'an Jiaotong University, Xi'an 710004, China

² Department of Radiation Therapy, The Second Affiliated Hospital of Medical College, Xi'an Jiaotong University, Xi'an 710004, China

Abstract

Objective This study aimed to investigate the effects of vitamin B12 mixed oral liquid in the treatment of radiation-induced esophagitis in patients with esophageal cancer.

Methods Seventy-five patients with esophageal cancer who met the enrollment criteria were randomly divided into the vitamin B12 mixed oral liquid group (39 patients in the study group) and the gentamicin mixed oral liquid group (36 patients in the control group). The effects of the two treatment methods on esophagitis grading, pain degree, body weight loss, and Karnofsky performance status (KPS) score in patients with radiation esophagitis were observed.

Results In the control group, grade 1 radiation esophagitis accounted for 27.8% of the total patients, grade 2 accounted for 41.7%, and grades 3 and 4 accounted for 30.6%. In the vitamin B12 treatment group, grade 1 radiation esophagitis accounted for 66.7% of the total patients, grade 2 accounted for 25.6%, and grades 3 and 4 accounted for 7.7%; there was a significant difference between the vitamin B12 treatment group and control group ($P < 0.01$). Similarly, pain caused by radiation esophagitis was significantly improved in the vitamin B12 group compared with the control group ($P < 0.05$). After treatment, the average weight loss of the control group was (2.18 ± 0.36) kg, while that of the vitamin B12 treatment group was (0.90 ± 0.43) kg ($P < 0.05$). The KPS scores of the vitamin B12 group were higher than those of the control group, which were 86.2 ± 1.2 and 85.6 ± 1.5 , respectively, but there was no statistical difference ($P > 0.05$).

Conclusion Vitamin B12 mixed oral liquid can effectively reduce the severity of radiation esophagitis, relieve pain, improve patients' quality of life, and increase treatment compliance.

Key words: esophagitis; vitamin B12; quality of life; Karnofsky performance status (KPS)

Received: 15 July 2019

Revised: 3 September 2019

Accepted: 25 September 2019

Esophagitis is the common side effect of radiotherapy for esophageal cancer, which adversely affects the treatment efficacy and quality of life of patients who receive this treatment [1]. With the increasing use of radiotherapy in the treatment of thoracic tumors, despite achieving significant results, the incidence of radiation-induced esophagitis has gradually increased. When the dose of radiotherapy reaches 20–30 Gy, different degrees of radiation esophagitis occur [2]; related studies show that the incidence of severe radiation esophagitis in lung

cancer patients is as high as 15%–25% [3]. In a randomized clinical study, radiation treatment was discontinued in 21% of cancer patients owing to the occurrence of severe radiation-induced esophagitis [4].

Congestion, edema, erosion, or ulcer in the esophageal mucosa is the main pathological manifestation of radiation esophagitis. The patient with this condition may experience throat drying, dysphagia, nausea and vomiting, and retrosternal pain. Radiation esophagitis initially occurs as an aseptic inflammation, which

✉ Correspondence to: Hongbing Ma. Email: mhbxiidn@126.com
Baofeng Wang. Email: wangbf1680@126.com

* Supported by a grant from the National Natural Sciences Foundation of China (No. 81872471).

© 2019 Huazhong University of Science and Technology

may be accompanied by infection in the later stage and further aggravates the condition. In severe cases, dehydration, electrolyte imbalance, and insufficient nutrient intake may occur. Especially when radiotherapy and chemotherapy are carried out at the same time, the symptoms are more obvious, eventually increasing the incidence of complications and affecting the radiation response of the tumor^[5-6].

Therefore, the cure of radiation esophagitis is essential to the success of tumor radiation therapy. In the traditional clinical treatment of radiation esophagitis, patients are often treated with antibiotics combined with hormone therapy, are placed on liquid diet, and receive parenteral nutrition, which can partially relieve pain but cannot be used to treat radiation esophagitis. Currently, there are no available drugs that can effectively treat radiation esophagitis^[2,7]. Thus, there is a need to develop a new drug that can be used for patients with radiation-induced esophagitis.

Vitamin B12 is a water-soluble vitamin that exerts significant antioxidant effects by scavenging reactive oxygen species (ROS). It also reduces inflammatory responses by regulating the expression of cytokines and prevents immune damage in tissues^[8-9]. At the same time, previous clinical trials have found that vitamin B12 can significantly reduce radiation-induced mucosal damage^[10]. Over the years, vitamin B12 mixed oral liquid has proven to be an effective formula for the treatment of radiation esophagitis in our cancer treatment centers (The Second Affiliated Hospital of Medical College, Xi'an Jiaotong University, China). From January 2015 to December 2018, our department has treated 75 patients with radiation-induced esophagitis with vitamin B12 mixed oral liquid. This study aimed to determine the use and positive role of vitamin 12 mixed oral liquid during the course of radiotherapy and provide a clinical reference point on how to avoid or reduce esophageal toxicity during thoracic cancer radiotherapy.

Material and methods

General information

From January 2015 to December 2018, 78 patients with esophageal cancer who met the enrollment criteria were randomized as follows: vitamin B12 mixed oral liquid group or study group (40 patients) and control group (38 patients). One patient from the study group and two from the control group were excluded from the study. Finally, 39 patients from the study group and 36 from the control group were included in the follow-up studies. Of the total participants, 64 were men and 11 were women, aged 45–80 years. The baseline characteristics of the patients are shown in Table 1. There were no significant differences in gender, age, tumor size, and radiation dose between

Table 1 Patients and treatment characteristics (*n*)

Group	Study group (<i>n</i> = 39)	Control group (<i>n</i> = 36)
Age (years)	65.5 ± 9.3	66.7 ± 9.5
Histology		
ESCC	37	33
EAC	2	3
Gender		
Male	33	31
Female	6	5
Marriage		
Yes	37	35
No	2	1
Grade		
G1	3	2
G2–3	36	34
Weight loss		
≤ 5%	29	28
> 5%–10%	10	8
Smoking		
Yes	25	23
No	14	13
Length (cm)		
≤ 5	13	11
> 5	26	25
KPS	81.3 ± 1.4	81.1 ± 1.5
Radiation dose (Gy)		
≤ 60	13	12
> 60	26	24

Note: *P* > 0.05. ESCC: Esophageal squamous-cell cancer; EAC: Esophageal adenocarcinoma; KPS: Karnofsky performance status

the two groups.

Inclusion criteria

Patients (1) with esophageal cancer confirmed by esophagoscopy biopsy; (2) who were generally in good condition, aged ≤ 80 years, with a Karnofsky performance status (KPS) score of ≥ 70, and with life expectancy of ≥ 3 months; (3) with no previous history of esophageal disease and neck and chest radiotherapy; (4) who consumed a liquid diet before treatment; (5) with no tracheal invasion and no pre-perforation signs on X-ray examination; (6) without obvious heart, liver, lung, and kidney function abnormalities and with normal electrocardiogram (ECG) findings; and (7) who had better understanding of their condition, knew the role of the relevant treatment and adverse reactions, and voluntarily received the treatment were included in the study.

Exclusion criteria

Patients (1) whose esophageal cancer was diagnosed only based on the imaging data without pathological confirmation; (2) aged > 80 years, with poor general condition, with KPS score of < 70, and with life

expectancy of < 3 months; (3) with history of esophageal disease or neck and chest radiotherapy; (4) who did not consume a liquid diet before treatment; (5) with signs of tracheal invasion or combined esophageal perforation on X-ray; (6) with abnormal heart, liver, lung, and kidney function, and abnormal ECG findings; (7) were pregnant or lactating; and (8) who were not familiar with the treatment or refused to receive the treatment were excluded.

Treatment and radiotherapy

Patients with esophageal cancer who met the conditions were administered with a mixed oral solution every day after 20 Gy of radiotherapy. The study group received the following treatment: vitamin B12 5 mg + lidocaine 200 mg + gentamicin 320 000 U added to 500 mL of saline. The control group received the following treatment: lidocaine 200 mg + gentamicin 320 000 U added to 500 mL of saline. The patients were positioned flat on the bed while receiving the mixed oral solution, were asked to swallow the solution slowly, and were not allowed to eat or drink anything for half an hour before and after treatment, so that the drug has sufficient time to act on the esophageal mucosa. The medication was administered three times a day at a dose of 20–25 mL until the end of radiotherapy. Vitamin B12 was administered at a dose of 0.5 mg (Fangming Pharmaceutical Group Co., Ltd., China); lidocaine, 100 mg (Tiansheng Pharmaceutical Group Co., Ltd., China); and gentamicin injection, 2 mL: 80 mg (80 000 U) (Chengxin Pharmaceutical Co., Ltd., China). All treatments were carried out with a linear accelerator (Varian Medical Systems Inc., CA, USA), using 6-MV photon energies delivered in 1.8–2 Gy per fraction 5 days a week at a dose rate of 400 cGy/min. The total radiation dose administered was 50.4–66 Gy.

Diagnostic criteria

Radiation-induced esophagitis was defined as the occurrence of esophageal inflammation after radiotherapy, such as local congestion, edema, and superficial ulcer. The primary symptoms include odynophagia, dysphagia, and retrosternal pain, and the diagnosis was made based on the history of radiotherapy and patients' symptoms^[1]. According to the Radiation Therapy Oncology Group acute radiation-induced esophageal morbidity (ARIE) scoring criteria, ARIE was classified into five grades^[11] (Table 2).

Observation indicators and evaluation methods

During radiotherapy, changes in the patient's radiation-induced esophagitis grading, weight, pain, and nutritional status were observed and recorded.

Table 2 Description of radiation esophagitis grade

Grade	Description
Grade 0	No change
Grade I	Mild dysphagia or odynophagia, requiring topical anesthetic, non-narcotic agents, or soft diet
Grade II	Moderate dysphagia or odynophagia. Pain drugs or pure liquid diet might be needed
Grade III	Severe dysphagia or odynophagia with dehydration, weight loss > 15%. Nasogastric tube might be required for nutrition
Grade IV	Complete obstruction, ulceration, perforation or fistula was formed

Esophagitis pain judgment criteria

The score is measured using a 10-point visual analog scale: 0 points: no pain; 3 points or less: slight bearable pain; 4–6 points: pain affects patient's sleep but is still bearable; and 7–10 points: gradual increase in pain intensity, pain is becoming unbearable, and it affects appetite and sleep. Radiation-induced esophagitis grading and esophagitis pain scores were evaluated once a week during treatment. For statistical analysis, patients with the highest ARIE grade and the most severe pain were selected for analysis.

Evaluation criteria of quality of life

The physical condition of the patient was evaluated using the KPS established by the World Health Organization and was evaluated and recorded before and after the treatment.

Quality control

Before undertaking the study, all participants of the clinical team were trained to master the management of radiation esophagitis, including grading of esophagitis and usage of these evaluation tools. All researchers were required to strictly adhere to the standard operating procedures when performing all necessary interventions and when recording data.

Statistical analysis

Quantitative data were presented as the mean ± standard error of the mean (SEM) and analyzed by one-way analysis of variance. Statistical analyses were performed using SPSS software (version 18.0). Qualitative data was measured by χ^2 test, and a *P* value of < 0.05 was considered significant.

Results

Changes of radiation esophagitis grade after treatment

Two groups of patients had different levels of dysphagia or pain when swallowing during radiotherapy. In the

Table 3 The classification of radiation esophagitis after treatment (n)

Group	Radiation esophagitis (classification)					χ^2	F
	0	1	2	3	4		
Study group	0	26	10	2	1		
Control group	0	10	15	8	3	12.61	0.0056

Note: $P < 0.01$, compared with the control group

Table 4 Comparison of pain between the two groups (n)

Group	Grade				χ^2	F
	No	Mild	Moderate	Severe		
Study group	0	31	5	3		
Control group	0	18	12	6	7.223	0.027

Note: $P < 0.05$, compared with the control group

control group, 10 (27.8%) patients had grade 1 radiation esophagitis, 15 (41.7%) had grade 2, and 11 (30.6%) had grades 3 and 4. In the vitamin B12 treatment group, 26 (66.7%) patients had grade 1 radiation esophagitis; 10 (25.6%) had grade 2, and 3 (7.7%) had grades 3 and 4. There was a significant difference between the vitamin B12 treatment group and control group, indicating that the severity of radiation esophagitis was significantly reduced by vitamin B12 mixed oral solution ($P < 0.01$; Table 3).

Comparison of pain scores between the two groups

The pain scores of the two groups are shown in Table 4. None of the patients from the vitamin B12 group and control group had absence of pain. In the vitamin B12 group, 31 patients had mild pain, while 8 had moderate to severe pain. In the control group, 18 patients had mild pain, and 18 had moderate to severe pain. There was a significant difference between the two groups ($P < 0.05$).

Weight changes after radiation therapy

In the two groups, only 16.7% of the patients from the control group had an increase in body weight after the end of treatment, and the rest of the patients had different degrees of reduction in body weight. The average weight loss of the control group was (2.18 ± 0.36) kilograms. On the vitamin B12 treatment group, 41.0% of the patients had an increase in body weight, while the average weight loss was (0.90 ± 0.43) kilograms. Compared with the control group, the difference was significant ($P = 0.029$; Fig. 1).

Changes in quality of life

The KPS score was 81.1 ± 1.5 and 81.3 ± 1.4 in the control group and vitamin B12 group, respectively, at the beginning of radiotherapy. After radiation, the KPS scores of the vitamin B12 group and control group were significantly increased (86.2 ± 1.2 and $85.6 \pm$

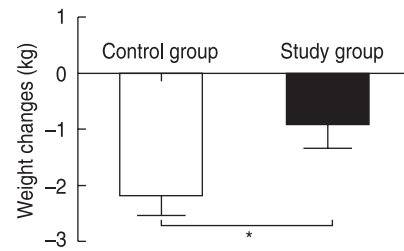


Fig. 1 Weight changes after radiation therapy. In the control group, the average weight loss was (2.18 ± 0.36) kilograms. In the vitamin B12 study group, the average weight loss was (0.90 ± 0.43) kilograms. Compared with the control group, the difference was significant ($P = 0.0442$).

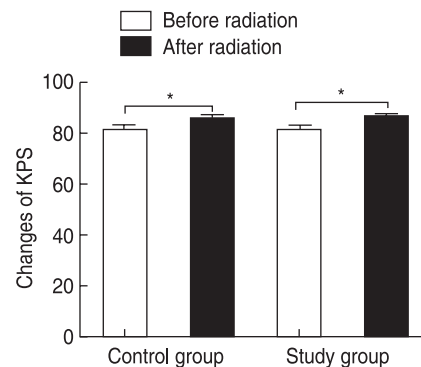


Fig. 2 KPS score changes after radiation therapy. The KPS scores of the vitamin B12 group and control group were significantly increased after radiation (86.2 ± 1.2 and 85.6 ± 1.5 , respectively). There was a statistically significant difference between the post-radiation KPS scores and pre-radiation scores of each group ($P < 0.05$), but no statistical difference was observed between the two groups ($P > 0.05$).

1.5, respectively). There was a statistically significant difference between the post-radiation KPS scores and pre-radiation scores of each group ($P < 0.05$; Fig. 2), but there was no statistical difference between the two groups ($P > 0.05$; Fig. 2). This may be due to the fact that the increase in KPS scores of esophageal cancer patients was not only related to the improvement of radiation esophagitis, but was also related to the improvement of the disease itself.

Discussion

Radiation esophagitis is the most common side effect of radiotherapy for esophageal cancer, and it often occurs throughout the treatment period. Severe radiation-induced esophagitis can lead to pain, swallowing difficulties, depression, malnutrition, severe physical decline, and even disruption of radiation therapy, ultimately affecting the treatment of the tumor. The study found that the local tumor control rate is related to the total time of radiotherapy, and the extension of the total treatment time reduces the local control of the tumor [12].

Xu *et al*^[13] found that the interrupted time (IT) of more than 4 days during intensity-modulated radiotherapy may decrease the survival outcomes of nasopharyngeal cancer patients. Moreover, IT (> 4 days vs ≤ 4 days) was found to be an independent prognostic factor for progression-free survival and overall survival.

To date, the clinical treatment of radiation esophagitis is aimed at achieving convergence, achieving anti-inflammatory effects, promoting esophageal mucosal repair, achieving analgesic effects, and promoting nutritional support. There are several treatments used to manage radiation esophagitis. These include oral glutamine, gentamicin, and procaine oral solution; epicatechin-3-gallate; and traditional Chinese medicine^[14-17], and they all achieved certain clinical effects. However, there are no standard guidelines for the treatment of radiation esophagitis.

In the process of radiotherapy of tumors, radiation also acts on the esophageal mucosa not only to activate the inflammatory response, but also to decompose H₂O in the esophagus into oxygen free radicals by ionization. Oxygen free radicals generated in large amounts in local tissues can cause oxidative damage to the esophageal mucosa and produce malondialdehyde (MDA) and superoxide dismutase, which can increase the cell membrane permeability, destroy lysosomes, induce apoptosis, aggravate inflammatory response, and further cause damage to the esophagus^[18-21].

Vitamin B12, or cobalamin, is an essential water-soluble vitamin that can directly scavenge ROS, especially superoxides, and exerts antioxidant properties^[8]. In addition, vitamin B12 can reduce the inflammatory response by regulating the expression of cytokines and growth factors to protect against tissue damage caused by immune responses^[9]. A joint study of patients with Alzheimer's disease found that patients with vitamin B12 deficiency had higher levels of interleukin-6 than those with normal vitamin B12 levels^[22]. Studies of B12-deficient rats and patients with severe B12 deficiency also showed an increase in tumor necrosis factor alpha and a decrease in epidermal growth factor levels compared with controls. Other experimental results also showed that the ROS level in cobalamin-deficient melanocytes is extremely increased compared with that in controls^[23]. Previous studies further confirmed that vitamin B12 protects against oxidative stress caused by an immune response by regulating the production of cytokines and growth factors. Chen *et al*^[10] found that vitamin B12 causes obvious and rapid repair and regeneration of functions on radiation-damaged mucosal epithelial cells and vascular endothelial cells, accelerating the formation of new tissues. Moreover, it can directly act on the pain receptors of the free nerve endings after being absorbed by the damaged part and has a significant peripheral and

central analgesic effect.

Gentamicin is a broad-spectrum antibiotic suitable for the treatment of intestinal infections, pelvic infections, and skin and soft tissue infections caused by sensitive Gram-negative bacilli and staphylococcus. Through oral administration, gentamicin acts directly on the damaged mucosa to reduce the inflammatory reaction, so that the damaged mucosa does not delay the repair of the injury due to infection. Lidocaine has a surface anesthetic effect, which can relieve pain symptoms for those with severe pain. This oral mixture is a comprehensive treatment for the clinical symptoms of radiation esophagitis. Patients were positioned flat on bed while the mixed oral liquid was administered. They were asked to swallow the solution slowly and were not allowed to eat or drink anything for half an hour before and after administering the medication, so that the drug has sufficient time to act on the esophageal mucosa.

Our results showed that patients who were treated with vitamin B12 had higher incidence of grades 1 and 2 radiation esophagitis, while those in the control group had higher incidence of grades 3 and grade 4 radiation esophagitis. The distribution of changes in the pain scores of the two groups were similar to that of grades in radiation esophagitis. Most of the patients in the study group experienced mild pain, and had lower incidence of moderate and severe pain than that of the control group. Changes in the distribution of radiation esophagitis and pain also affected the patients' quality of life. This study found that the quality of life of the two groups was similar to that before treatment. Moreover, the degree of weight loss in the study group was significantly lower than that in the control group after treatment, and the difference was significant. Although the quality of life in the study group improved compared with the control group, there was no statistical difference between the two groups. It may be because the increase in the KPS scores of the esophageal cancer patients was not only related to the improvement of radiation esophagitis, but was also related to the improvement of the disease itself. In addition, as the pain caused by radiation esophagitis was relieved, the radiotherapy treatment of the patients in the study group was not interrupted, which ensured the successful completion of the treatment. In the control group, two patients continued to undergo radiotherapy as their treatment was interrupted for 2-5 days due to the side effect. During the course of radiotherapy, we closely observed the patient's pain status and the changes in diet, mental, and other general conditions. If the patient experienced severe pain, which affected his or her quality of life or sleep, adjuvant treatments (such as analgesics and nutritional support), were provided. The study group did not develop toxicities associated with vitamin B12 treatment. After clinical observation, we found that the

mixed oral liquid has no toxic and side effects, is safe and reliable, and is an effective treatment for radiation esophagitis.

In summary, our preliminary results show that vitamin B12 mixed oral solution can significantly reduce the symptoms of radiation esophagitis, improve the quality of life of patients, ensure the smooth completion of treatment, and is convenient and economical. However, this study also has certain limitations. Hence, a multi-center, large-sample, double-blind clinical study is warranted.

Ethics approval and consent to participate

All procedures involving human participants were performed in accordance with the ethical standards of the institutional and national research committee and with the 1964 Helsinki Declaration and its later amendments or comparable ethical standards. Verbal consent was obtained from all participants, and the study documents were reviewed and approved by the Medical Ethics Committee of the Second Affiliated Hospital of Medical College, Xi'an Jiaotong University, China (approval No. 2019015).

Conflicts of interest

The authors indicate no potential conflicts of interest.

References

- Murro D, Jakate S. Radiation esophagitis. *Arch Pathol Lab Med*, 2015, 139: 827–830.
- Werner-Wasik M, Yorke E, Deasy J, *et al*. Radiation dose-volume effects in the esophagus. *Int J Radiat Oncol Biol Phys*, 2010, 76 (3 Suppl): S86–S93.
- Palma DA, Senan S, Oberije C, *et al*. Predicting esophagitis after chemoradiation therapy for non-small cell lung cancer: an individual patient data meta-analysis. *Int J Radiat Oncol Biol Phys*, 2013, 87: 690–696.
- Aupérin A, Le Péchoux C, Rolland E, *et al*. Meta-analysis of concomitant versus sequential radiochemotherapy in locally advanced non-small-cell lung cancer. *J Clin Oncol*, 2010, 28: 2181–2190.
- Hawkins PG, Boonstra PS, Hobson ST, *et al*. Prediction of radiation esophagitis in non-small cell lung cancer using clinical factors, dosimetric parameters, and pretreatment cytokine levels. *Transl Oncol*, 2018, 11: 102–108.
- Gao F, Jia L, Han JJ, *et al*. Predictive value of serum levels of transforming growth factor beta 1 for the short-term effects of radiotherapy and chemotherapy in patients with esophageal cancer. *Oncol Transl Med*, 2018, 4: 1–5.
- Feng M, Smith DE, Normolle DP, *et al*. A phase I clinical and pharmacology study using amifostine as a radioprotector in dose-escalated whole liver radiation therapy. *Int J Radiat Oncol Biol Phys*, 2012, 83: 1441–1447.
- Green R, Allen LH, Bjørke-Monsen AL, *et al*. Correction: Vitamin B12 deficiency. *Nat Rev Dis Primers*, 2017, 3: 17054.
- van de Lagemaat EE, de Groot LCPGM, van den Heuvel EGHM. Vitamin B12 in relation to oxidative stress: A systematic review. *Nutrients*, 2019, 11: pii: E482.
- Chen XL, Shi YS. Effect of vitamin B12 mixed solution inhalation for acute radiation-induced mucosal injury. *J South Med Univ (Chinese)*, 2006, 26: 512–514.
- Cox JD, Stez J, Pajak TF. Toxicity criteria of the Radiation Therapy Oncology Group (RTOG) and the European Organization for Research and Treatment of Cancer (EORTC). *Int J Radiat Oncol Biol Phys*, 1995, 31: 1341–1346.
- Li PJ, Jin T, Luo DH, *et al*. Effect of prolonged radiotherapy treatment time on survival outcomes after intensity-modulated radiation therapy in nasopharyngeal carcinoma. *PLoS One*, 2015, 10: e0141332.
- Xu GZ, Li L, Zhu XD. Effect of interrupted time during intensity modulated radiation therapy on survival outcomes in patients with nasopharyngeal cancer. *Oncotarget*, 2017, 8: 37817–37825.
- Tutanc OD, Aydogan A, Akkucuk S, *et al*. The efficacy of oral glutamine in prevention of acute radiotherapy-induced esophagitis in patients with lung cancer. *Contemp Oncol (Pozn)*, 2013, 17: 520–524.
- Wang LJ, Lu JZ, Cai BN, *et al*. Effect of compound Zhuye Shigao Granule on acute radiation-induced esophagitis in cancer patients: A randomized controlled trial. *Chin J Integr Med*, 2017, 23: 98–104.
- Chang SC, Lai YC, Hung JC, *et al*. Oral glutamine supplements reduce concurrent chemoradiotherapy-induced esophagitis in patients with advanced non-small cell lung cancer. *Medicine (Baltimore)*, 2019, 98: e14463.
- Zhao H, Xie P, Li X, *et al*. A prospective phase II trial of EGCG in treatment of acute radiation-induced esophagitis for stage III lung cancer. *Radiother Oncol*, 2015, 114: 351–356.
- Park BK, Lee JH, Seo HW, *et al*. Icaritin protects against radiation-induced mortality and damage *in vitro* and *in vivo*. *Int J Radiat Biol*, 2019, 95: 1094–1102.
- Chaurasia M, Gupta S, Das A, *et al*. Radiation induces EIF2AK3/PERK and ERN1/IRE1 mediated pro-survival autophagy. *Autophagy*, 2019, 15: 1391–1406.
- Rezaeyan A, Haddadi GH, Hosseinzadeh M, *et al*. Radioprotective effects of hesperidin on oxidative damages and histopathological changes induced by X-irradiation in rats heart tissue. *J Med Phys*, 2016, 41: 182–191.
- Chen MF, Chen PT, Chen WC, *et al*. The role of PD-L1 in the radiation response and prognosis for esophageal squamous cell carcinoma related to IL-6 and T-cell immunosuppression. *Oncotarget*, 2016, 7: 7913–7924.
- Politis A, Olgiaiti P, Malitas P, *et al*. Vitamin B12 levels in Alzheimer's disease: association with clinical features and cytokine production. *J Alzheimers Dis*, 2010, 19: 481–488.
- Rzepka Z, Respondek M, Rok J, *et al*. Vitamin B12 deficiency induces imbalance in melanocytes homeostasis – A cellular basis of hypcobalaminemia pigmentary manifestations. *Int J Mol Sci*, 2018, 19: pii: E2845.

DOI 10.1007/s10330-019-0367-7

Cite this article as: Tian YD, Guo Y, Ke Y, *et al*. Determining the efficacy of vitamin B12 mixed oral liquid in the treatment of radiation-induced esophagitis. *Oncol Transl Med*, 2019, 5: 223–228.

Treatment results of childhood extracranial malignant germ cell tumors and the salvage approach for recurrent and refractory cases: a single-center report

Kejun He, Xiaojun Yuan (✉), Zhen Tan

Department of Pediatric Hematology/Oncology, Xinhua Hospital Affiliated to Shanghai Jiao Tong University School of Medicine, Shanghai 200092, China

Abstract

Objective The aim of this study is to report the treatment result of childhood extracranial malignant germ cell tumors and discuss the experience for recurrent and refractory cases treatment from our center.

Methods We have retrospectively analyzed 58 extracranial malignant germ cell tumor patients treated with surgery and chemotherapy from our center over a 9-year period. Another 14 recurrent and refractory cases referred from other centers were added to the study for salvage approach. We evaluated the treatment results for primary cases and relapsed cases with a median follow-up of 61.5 months. Several factors were analysed to evaluate their power to the outcome of these cases.

Results The 5-year event-free and overall survival for primary cases were $74.1\pm 5.7\%$ and $86.2\pm 4.5\%$, respectively. 25 recurrent or refractory cases entered the salvage approach study, and 17 patients were alive till the end of follow-up. We demonstrated superior survival outcome for those with successful local control through pre-operative and post-operative radiotherapy, second-look surgery and multi-drug second-line chemotherapies.

Conclusion The outcome for childhood extracranial malignant germ cell tumors is generally favorable. For recurrent and refractory cases, multi-modality treatment approaches including radiotherapy, salvage chemotherapy and second-look surgery are important for better local control.

Key words: chemotherapy; germ cell tumor; radiotherapy; surgery; children

Received: 29 May 2019
Revised: 10 June 2019
Accepted: 25 June 2019

Germ cell tumors (GCTs) are infrequent in childhood, developing at a rate of 2.4 cases per million children and representing approximately 2% to 3% of cancers diagnosed in children and adolescents aged < 15 years^[1]. Extracranial GCTs can be categorized as gonadal or extragonadal according to their original sites. GCTs are derived from pluripotent precursor cells known as primordial germ cells, yet they can present as a heterogeneous group of tumors in distinct phenotype^[2]. Yolk sac tumors (YSTs), the most common pure malignant GCTs in young children, are confirmed if the precursor cells differentiate to resemble extraembryonic structures. Malignant teratomas (MTs) are teratomas containing at least one of the malignant germ cell elements. YSTs and MTs account

for most of the extracranial malignant germ cell tumors (MGCTs) in children and young adolescents^[3].

The treatment outcome for childhood MGCTs has greatly improved in the past two decades due to the introduction of platinum-based chemotherapy along with effective pediatric surgery and better supportive care^[4-6]. Despite these achievements, approximately 15% of the cases are recurrent or refractory. These cases would have dismal prognosis if no effective salvage treatment was performed, especially in patients from developing countries with limited medical resources^[4,7]. This report has two aims: (1) to study the result of current treatment with surgery and carboplatin, etoposide, bleomycin (JEB) regimen chemotherapy for extracranial MGCTs in

Chinese children and (2) to evaluate the safety and efficacy of the multimodality salvage approach for recurrent and refractory MGCT cases in our center.

Patients and methods

Patients diagnosed with MGCTs between March 2007 and December 2015 at Xin Hua Hospital Affiliated to Shanghai Jiao Tong University School of Medicine were enrolled. The recurrent or refractory cases along with cases referred from other centers during this period were analyzed in the study on the salvage approach. Recurrent cases were defined as cases that relapsed after remission, and refractory cases as no or minor response to conventional treatment. Clinical and laboratory data were collected from patients' medical records.

The diagnosis of MGCT was confirmed through histopathologic examination of surgical resection or biopsy specimen and serum tumor marker [α -fetoprotein (AFP) and β -human chorionic gonadotropin] test by experienced pathologists. Since AFP levels have a wide variation and variability in $t_{1/2}$ at different ages within the first year of life, we obtained established normal ranges at various ages as reference for evaluation^[8]. The Children's Oncology Group (COG) criteria of gonadal and extragonadal tumors were used for staging^[9]. Imaging evaluation for staging included computed tomography of the chest, brain, and original site and technetium-99m bone scan.

In our center, a multidisciplinary consultation of any patient suspected of having GCT was organized to discuss the probable histology and optimal surgical approach. Radical surgery would be performed if this was possible without major morbidity. Delayed resection following biopsy and neoadjuvant chemotherapy was implemented to prevent mutilating surgery and ensure complete resection afterward. When a high-risk procedure is encountered at presentation or malignant histologies are strongly suspected (elevated markers), biopsy could be omitted in the premise that surgery was planned in the short term. Radical inguinal orchiectomy was performed on the testicular tumor with high ligation of the spermatic cord. Coccygectomy was performed with excision of the original tumor in sacrococcygeal cases.

JEB regimen was used for chemotherapy in our center. Stage I testicular tumors were monitored after radical resection if the marker was negative. Otherwise, chemotherapy was performed. Chemotherapy was performed in patients with infantile immature teratoma who developed malignant YST recurrence. These children were categorized into the malignant teratoma group in the analysis. The JEB regimen consists of etoposide (120 mg/m² infusion on days 1–3), carboplatin (600 mg/m² infusion on day 2), and bleomycin (15 mg/m² infusion on

day 3). If the glomerular filtration rate (GFR) could be obtained, the formula for carboplatin dosage was used^[10]:

$$D \text{ (mg/m}^2\text{)} = \text{target AUC (mg}\cdot\text{min/mL)} \times [0.93 \times \text{GFR (mL/min/m}^2\text{)} + 15]$$

The target area under the plasma carboplatin concentration-vs-time curve (targetAUC) was set as 6 mg \cdot min/mL in the JEB regimen for MGCTs. Radiotherapy (RT) and second-look surgery were the major approaches for patients with recurrent and refractory tumors. Local irradiation with a total volume of 27.0–50.4 Gy was performed by the RT team of our center. Second-look surgery was performed to re-excise the lesion and sampling for histologic re-evaluation. We assessed and categorized tumor response after surgery as follows: R0, tumor totally removed, no residual tumor detectable macroscopically or microscopically; R1, tumor mostly removed, no tumor detectable macroscopically but residual tumor tissue detected microscopically; and R2, tumor resection, residual tumor detectable macroscopically.

Second-line chemotherapy regimens including PEI (cisplatin 20 mg/m² infusion on d1–5, etoposide 100 mg/m² infusion on days 1 to 5, and ifosfamide 1.5 g/m² infusion on d1–5)^[11] and IN (irinotecan 10 mg/m²/dose 5 days a week for 2 weeks and nedaplatin 100 mg/m² on d1)^[12–13] were preferred in cases with poor response to JEB regimen. Courses were conducted every 21–28 days depending on hematologic recovery. Chemotherapy response was indicated by a decrease in tumor in size in imaging or a satisfactory calculated decline in tumor marker. It was considered that remission was achieved when AFP levels had normalized, in which time imaging showed generally either confirmed remission or considerable reduction in tumor size. Two further courses were conducted after

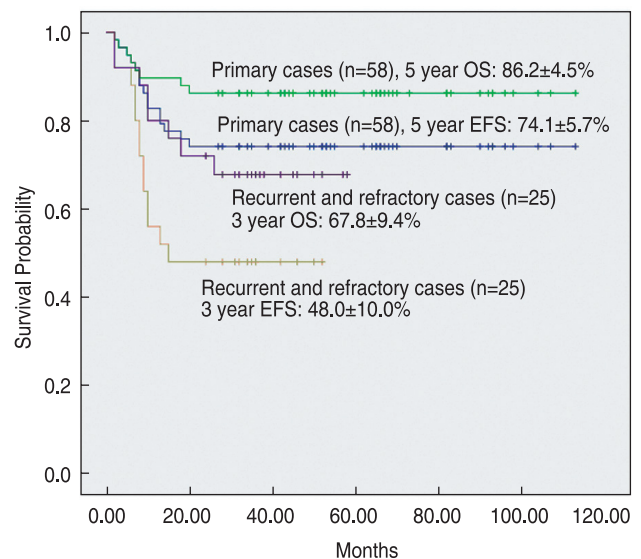


Fig. 1 Survival curve of two patient groups for EFS and OS

complete remission for consolidation. Patients with recurrent and refractory tumors were treated under the supervision of a multidisciplinary team of our center, and this treatment protocol for MGCTs was approved by the hospital's ethics committee. The general treatment plan for MGCTs was shown in Fig. 1.

The last follow-up date was December 31, 2017. Overall survival (OS) or event-free survival (EFS) was calculated as time (in months) from diagnosis to death of any cause or event. Event included disease progression, recurrence, or abandonment.

The tumor marker was examined monthly after treatment completion in the first year of follow-up, then every three months in the second and third years, and every six months in the fourth and fifth years. Physical examination and necessary imaging evaluation were also performed every visit.

The NCI Common Terminology Criteria for Adverse Events (CTCAE, version 4.03) was used in the toxicity assessment.

Data analysis was performed using Statistical Package for the Social Sciences version 20.0 (IBM, USA). The survival rates were reported as mean ± standard SE using the Kaplan-Meier method. Comparison of survival between the different groups was performed using the bilateral log-rank test. A *P*-value < 0.05 was considered statistically significant. A multivariate analysis using a proportional hazards model was conducted to identify risk factors and the risk model.

Results

In a 9-year period, 72 patients with MGCT were enrolled, with a median follow-up duration of 61.5 months (2–113 months). There were 30 boys and 42 girls.

Among 58 primary cases that were initially diagnosed and treated in our center, the subtypes included YST (46), malignant teratoma (11), and dysgerminoma (one ovarian case). The age of the patients ranged from 6 months to 12 years (due to the age limitation for admission) with a median of 26.5 months. According to the COG staging system, the numbers of cases classified as stages I, II, III, and IV were 12, 6, 24, and 16, respectively. The primary sites and their histologic diagnosis are summarized in Table 1. Four patients with stage I testicular YST underwent chemotherapy according to the guardians' strong willingness and physicians' approval and have EFS. The 5-year EFS and OS were 74.1 ± 5.7% and 86.2 ± 4.5%, respectively. At the end of the follow-up, stage I and II cases have good outcomes with 100% OS. Fourteen patients with testicular tumors, whose histologic types were exclusively YST, have EFS. The survival probability is shown in Fig. 2. The outcomes among different groups based on the clinical and biologic features were shown

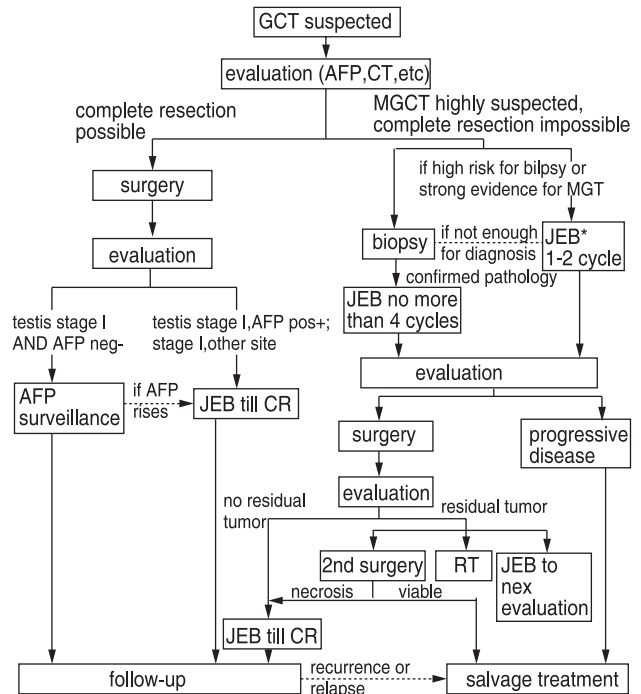


Fig. 2 General treatment schema for pediatric germ cell tumors in our center

in Table 2 and 3. No difference in EFS or OS was shown among different AFP groups.

Among 58 cases initially diagnosed in our center, 11 were recurrent and refractory. These cases, together with 14 referral cases, were studied in the salvage group. These patients were pretreated with surgery along with JEB or PEb chemotherapy. In this series with 25 patients, 7 patients had poor response, 13 had initial relapse, and 5 had multiple relapses. Among 16 patients who underwent second-look surgery, post-surgical evaluation demonstrated that 8 patients had finally achieved R0, 4 achieved R1, and 4 achieved R2. Further histopathologic examination revealed tumor necrosis in 9 specimens, malignant teratoma in 4, and viable tumor in 3. It should be noted that patients with R0 resection and necrotic tissue after second-look surgery survived. Eighteen patients underwent local irradiation. Preoperative irradiation of 18.0–23.4 Gy in 10–13 fractions was performed in 10 patients. Moreover, these patients received postoperative RT. Chemotherapy was performed in all 25 patients. Eleven received the same JEB regimen as initial treatment, 8 received JEB plus PEI regimens, and six received IN with JEB and PEI regimens. Except for five episodes that are unsuitable for response evaluation, the response rates of chemotherapy were 33.3% (2/6) in the poor response group, 55.5% (5/9) in the multiple relapse group, and 58.3% (7/12) in the initial relapse group. The clinical

Table 1 Characteristics of 58 patients with primary MGCT by tumor site (*n*)

	Testis (14)	Ovary (8)	Retroperitoneal and sacrococcygeal region (30)	Vagina (3)	Thorax (3)	Total
Age at diagnosis (years)						
0–1	0	0	4	1	0	5
1–5	11	1	24	2	0	38
5–12	3	7	2	0	3	15
Stage						
I	9	1	2	0	0	12
II	2	1	3	0	0	6
III	3	4	13	2	2	24
IV	0	2	12	1	1	16
AFP (ng/mL)						
< 10,000	11	4	7	1	2	25
10,000 to < 100,000	3	3	16	2	1	25
≥ 100,000	0	1	7	0	0	8
Histology						
Yolk sac tumor	14	4	24	3	1	46
Malignant teratoma	0	3	6	0	2	11
Others	0	1	0	0	0	1

Table 2 Survival analysis of malignant germ cell tumors based on different factors (*n*)

	No. of patients	5-year EFS (%)	<i>P</i> value	5-year OS (%)	<i>P</i> value
Sex					
Male	25	88.0 ± 6.5	0.042	96.0 ± 3.9	0.07
Female	33	63.6 ± 8.4		78.8 ± 7.1	
Age (years)					
< 1	7	57.1 ± 18.7	0.433	57.1 ± 18.7	0.033
1–5	36	75.0 ± 7.2		88.9 ± 5.2	
5–12	15	80.0 ± 10.3		93.3 ± 6.4	
Stage					
I	12	91.7 ± 8.0	0.314	100	0.074
II	6	83.3 ± 15.2		100	
III	24	70.8 ± 9.3		87.5 ± 6.8	
IV	16	62.5 ± 12.1		68.8 ± 11.6	
Sites					
Testis	14	100	0.047	100	0.222
Ovary	8	75.0 ± 15.3		87.5 ± 11.7	
Extragenital	36	63.9 ± 8.0		80.6 ± 6.6	
Histology					
YST	46	78.3 ± 6.1	0.147	87.0 ± 5.0	0.693
Non-YST	12	58.3 ± 14.2		83.3 ± 10.8	
AFP level (ng/mL)					
< 10,000	25	68.0 ± 9.3	0.113	88.0 ± 6.5	0.940
10,000–100,000	27	85.2 ± 6.8		85.2 ± 6.8	
≥ 100,000	6	50.0 ± 20.4		83.3 ± 15.2	

Recurrent and refractory cases (*n* = 25)**Table 3** Prognostic factors analysis of event-free and overall survival for 25 recurrent and refractory malignant germ cell tumors

Category	No. of patients	3-year EFS (%)	<i>P</i> value	3-year OS (%)	<i>P</i> value
Local irradiation					
Yes	18	50.0 ± 11.8	0.677	77.4 ± 10.0	0.045
No	7	42.9 ± 18.7		42.9 ± 18.7	
Second-look surgery					
Yes	16	62.5 ± 12.1	0.053	80.8 ± 10.0	0.025
No	9	22.2 ± 13.9		44.4 ± 16.6	

Table 4 Clinical parameters and treatment outcomes of 25 recurrent and refractory cases (*n*)

Patient No.	Months after		Recurrence times or Poor response	Sites of recurrence	Histology at		Post-surgical assessment ^a	AFP ^b	Radiation therapy ^c (Gy)	CT regimens	Reponse of CT ^d	Status ^e	Survival Time (months)
	Diagnosis	End of previous treatment			Diagnosis	Last Surgery							
1	8			Local	YST	/	/	↑↑	/	JEB	No	DOD	10
2	4	1	multiple	Local	YST	/	/	↑↑↑	/	JEB,PEI	Yes	PD	
	8	2		Combined		/	/	↑↑	/	JEB,PEI,IN	No	DOD	10
3	2	0	Poor response	Combined	YST	/	/	↑↑	/	JEB	No	DOD	2
4	5	0	Poor response	Local	YST	/	/	↑↑↑	/	JEB	No	DOD	2
5	13	6	1st	Local	YST	necrosis	R0	↑↑	45	JEB	Yes	2° CR	52+
6	8	1	1st	Local	YST	necrosis	R1	↑↑	45	JEB,PEI	Yes	SD	58+
7	3	0	Poor response	Local	MT	MT	R2	↑	18+27	JEB	No	2° CR	34+
8	15	9	1st	Local	MT	necrosis	R0	-	18+27	JEB	Yes	SD	38+
9	14	8	multiple	Local	YST	viable	R0	↑↑↑	23.4+21.6	JEB	No	PR	
	17	0		Local		necrosis	R0	↑↑	/	JEB,PEI,IN	No	PR	50+
10	10	4	multiple	Distant	MT	MT	R1	↑↑	/	JEB,PEI	N/A	PR	
	16	1		Local		/	/	↑	/	JEB,PEI	Yes	PR	
	22	2		Local		MT	R0	↑	/	JEB,PEI	Yes	SD	37+
11	16	7	1st	Local	MT	MT	R0	↑	23.4+27	JEB	No	SD	57+
12	6	2	Poor response	Distant	YST	/	/	↑↑	36	JEB,PEI,IN	Yes	PR	45+
13	4	1	multiple	Local	YST	/	/	↑↑↑	45	JEB	Yes	PR	
	6	0		Distant		/	/	↑↑	/	JEB,PEI	Yes	PD	
	13	1		Combined		/	/	↑↑↑	/	JEB,PEI,IN	No	DOD	15
14	21	13	1st	Local	MT	MT	R1	↑↑	45	JEB	N/A	2° CR	31+
15	9	3	1st	Distant	YST	necrosis	R1	↑↑↑	/	JEB,PEI,IN	No	SD	39+
16	7	2	multiple	Local	YST	necrosis	R1	↑↑	23.4+21.6	JEB,PEI	N/A	2° CR	
	15	3		Combined		necrosis	R0	↑↑	/	JEB,PEI	N/A	3° CR	28+
17	6	1	1st	Local	YST	necrosis	R2	↑↑	18+27	JEB,PEI	Yes	2° CR	42+
18	14	5	1st	Local	MT	viable	R2	↑↑	18+27	JEB	No	DOD	26
19	6	0	Poor response	Combined	MT	viable	R1	↑	18+27	JEB,PEI	No	DOD	18
20	8	2	1st	Local	YST	/	/	↑↑↑	45	JEB,PEI	No	DOD	8
21	9	2	1st	Local	YST	necrosis	R0	↑↑	/	JEB,PEI	Yes	2° CR	38+
22	7	1	1st	Local	YST	/	/	↑	45	JEB	Yes	2° CR	46+
23	10	3	1st	Local	YST	/	/	↑↑	45	JEB	Yes	2° CR	36+
24	6	2	Poor response	Local	YST	necrosis	R2	↑↑↑	18+27	JEB,PEI,IN	Yes	2° CR	24+
25	4	1	Poor response	Local	YST	viable	R0	↑↑	18+27	JEB,PEI	N/A	2° CR	36+

a: R0, tumor totally removed, no residual tumor detectable macroscopically or microscopically; R1, tumor mostly removed, no tumor detectable macroscopically but residual tumor tissue detected microscopically; R2, tumor resection, residual tumor detectable macroscopically.

b: ↑↑, <1,000 ng/mL; ↑↑↑, 1000-<10,000 ng/mL; ↑↑↑↑, >10,000 ng/mL.

c: Local volume of irradiation is shown as preoperative dose + postoperative dose. If not indicated, the entire dose was administered postoperatively.

d: CT, chemotherapy; chemotherapy response was indicated by a decrease in tumor in size in imaging or satisfactory calculated decline in tumor marker.

e: DOD, die of disease; CR, complete remission, the absence of any detectable disease, including normal serum levels of α-fetoprotein; PR, partial remission, the absence of new lesions and at least a 30% decrease in the sum of the longest diameters of target lesions; PD, progressive disease; on the basis of any of the following criteria: a ≥ 20% increase in the sum of the longest diameters of target lesions, new lesions, or disease sites or increases in the serum tumor levels; SD, stable disease, for responses that did not meet the criteria for complete remission, partial remission, or progressive disease.

parameters, treatment responses, and outcomes of these recurrent and refractory cases are shown in Table 4. With a median follow-up duration of 36 months, 17 patients survived, and the 3-year EFS and OS in the patients in this series were 48.0 ± 10.0% and 67.8 ± 9.4%, respectively. In the univariate analysis of prognostic factors, we found a significant difference in OS between patients treated

with or without local irradiation (77.4 ± 10.0% vs 42.9 ± 18.7%, *P* = 0.045) and those treated with or without second-look surgery (80.8 ± 10.0% vs 44.4 ± 16.6%, *P* = 0.025). All abovementioned factors were included in the multivariate Cox proportional-hazards regression model. The result revealed that no second-look surgery (*P* = 0.047; 95% confidence interval, 1.02–20.93) could

Table 5 Multivariate analysis with COX regression for recurrent and refractory cases

Factors	Number	HR ^a	95% CI ^b	P value
AFP < 10,000 ng/mL	10	2.43	0.45–13.18	0.302
No local irradiation	7	5.65	0.99–32.25	0.051
No second-look surgery	9	5.38	1.15–25.20	0.033

a: HR stands for hazard ratio

b: CI stands for confidence interval

Table 6 Toxicity of salvage chemotherapies

Factors	JEB (n = 97)	PEI (n = 37)	IN (n = 15)
Hematologic toxicity			
Grade 3/4 neutropenia	43	34	6
Grade 3/4 thrombocytopenia	37	34	5
Grade 3/4 infections	9	15	4
Next course delayed > 28 days	16	22	3
Hearing impairment	0	2	0
Renal toxicity			
Acute kidney injury	0	4	0
Hematuria	0	2	0
Tubular dysfunction	0	1	0
Ifosfamide induced neurotoxicity	/	1	/

be considered as individual factor contributing to shorter survival (Table 5).

Among 58 patients with primary tumors, 53 received a total of 278 courses of JEB regimen chemotherapy. The principal toxicities were hematologic abnormalities, mainly neutropenia and thrombocytopenia. A total of 37 courses of PEI and 15 courses of IN were performed in patients with recurrent and refractory tumors. We have observed neither secondary malignancy nor pulmonary fibrosis due to chemotherapy in survivors. Hearing impairment and renal toxicity were rare in patients treated with JEB regimen. One patient developed moderate ifosfamide-induced neurotoxicity and was detoxified with methylene blue. The chemotherapy complications are presented in Table 6.

Discussion

In this study, we enrolled children and adolescents aged < 12 years with extracranial MGCTs. We found that these children had generally good outcomes. The EFS and OS are slightly inferior compared to the COG or United Kingdom study group's result^[14]. Among 8 death events in our center, 4 occurred in the first six months after diagnosis. Two patients had just undergone one to two courses of chemotherapy and abandoned the treatment due to financial restraint and eventually died. One 10-month-old boy died due to severe infection after chemotherapy. With the gradual improvement of the

medical security system and supportive care in the last few years, the abandonment and treatment-related death rates in GCTs are now extremely low in our center.

Cisplatin-based PEb and carboplatin-based JEB regimens are both first-line chemotherapies for pediatric and adolescent patients with GCTs^[6,15]. Our hospital was one of the first few pediatric cancer centers in China that adopted JEB chemotherapy, and this study has shown the general outcome of childhood MGCTs in the Chinese population aged < 12 years. Due to the age limitation for admission in our center, histologic types, which are more prevalent in adolescents and young adults such as germinoma, embryonal carcinoma, choriocarcinoma, ovarian tumors, and testicular non-YSTs, are rarely observed in this age group. Therefore, the distribution of cases with respect to tumor site or histologic type and outcome of specific subgroups may have some difference from those in existing literature. Patients with stage I testicular tumor showed excellent outcomes and are recommended to undergo a “watch and see” strategy if the AFP level normalizes postoperatively^[16]. Four boys in the study had “overtreatment” of postoperative chemotherapy and had EFS. They were not excluded from the analysis.

Although the outcome of pediatric MGCTs with the combined effort of surgical resection and platinum-based chemotherapy is generally optimistic, a challenge still exists on improving the prognosis for recurrent and relapse cases, especially in a pediatric cancer institution with limited medical resources. In our study, recurrent and refractory cases among primary cases were organized and evaluated together with cases referred from other centers.

Increased serum AFP levels usually indicate either residual tumor postoperatively or tumor progression, and tumor relapses of MGCTs are always reflected in the AFP level. In the COG AGCT 0132 study, 23 of 25 patients with stage I ovarian tumors had elevated AFP levels at diagnosis, and all 12 relapse episodes were induced by AFP level elevation^[17]. In this study, 54 of 58 patients with primary MGCT had elevated serum AFP levels at diagnosis. Ten of eleven patients with recurrent and refractory tumors had elevated AFP levels during the occurrence of the event. A study on adult GCTs demonstrated that the rate of AFP level decline during chemotherapy has prognostic value independent of risk^[18]. Therefore, AFP was considered to be an ideal marker for tumor surveillance and response evaluation in chemotherapy.

Many children with recurrent GCTs will have local relapse rather than disseminated relapse in adults; therefore, multimodality efforts with the aim of achieving good local control are considered the mainstay of the salvage approach. In the German MAKEI study, the 5-year EFS and OS in all 22 patients with relapse MGCT

reached 0.3 ± 0.1 and 0.42 ± 0.11 , respectively, with salvage therapy and indicated that complete resection of the local lesion was critical in salvage treatment. For most relapse or refractory tumors, resection might be impossible when tumors have infiltrated adjacent nerves and bones because radical surgery can be mutilating. Preoperative platinum-based chemotherapy, combined with local regional thermochemotherapy, might facilitate complete tumor resection. Local irradiation with doses > 45 Gy contributed to a favorable outcome in patients with residual tumor^[19]. In the later MAKEI phase 2 study on regional deep hyperthermia for salvage treatment of children and adolescents with refractory or recurrent non-testicular MGCTs, a multimodal strategy integrating PEI-regional deep hyperthermia and surgical resection with or without radiation had successfully promoted the long-term outcome of these patients with treatment almost similar to those undergoing first-line treatment^[20]. However, regional deep hyperthermia is resource consuming and not accessible in many children's cancer centers. Besides postoperative RT, preoperative RT could be considered in childhood unresectable tumors to facilitate surgical resection. In studies on adult patients with rectal cancer, a relative improvement of 24% in disease-free survival was recorded in patients undergoing preoperative RT^[21]. Preoperative RT had shown its value in local control in pediatric and young adult patients with unresectable nonrhabdomyosarcoma soft-tissue sarcoma^[22]. We have observed some effects on the tumor shrinkage and inhibition of vascularization of preoperative irradiation in previous clinical practice. In this study, patients undergoing preoperative RT had achieved satisfactory outcomes (5/10 had complete remission, 1/10 had partial remission, 2/10 had stable disease, and 2/10 died of the disease) comparable to those in MAKEI PEI-regional deep hyperthermia salvage therapy.

The major goal of chemotherapy for relapse MGCTs should be bridging to complete tumor resection. The regimen administered before relapse or progression is an important concern. It seems that patients with recurrent sacrococcygeal MGCTs who were treated with less-intensive regimens (such as insufficient dose of etoposide and carboplatin) can be successfully treated with intensive chemotherapy^[23-24]. However, treatment of patients with an intensive pretreatment may be problematic^[18]. Studies on adults receiving GOP (gemcitabine, oxaliplatin, paclitaxel), TIP (paclitaxel, ifosfamide, cisplatin) and IN regimens for relapse GCTs indicated that platinum-based second-line chemotherapy might be utilized for recurrent and refractory childhood MGCTs to facilitate local control^[12, 25-26]. The initial chemotherapy in this cohort was mainly the JEB regimen. At the time of recurrence, JEB, PEI, and IN regimens had been administered to these patients. The single relapse group

had higher response rate to chemotherapy than the other two groups. Nishikawa et al. reported that IN regimen led to normalization of serum tumor marker levels in 45% of patients with relapse tumors who underwent surgical resection^[12]. Six patients (Nos. 2, 6, 10, 13, 17, 21) achieved response after PEI regimen, and 2 patients (Nos. 12, 14) showed responses to IN regimen after failure of JEB and PEI regimens. The efficacy of these salvage regimens needs to be further verified through a uniform study design. Patients with recurrent or refractory tumors treated with or without RT and second-look surgery have revealed a significant difference in survival rate. After including the AFP group, staging, and these factors in the multivariate Cox regression model, the multivariate analysis demonstrated that no surgery could be considered as individual factor contributing to poorer prognosis. This result has confirmed the viewpoint that a complete resection of local recurrent tumor represents the cornerstone of salvage treatment^[27]. We attribute this salvage rate in our center to the successful implementation of preoperative and postoperative local irradiation, second-line chemotherapy, careful surgery, and sincere cooperation of the multidisciplinary team in the children's cancer center. There were no treatment-related death, secondary malignancy, or lung fibrosis and few nephrotoxicities, ototoxicities, and neurotoxicities in the chemotherapy group in the median follow-up duration of 36 months. However, local irradiation in pediatric patients at the gonadal and extragonadal sites may cause a series of short-term and long-term side effects. Further follow-up is needed to observe the subacute and late visceral effects among survivors^[28-29].

Conclusion

The treatment result from our center for childhood extracranial MGCTs is generally optimistic. For recurrent and refractory cases, the treatment approaches for local control including pre- and postoperative RT, salvage chemotherapy such as PEI and IN regimens, and second-look surgery were successfully performed, and satisfactory outcomes were achieved without major morbidity.

Acknowledgments

We greatly appreciate the pediatric cancer multidisciplinary team from our center (including pediatric oncologists, surgeons, radiation therapists, radiologists, pathologists, specialty nurses, and social workers) for their collaborative work to the treatment plan and dedication to the care of our patients and their families.

Conflicts of interest

The authors indicate no potential conflicts of interest.

References

- Ward E, DeSantis C, Robbins A, *et al.* Childhood and Adolescent Cancer Statistics, 2014. *CA Cancer J Clin*, 2014, 64: 83–103.
- Schneider DT, Schuster AE, Fritsch MK, *et al.* Multipoint imprinting analysis indicates a common precursor cell for gonadal and nongonadal pediatric germ cell tumors. *Cancer Res*, 2001, 61: 7268–7276.
- Schneider DT, Calaminus G, Koch S, *et al.* Epidemiologic analysis of 1,442 children and adolescents registered in the German germ cell tumor protocols. *Pediatr Blood Cancer*, 2004, 42: 169–175.
- Mann JR, Pearson D, Barrett A, *et al.* Results of the United Kingdom Children's Cancer Study Group's malignant germ cell tumor studies. *Cancer*, 1989, 63: 1657–1667.
- Mann JR, Raafat F, Robinson K, *et al.* The United Kingdom Children's Cancer Study Group's second germ cell tumor study: carboplatin, etoposide, and bleomycin are effective treatment for children with malignant extracranial germ cell tumors, with acceptable toxicity. *J Clin Oncol*, 2000, 18: 3809–3818.
- Cushing B, Giller R, Cullen JW, *et al.* Randomized comparison of combination chemotherapy with etoposide, bleomycin, and either high-dose or standard dose cisplatin in children and adolescents with high-risk malignant germ cell tumors: a pediatric intergroup study-Pediatric Oncology Group 9049 and Children's Cancer Group 8882. *J Clin Oncol*, 2004, 22: 2691–2700.
- Wessalowski R, Kruck H, Pape H, *et al.* Hyperthermia for the treatment of patients with malignant germ cell tumors: a phase I/II study in ten children and adolescents with recurrent or refractory tumors. *Cancer*, 1998, 82: 793–800.
- Blohm ME, Vesterling-Horner D, Calaminus G, *et al.* Alpha 1-fetoprotein (AFP) reference values in infants up to 2 years of age. *Pediatr Hematol Oncol*, 1998, 15: 135–142.
- Rogers PC, Olson TA, Cullen JW, *et al.* Treatment of children and adolescents with stage II testicular and stages I and II ovarian malignant germ cell tumors: A Pediatric Intergroup Study-Pediatric Oncology Group 9048 and Children's Cancer Group 8891. *J Clin Oncol*, 2004, 22: 3563–3569.
- Marina NM, Rodman J, Shema SJ, *et al.* Phase I study of escalated targeted doses of carboplatin combined with ifosfamide and etoposide in children with relapsed solid tumors. *J Clin Oncol*, 1993, 11: 554.
- Farhat F, Culine S, Théodore C, *et al.* Cisplatin and ifosfamide with either vinblastine or etoposide as salvage therapy for refractory or relapsing germ cell tumor patients: the Institut Gustave Roussy experience. *Cancer*, 1996, 77: 1193–1197.
- Nishikawa M, Miyake H, Fujisawa M. Irinotecan and nedaplatin as salvage therapy for patients with advanced germ cell tumors following intensive treatment with cisplatin-based combination chemotherapies. *Int J Clin Oncol*, 2016, 21: 162–167.
- Bagatell R, London WB, Wagner LM, *et al.* Phase II study of irinotecan and temozolomide in children with relapsed or refractory neuroblastoma: a Children's Oncology Group study. *J Clin Oncol*, 2011, 29: 208–213.
- Frazier AL, Hale JP, Rodriguez-Galindo C, *et al.* Revised risk classification for pediatric extracranial germ cell tumors based on 25 years of clinical trial data from the United Kingdom and United States. *J Clin Oncol*, 2015, 33: 195–201.
- Williams SD, Birch R, Einhorn LH, *et al.* Treatment of disseminated germ-cell tumors with cisplatin, bleomycin, and either vinblastine or etoposide. *N Engl J Med*, 1987, 316: 1435–1440.
- Schlatter M, Rescorla F, Giller R, *et al.* Excellent outcome in patients with stage I germ cell tumors of the testes: a study of the Children's Cancer Group/Pediatric Oncology Group. *J Pediatr Surg*, 2003, 38: 319–324.
- DF Billmire, JW Cullen, FJ Rescorla. *et al.* Surveillance after initial surgery for pediatric and adolescent girls with stage I ovarian germ cell tumors: report from the Children's Oncology Group. *J Clin Oncol*, 2014, 32: 465–470.
- Mazumdar M, Bajorin DF, Bacik J, *et al.* Predicting outcome to chemotherapy in patients with germ cell tumors: the value of the rate of decline of human chorionic gonadotrophin and alpha-fetoprotein during therapy. *J Clin Oncol*, 2001, 19: 2534–2541.
- Schneider DT, Wessalowski R, Calaminus G, *et al.* Treatment of recurrent malignant sacrococcygeal germ cell tumors: analysis of 22 patients registered in the German protocols MAKEI 83/86, 89, and 96. *J Clin Oncol*, 2001, 19: 1951–1960.
- Wessalowski R, Schneider DT, Mils O, *et al.* Regional deep hyperthermia for salvage treatment of children and adolescents with refractory or recurrent non-testicular malignant germ-cell tumours: an open-label, non-randomised, single-institution, phase 2 study. *Lancet Oncol*, 2013, 14: 843–852.
- Sebag-Montefiore D, Stephens RJ, Steele R, *et al.* Preoperative radiotherapy versus selective postoperative chemoradiotherapy in patients with rectal cancer (MRC CR07 and NCIC-CTG C016): a multicentre, randomised trial. *Lancet*, 2009, 373: 811–820.
- Smith KB, Indelicato DJ, Knapik JA, *et al.* Definitive radiotherapy for unresectable pediatric and young adult nonrhabdomyosarcoma soft tissue sarcoma. *Pediatr Blood Cancer*, 2011, 57: 247–251.
- Baranzelli MC, Kramar A, Bouffet E, *et al.* Prognostic factors in children with localized malignant nonseminomatous germ cell tumors. *J Clin Oncol*, 1999, 17: 1212–1218.
- Schneider DT, Calaminus G, Reinhard H, *et al.* Primary mediastinal germ cell tumors in children and adolescents: results of the German cooperative protocols MAKEI 83/86, 89, and 96. *J Clin Oncol*, 2000, 18: 832–839.
- Bokemeyer C, Oechsle K, Honecker F, *et al.* Combination chemotherapy with gemcitabine, oxaliplatin, and paclitaxel in patients with cisplatin-refractory or multiply relapsed germ-cell tumors: a study of the German Testicular Cancer Study Group. *Ann Oncol*, 2008, 19: 448–453.
- Kondagunta GV, Bacik J, Donadio A, *et al.* Combination of paclitaxel, ifosfamide, and cisplatin is an effective second-line therapy for patients with relapsed testicular germ cell tumors. *J Clin Oncol*, 2005, 23: 6549–6555.
- Göbel U, Schneider DT, Calaminus G, *et al.* Multimodal treatment of malignant sacrococcygeal germ cell tumors: A prospective analysis of 66 patients of the German cooperative protocols MAKEI 83/86 and 89. *J Clin Oncol*, 2001, 19: 1943–1950.
- Kenney LB, Cohen LE, Shnorhavorian M, *et al.* Male reproductive health after childhood, adolescent, and young adult cancers: a report from the Children's Oncology Group. *J Clin Oncol*, 2012, 30: 3408–3416.
- Wo JY, Viswanathan AN. Impact of radiotherapy on fertility, pregnancy, and neonatal outcomes in female cancer patients. *Int J Radiat Oncol Biol Phys*, 2009, 73: 1304–1312.

DOI 10.1007/s10330-019-0362-2

Cite this article as: He KJ, Yuan XJ, Tan Z. Treatment results of childhood extracranial malignant germ cell tumors and the salvage approach for recurrent and refractory cases: a single-center report. *Oncol Transl Med*, 2019, 5: 229–236.

Efficacy and safety of combined decitabine and ruxolitinib in the treatment of chronic myelomonocytic leukemia*

Jiaming Li, Sujiang Zhang (✉), Yubao Chen, Zeying Yan, Ying Wang, Zhiyin Liu, Haimin Sun, Yu Chen

Department of Hematology, Ruijin Hospital North affiliated to Shanghai JiaoTong University School of Medicine, Shanghai 201800, China

Abstract

Objective The aim of the study was to evaluate the clinical efficacy of decitabine (DEC) combined with ruxolitinib (RUX) in the treatment of chronic myelomonocytic leukemia (CMML).

Methods The clinical characteristics of 12 patients with CMML were analyzed retrospectively and subsequent target sequencing was performed to investigate the efficacy of the combined treatment with DEC and RUX and the molecular signatures therein.

Results Among the 12 cases, clinical improvement was observed in all patients (100%), spleen reduction was observed in six patients (67%), and hematologic improvement was observed in four patients (33%). In the CMML-1 group, the overall response was 50% (3/6), one case achieved complete response, one achieved bone marrow remission, and one achieved hematological improvement. In the CMML-2 group, the overall response was 17% (1/6), one case achieved complete response, four showed disease progression (PD), and one exhibited no response. As expected, ASXL1 mutation was predictive for the outcome of CMML (hazard ratio of 2.97, 95% confidence interval of 1.21–7.06; $P = 0.02$).

Conclusion The use of DEC combined with RUX in the treatment of CMML effectively improved the clinical response and quality of life, especially for CMML-1 patients. Ongoing clinical trials will further evaluate the safety and efficacy of this novel therapeutic approach.

Key words: decitabine (DEC); ruxolitinib (RUX); chronic myelomonocytic leukemia (CMML)

Received: 8 April 2019
Revised: 29 August 2019
Accepted: 20 September 2019

Chronic myelomonocytic leukemia (CMML) is a clonal disease of bone marrow hematopoietic stem cells. Its incidence rate is approximately 1 to 2 in 100 000, and it occurs more commonly among the elderly, with a median age of onset of 65–75 years. The survival period is 20 to 40 months, and 15% to 30% of patients experience progression into acute leukemia. However, CMML is not treated satisfactorily. We retrospectively analyzed the clinical features and efficacy of decitabine (DEC) combined with ruxolitinib (RUX) in six patients with CMML-1 and six patients with CMML-2.

Patients and methods

Patients

This observational study began in 2016 and is currently ongoing. Ethical approval for the study was obtained from Ruijin Hospital affiliated to Shanghai JiaoTong University School of Medicine, China. The inclusion criteria of all patients included diagnosis of CMML according to the guidelines of the American Society of Hematology, with a duration of less than one month. Table 1 summarizes the patients' main characteristics at baseline. There were 8 males and 4 females, with a median age of 63 (38–72) years. The median percentage of primitive monocytes in

✉ Correspondence to: Sujiang Zhang. Email: zsj721108@163.com.

* Supported by a grant from the Fund of Ruijin Hospital North affiliated to Shanghai JiaoTong University School of Medicine (No: 2018ZY03).

© 2019 Huazhong University of Science and Technology

Table 1 Baseline patient demographics (n)

	CMML-1 (n = 6)	CMML-2 (n = 6)	All (n = 12)
Median age (years)	61 (38–68)	63 (60–72)	63 (38–72)
Male	5	3	8
Female	1	3	4
ECOG			
0–1	1 (16.7%)	0 (0.0%)	1 (8.0%)
2–3	5 (83.3%)	6 (100.0%)	11 (92.0%)
Gene mutation			
TET2	4 (66.7%)	3 (50.0%)	7 (58.0%)
ASXL1	4 (66.7%)	1 (16.7%)	5 (42.0%)
SRSF2	2 (33.3%)	3 (50.0%)	5 (42.0%)
NRAS	1 (16.7%)	2 (33.3%)	3 (25.0%)
DNMT3A	0 (0.0%)	1 (16.7%)	1 (8.0%)
JAK2	0 (0.0%)	2 (33.3%)	2 (16.7%)
TP53	0 (0.0%)	1 (16.7%)	1 (8.0%)
RUNX1	1 (17.7%)	1 (16.7%)	2 (16.7%)
Blasts	9% (3%–9%)	13% (12%–17%)	
Karyotype			
Normal	4 (66.7%)	4 (66.7%)	8 (67.0%)
Complex	2 (33.3%)	1 (16.7%)	3 (35.0%)

the bone marrow smear and number of white blood cells in the peripheral blood among all patients were 11% (3%–17%) and $17 (6–27) \times 10^9$ cells/L, respectively. The level of hemoglobin and the number of platelets decreased, with a median of 45 (36–97) g/L and $40 (10–234) \times 10^9$ cells/L, respectively. Abdominal B ultrasound showed that nine patients had different degrees of splenomegaly, the largest with a spleen thickness of 96 mm and a long diameter of 228 mm.

Gene sequencing

After initial diagnosis and treatment, bone marrow was extracted from the patients and sent to Shanghai Aositai

Biotechnology (China) for DNA sequencing. Detection of 22 myelodysplastic syndrome (MDS)/myeloproliferative neoplasm (MPN) genome sets including SF3B1, SRSF2, U2AF1, DNMT3A, Iso-lemon IDH1, IDH2, TET2, TP53, RUNX1, NRAS, EZH2, JAK2, CBL, ETV6, and ASXL1 was performed. We found four patients with CBL gene mutations, three with SRSF2 gene mutations, three with TET2 gene mutations, two with ASXL1 gene mutations, one with RUNX1 gene mutation, one with SETBP1 gene mutation, one with NRAS gene mutation, and one with JAK2 gene mutation.

Administration and criteria for response

Treatment was determined based on the patient's condition and willingness. DEC at 20 mg/(m²·d), on days 1–3 and RUX at 5–20 mg, qd (adjusted according to the number of platelets), on days 1–28, were administered every 4–6 weeks during one course of treatment (Table 2). Bone marrow evaluation (including cytogenetic and molecular studies) was performed at the end of each course of treatment. Therapy continued until disease progression was observed, unacceptable toxicity has developed, concurrent illness prevented further treatment, or the patient requested withdrawal from the study. Prevention of infection, blood transfusion of components, and other supportive treatment during the period of myelosuppression were acceptable. The criteria for response to treatments according to the literature^[1] were as follows: complete remission (CR), bone marrow remission (mCR), hematologic improvement (HI), no response (NR), and disease progression (PD).

Follow-up

The follow-up period began on the date of treatment after the diagnosis of the disease, and the follow-up deadline was July 1, 2019. Follow-up was conducted by

Table 2 The efficacy of DEC and RUX in the treatment of CMML

Patient	Starting dose of Rux	Maintenance dose of Rux	Duration of Rux (months)	Number of cycles of therapies	Sequence of treatment	Duration of follow-up (months)
1	5 mg bid	5 mg bid	9	3	DEC + RUX	15
2	5 mg bid	5 mg bid	4	1	DEC + RUX	22
3	5 mg qd	5 mg qd	5	1	DEC + RUX	9
4	5 mg qd	5 mg qd	1	4	DEC + RUX	13
5	5 mg bid	5 mg bid	19	3	DEC + RUX	19
6	5 mg bid	5 mg bid	1	1	RUX + DEC	1
7	5 mg bid	10 mg bid	13	2	RUX + DEC	17
8	5 mg bid	10 mg bid	7	5	RUX + DEC	23
9	5 mg bid	5 mg bid	1	3	DEC + RUX	9
10	5 mg bid	5 mg bid	4	3	DEC + RUX	13
11	5 mg qd	5 mg qd	3	4	DEC + RUX	15
12	5 mg bid	5 mg bid	8	6	DEC + RUX	28

Note: bid, twice a day; qd, once a day

telephone contact.

Results

Efficacy of treatment

Some objective responses (clinical improvement, spleen reduction, and hematologic improvement) were evaluated. Before treatment, constitutional symptoms (fatigue, fever, chills, night sweats, and loss of muscle mass) were present in CMML patients. After treatment, there were some improvements in terms of fatigue, loss of muscle mass, and weight loss in all patients. The spleen sizes of six patients (67%) were reduced to various extents compared to those before treatment. For example, palpable splenomegaly decreased to 9 cm in case 1, 8 cm in case 9, and 4 cm in case 11. At the time of diagnosis, red blood cell (RBC) transfusion was required every two weeks for case 1, 2, 8, and 12. After two cycles of treatment, RBC transfusion was required on a monthly basis.

The efficacy of treatment was also evaluated. The overall response rate of all patients to the combination of DEC and RUX was 33%. In the CMML-1 group, the overall response was 50% (3/6), one case achieved CR, one achieved mCR, one achieved HI, two had NR, and one showed PD. In the CMML-2 group, the overall response was 17% (1/6), one case achieved CR, one had NR, and four showed PD. The efficacy and outcome of the 12 patients after treatment are shown in Table 3.

Safety of treatment

All patients completed the therapeutic schedule for more than one cycle. DEC and RUX were well tolerated, although some patients experienced mild gastrointestinal

reactions such as nausea, vomiting, and diarrhea. Myocardial suppression occurred in 10 patients after chemotherapy. Among them, myelosuppression was the most severe and the longest period of myelosuppression was observed in case 1, 7, and 10. The computed tomography chest scans of case 1, 2, 3, 7, and 10 showed pulmonary infection. These patients were treated with active anti-infection (anti-bacterial and anti-fungal) agents, and all of them showed improvements after treatment.

Molecular genetic abnormalities

Three patients showed complex karyotype abnormalities, two being in the CMML-1 group (45, XY, -7, -5q karyotype, with ASXL-1 and TET2 gene mutations; 48, XY, +8, +10 karyotype, with ASXL-1 and RUNX1 gene mutations) and one in the CMML-2 group (47, XY, +8 karyotypes, with JAK2, TET2, and SRSF2 gene mutations).

According to the results of 22 MDS/CMML-related gene mutations, positive mutations were detected in all patients. Further analysis of the effect of gene mutations on the response rate revealed that two patients with TET2 mutations showed HI and mCR, two with NRAS mutations showed HI and CR, three with ASXL1 mutations showed PD, two with ASXL1 mutations showed NR, two with JAK2 and TET2 mutations obtained PD, one with TP53 mutation in the CMML-2 group showed PD, and one with RUNX1 mutation showed PD. The ASXL1 mutation was common among CMML patients, and it is predictive for the outcome of CMML (hazard ratio of 2.97, 95% confidence interval of 1.21–7.06; $P = 0.02$).

Table 3 Clinical outcomes of CMML patients treated with DEC and RUX

Case	Constitutional symptom (pre-Tx)	Improvement in symptoms (post-Tx)	Spleen size (cm)		Peripheral blasts (%)		Response
			Pre-Tx*	Post-Tx**	Pre-Tx*	Post-Tx**	
1	F, NS, WL, LM	All	23	14	4	5	HI
2	F, LM, F/C	All	15	14	9	13	NR
3	F, WL, P	Weight gain	19	15	7	37	PD
4	F, NS, WL, F/C	Weight gain	N	N	15	17	PD
5	F, NS, P, F/C	All	23	21	3	1	CR
6	F, NS, WL, LM, F/C	Weight gain	14	13	15	24	PD
7	F, NS, LM, F/C	All	23	21	7	18	NR
8	F, P, F/C	No fever	18	10	17	30	PD
9	F, WL, F/C	Weight gain, No fever	12	11	14	42	PD
10	F, NS, WL	All	13	9	13	16	NR
11	F, NS, P	All	N	N	4	1	mCR
12	F, NS, F/C	All	N	N	15	3	CR

Note: Tx, treatment; F, fatigue; NS, night sweats; WL, weight loss; LM, loss of muscle mass; P, pruritus; F/C, fever and chills. * Pre-Tx: spleen size and peripheral blood blast percentage values were collected prior to initiation of either ruxolitinib or DNMT inhibitors. ** Post-Tx: spleen size and peripheral blood blast percentage values were collected when patients were on stable doses of both treatments

Discussion

CMML is a rare and often aggressive myeloid malignancy characterized by features of both MDS and MPNs. Therefore, therapeutic options for CMML are largely developed from those dealing with MDS and MPNs. CMML has shown poor prognosis, and effective treatment options are limited but include hydroxyurea, low-dose chemotherapy, supportive care, and hematopoietic stem cell transplantation. Because of comorbidities, poor tolerance to chemotherapy, and the lack of indication of transplantation, most elderly patients choose supportive treatment. Recently, a number of novel approaches using unapproved therapies (lenalidomide, ruxolitinib, sotatercept, and tipifarnib) have demonstrated some efficacy in CMML^[2].

Hypomethylating agents (HMAs) are usually the standard first-line therapy used to reverse the DNA methylation process and induce tumor cell differentiation or apoptosis. Many recent studies have attempted to identify CMML patients that can most likely benefit from HMAs^[3-5]. RUX is a Janus kinase (JAK)1/2 inhibitor for the treatment of myeloproliferative diseases that can inhibit tumor proliferation and thus achieve a significant spleen-reducing effect. Notably, responses were seen even in the absence of detectable JAK2 mutations. Recently, RUX has shown good efficacy in CMML-1 patients with high white blood cell count, and this drug can still effectively improve clinical symptoms and reduce the proportion of bone marrow blast cells after the failure of HMA treatment^[6-7]. The 12 CMML patients reported in this study revealed that a combination of DEC and RUX may be a safe and effective treatment scheme in CMML patients.

In this study, the complementary effects of DEC and RUX resulted in symptomatic relief and hematological improvement, potentially addressing relevant contributors to disease pathogenesis. In particular, 67% of the patients exhibited spleen reduction to varying degrees, 33% showed a decrease in the frequency of RBC transfusion, and some clinical improvement (fatigue, loss of muscle mass, and weight loss) was present in all patients. In addition, the combination of DEC and RUX in the treatment of CMML-1 achieved an effective response rate of 50%. Based on the results of this study, we confirmed the combination of DEC and RUX was safe and tolerable. Although patients treated with 20 mg of RUX attained the greatest blast count and spleen size reduction, patients treated with 5 mg of RUX were able to continue therapy for a longer duration. Collectively, this regimen may serve as a basis to which other novel/targeted therapeutic agents may be added to further improve efficacy against CMML.

Many studies have focused on somatic mutations as

drivers of pathogenesis in CMML patients, with the TET2 gene showing higher mutation frequency, followed by SRSF2, ASXL1, and RAS. Based on the results of the single-cell follow-up test, the priming-driven mutation of CMML occurred in TET2 and ASXL1^[8-9]. Patnaik and colleagues identified TET2-mutant patients without the ASXL1 mutation to have improved overall survival in comparison to non-mutant patients, who had the shortest survival^[10]. In this study, we further evaluated the impact of the ASXL1 mutation on the outcome of CMML. Indeed, three patients with ASXL1 mutations showed PD and two showed NR. It was suggested that the ASXL1 mutation is predictive for inferior outcome in CMML. Future studies will evaluate the functional consequence on protein function based on the type of ASXL1 mutation.

In summary, the preliminary results of this study showed that DEC combined with RUX effectively ameliorated the clinical symptoms and improved the quality of life of CMML patients. Because of the small number of participants and short follow-up period in this study, the safety and efficacy of DEC and RUX require further evaluation in large-scale clinical trials.

Ethics approval and consent to participate

Patient data were used after obtaining approval from the Ethics Committee of Ruijin Hospital affiliated to Shanghai JiaoTong University School of Medicine, China.

Conflicts of interest

The authors indicate no potential conflicts of interest.

References

1. Savona MR, Malcovati L, Komrokji R, *et al.* An international consortium proposal of uniform response criteria for myelodysplastic/myeloproliferative neoplasms (MDS/MPN) in adults. *Blood*, 2015, 125: 1857–1865.
2. Elmariah H, DeZern AE. Chronic myelomonocytic leukemia: 2018 update to prognosis and treatment. *Curr Hematol Malig Rep*, 2019, 14: 154–163.
3. Santini V, Allione B, Zini G, *et al.* A phase II, multicentre trial of decitabine in higher-risk chronic myelomonocytic leukemia. *Leukemia*, 2018, 32: 413–418.
4. Hunter AM, Zhang L, Padron E. Current management and recent advances in the treatment of chronic myelomonocytic leukemia. *Curr Treat Options Oncol*, 2018, 19: 67.
5. Zeidan AM, Hu X, Long JB, *et al.* Hypomethylating agent therapy use and survival in older patients with chronic myelomonocytic leukemia in the United States: A large population-based study. *Cancer*, 2017, 123: 3754–3762.
6. Francke S, Mies A, Meggendorfer M, *et al.* Disease-modifying activity of ruxolitinib in a patient with JAK2-negative CMML-2. *Leuk Lymphoma*, 2017, 58: 1271–1272.
7. Padron E, DeZern A, Andrade-Campos M, *et al.* A multi-institution phase I trial of ruxolitinib in patients with chronic myelomonocytic leukemia (CMML). *Clin Cancer Res*, 2016, 22: 3746–3754.

8. Sallman DA, Komrokji R, Cluzeau T, *et al.* ASXL1 frameshift mutations drive inferior outcomes in CMML without negative impact in MDS. *Blood Cancer J*, 2017, 7: 633.
9. Patnaik MM, Tefferi A. Chronic myelomonocytic leukemia: 2018 update on diagnosis, risk stratification and management. *Am J Hematol*, 2018, 93: 824–840.
10. Patnaik MM, Lasho TL, Vijayvargiya P, *et al.* Prognostic interaction between ASXL1 and TET2 mutations in chronic myelomonocytic leukemia. *Blood Cancer J*, 2016, 6: e385.

DOI 10.1007/s10330-019-0349-9

Cite this article as: Li JM, Zhang SJ, Chen YB, *et al.* Efficacy and safety of combined decitabine and ruxolitinib in the treatment of chronic myelomonocytic leukemia. *Oncol Transl Med*, 2019, 5: 237–241.

Expression of HERG in musculoskeletal tumors with different degrees of malignancy*

Lu Gan, Mo Li (Co-first author), Tongtao Yang (Co-first author), Jin Wu, Junjie Du, Zhuojing Luo (✉), Yong Zhou (✉)

Department of Orthopedics, Air Force Medical University, Xi'an 710032, China

Abstract

Objective The expression of HERG in common bone tumors is scarcely reported and there is a lack of dedicated studies. This study aimed to investigate the expression of HERG in several common musculoskeletal tumors.

Methods Immunohistochemical staining, RT-PCR, and Western blotting were used to observe HERG expression differences in various tissues and cell lines.

Results HERG was differentially expressed in different malignant tumors, both at a differential protein level and localization within tumors. HERG was not expressed in normal bone tissue. The HERG inhibitor E-4031 markedly inhibited the proliferation of osteosarcoma cell lines.

Conclusion HERG was highly expressed in malignant tumors. Blocking of HERG can effectively inhibit the proliferation of bone tumors.

Key words: HERG; potassium ion channel; musculoskeletal tumors; expression

Received: 26 August 2019
Revised: 29 September 2019
Accepted: 17 October 2019

Human Ether-a-go-go Related Gene (HERG) potassium channels play an important role in repolarization in cardiac action potentials. However, recent evidence has suggested a role for HERG in the proliferation and progression of multiple types of cancers, which may make it an attractive target for cancer therapy [1]. It has been confirmed that the existence of encoded potassium ion channels within tumor cell membranes has the ability to control the communication current of the cells. This can result in cell membrane depolarization at a deeper level due to specific biophysical properties [2]. HERG channels were reportedly expressed in tumor cell lines of various origins [3–4]. Additionally, HERG expression has been described in an array of human primary tumors including endometrial cancer, acute myeloid leukemia, and lymphocytic leukemia [5–7]. As is well known, tumorigenesis is a complex process. However, there is insufficient information regarding the expression of HERG in common bone tumors. Hernandez *et al* found that a significant anti-proliferative effect was associated with the HERG potassium channel in rat osteosarcoma

cells [8]. The BKCa potassium channel has the ability to inhibit osteosarcoma growth [9]. However, it is still unclear what the relationship of the HERG potassium channel is to the phenotype of bone tumors. Specifically, the questions that remain are if differences exist in HERG expression levels in bone tumors of various origins as well as malignant bone tumors. Using clinical bone tumor specimens with different degrees of malignancy, this study reports the expression levels of HERG and its correlation with bone tumor malignancy.

Materials and methods

Immunohistochemistry

Specimen collection

With the consent of the patients themselves and their families, 60 bone tumor patients (38 males and 22 females) were collated according to the requirements of the Medical Association. Specimens were collected in the operating room of our department from June 2007 to December 2009. Twenty-five and 35 patients were

✉ Correspondence to: Zhuojing Luo. Email: zjluo@fmmu.edu.cn
Yong Zhou. Email: gukezy@fmmu.edu.cn

* Supported by a grant from the Key Research and Development Program of Shaanxi Province Project (No. 2018YBXM-SF-12-2).
© 2019 Huazhong University of Science and Technology

characterized as having malignant and benign tumors, respectively.

Immunohistochemical staining

After routine de-waxing, tumor slices were treated with 3% hydrogen peroxide for 10 min and the antigen was retrieved using the microwave method. The primary antibody (CHEMICON Inc., AB5908-200 UL) was added and incubated at 4 °C overnight. The goat anti-mouse secondary antibody was subsequently added. Samples were washed with PBS and stained with DAB and HE. Slices were observed using a microscope camera, which was connected to a computer with auxiliary programs to capture images.

HERG mRNA expression level detection within different tumors using RT-PCR

Samples of approximately 1 g were selected for total RNA extraction and treated with TRIZOL (Invitrogen, USA). Total RNA extraction was conducted with an extraction kit (BETEKE, China).

cDNA synthesis

The TOYOBO First Strand cDNA Synthesis Kit was used. Briefly, 20 µL of reaction mix, 1 µL of Oligo (dT) 20, 1 µL of template RNA, and 9 µL of DEPC water were centrifugally mixed. After 5-min incubation at 65 °C, samples were put on ice and 4 µL of 5 × buffer, 1 µL of RNA inhibitor, 2 µL of dNTP mixture, and 1 µL of Rever TraAce were added. After centrifugal mixing, samples were incubated at 25 °C for 5 min, and 1 µL of reverse transcriptase was added. The reaction then proceeded at 30 °C for 10 min, 42 °C for 20 min, 85 °C for 5 min, and 4 °C for 5 min.

Polymerase chain reaction

Using β-actin as a control, HERG was amplified with PCR. The primers were as follows: HERG, 5'-AGA TGC TGC GGG TGC GG-3', 5'-CGA AGG CAG CCC TTG GTG-3'; β-actin, 5'-TCC ACC TTC CAG CAG ATG TG-3', 5'-GCA TTT GCG GTG GAC GAT-3'. The reaction system volume was 25 µL. The PCR reaction conditions for HERG were 98 °C for 10 min, 72 °C for 1 min, 94 °C for 40 s, 66 °C for 40 s, and 72 °C for 17 s for 35 cycles, with a final extension at 72 °C for 10 min. The PCR reaction conditions for β-actin were 94 °C for 2 min, 94 °C for 30 s, and 68 °C for 30 s for 35 cycles, with a final extension at 68 °C for 7 min.

Identification and analysis of PCR products

PCR products (20 µL) were separated using electrophoresis with a 15 g/L agarose gel with 70 V voltage electrophoresis. Observations and photographic results were recorded. Bands of the target and control genes were analyzed by BIORAD UNIVERSAL HOOD II-type gel imaging pixel.

Protein level detection of HERG (Western blot)

Protein extraction

Tissue from surgical excisions was weighed and cut into several smaller pieces. The pieces were put into a homogenizer per net weight, and the appropriate volume of lysis buffer was added. Supernatants were collected after centrifugation. Laemmli buffer was added to the supernatants, which were then further homogenized. The mixed sample was centrifuged at 10,000 g for 10 minutes before the supernatant was transferred to another tube. The sample was then ready for electrophoresis. Protein (50 µg) was loaded per lane for sodium dodecyl sulfate-polyacrylamide gel electrophoresis (SDS-PAGE). Samples were subsequently transferred to a nitrocellulose membrane. The membrane was blocked with skimmed milk powder and rinsed with TBST buffer 3 times for 10 min each time. Rabbit anti-HERG polyclonal antibody was added and incubated at 4 °C overnight. Horseradish peroxidase-labeled goat anti-rabbit secondary antibody was added and incubated for 2 h with oscillation at room temperature. A chemiluminescence color development system with light-sensitive X-ray film imaging was used to visualize the protein bands. The experiment was repeated twice.

Effect of K⁺ channel inhibitors on the proliferation of human osteosarcoma cells

Method

Cells in the logarithmic phase were collected and the concentration of the cell suspension was adjusted. 100 µL of the cell suspension containing 1,000–10,000 cells was added to each well. These were incubated in 5% CO₂ at 37 °C until the bottom of the wells were covered with single cell layer. A drug inhibitor was added after the adhesion of the cells. Cells were again incubated in 5% CO₂ at 37 °C for 16–48 h. The medium was carefully removed from each well and 50 µL of MTT solution (5 mg/mL or 0.5% MTT) was added into each well with a subsequent 4 h incubation. 150 µL of DMSO was added to each well. The plate was shaken with a low-speed oscillation for 10 min to fully dissolve the DMSO crystals. Absorption at OD 490 nm was measured with an enzyme-linked immunoassay instrument. The blank well and control well were used for calculations.

Results

In order to effectively observe the expression of HERG in tumor tissue, 57 cases of patients with bone tumors were selected in accordance with the common collate classification of bone tumors (Table 1). A normal human bone specimen was selected as a control. Immunohistochemical staining was used to detect the expression levels of HERG as well as western blot. RT-

Table 1 Classification of common bone tumors

Category	Benign (cases)	Malignant (cases)
Osteoplastic tumor	Benign osteblastoma (3)	Osteosarcoma (12); osteblastoma (1)
Cartilaginous tumors	Enchondrosis (1), chondroma (2), benign chondroblastoma (1), cartilage Fibroma (1)	Chondrosarcoma (6); malignant chondroblastoma (3); mesenchymal chondrosarcoma (2); dedifferentiated chondrosarcoma (0)
Multinucleated giant cell	Benign bone giant cell tumor (1)	Malignant bone giant cell tumor (2)
Marrow source tumor		Ewing sarcoma (2)
Connective tissue source tumor	Non-ossifying fibroma (1)	Malignant fibrosarcoma (2) squamous cell carcinoma (2)
Vascular oringal tumor	hemangioma	Hemangioendothelioma (0), hemangiopericytoma (0)
Adipose tissue oringin tumor	Lipoma (3)	Liposarcoma (0)
Nerve tissue oringin tumor	Neurilemmoma (2)	Malignant neurilemoma (1)
malignant neurilemoma		Chordoma (1)
Tumor-like lesion	Cyst (1) bone fibrous dysplasia (1) inflammatory granulation tissue (2)	

PCR was used to detect HERG mRNA expression levels with semi-quantitative software. The results showed that the expression of HERG was related to the degree of malignancy of bone tumors. HERG was not expressed in other samples except for a low degree of expression in the giant cell tumors of I-level, non-ossifying fibroma and chondroblastoma. A high expression of HERG with differing levels was seen in malignant tumors.

Immunohistochemical staining

Immunohistochemical staining showed that there was a significant difference between benign and malignant bone tumors for HERG expression levels. In order to measure this expression difference in positive tissue samples, software was used to quantify the positive stained cells (yellow earth). The grade was divided into 0, 1+, 2+, 3+ and 4. The results showed that 91.3% of benign lesions were negative, with the expression of two cases scoring just 1+ (Fig. 1).

As seen in Fig. 1, HERG was not expressed by the majority of the benign lesions. Low HERG expression was observed in bone giant cell tumors of I-level, non-ossifying fibroma and osteoblastoma origin. A relationship was shown between the HERG expression results and the origin of tumors and their malignancy. That there was high HERG expression levels in all malignant tumors showed that there was a relationship between benign and malignant tumors and their genesis (Fig. 2). This could be explained, as Fig. 1 demonstrates, by the lower level of HERG expression in some benign lesions as well as normal tissue samples. HERG participates in the regulation of cell proliferation and differentiation and so it is reasonable that there is a lower level of HERG expression in mesenchymal tissue excitatory cells, as is

observed in Fig. 1d, 1e and 1h, as well as benign lesions.

mRNA expression levels by RT-PCR

It was shown in the same patient samples that HERG mRNA expression levels corresponded with the immunohistochemical results (Fig. 3). In group A (benign tumor samples), expression of HERG was not detected, whereas a faint expression was observed for other potassium channels. It is hard to explain the relationship of HERG with the cell cycle. One suggested hypothesis was that the regulation of the cell volume plays a key role in the concentration of intracellular fluid, which is important for the cell's primary metabolism. Our results provide evidence that HERG is expressed at different levels in different malignant bone tumor cells. There is a stronger expression of HERG in malignant tumor cells. A number of other Kv family genes (for example Kv1.3) were not overexpressed. Further investigation is needed to understand the reason for this difference and its relationship with the cell cycle.

Western blot

The results of the western blot clearly showed the expression of HERG in both groups (Fig. 4).

MTT assay with HERG inhibitor to assess the proliferation of osteosarcoma cell lines

E-4031 (a HERG channel inhibitor) and different concentrations of non-specific inhibitor 4-AP (a Kv inhibitor) were added to three human osteosarcoma cell lines. After 48 hours incubation, an MTT assay was performed. Results showed that the inhibition of tumor cell proliferation occurred after incubation with the HERG channel inhibitor E-4031 (Fig. 5), although no

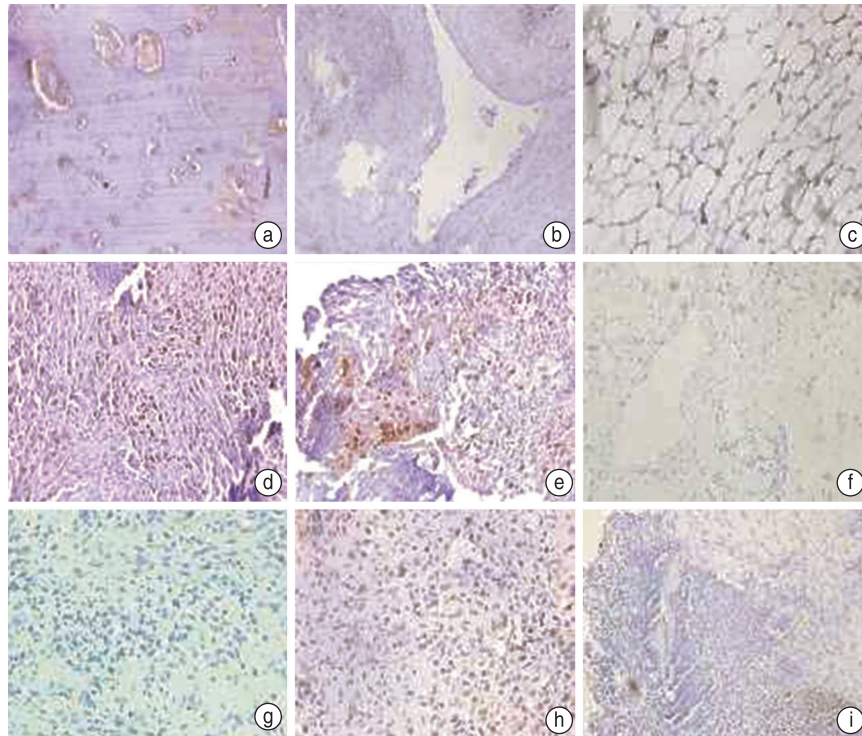


Fig. 1 Immunohistochemical staining for HERG in benign bone tumors. Detection of HERG in the 23 selected cases of benign tumors: normal bone tissue (a) -0; bone cyst (b) -0; fatty tumor (c) -0; bone giant cell grade I tumors (d) -1+; non-ossifying fibroma (e) -1+; hemangioma (f) -0; nerve sheath tumors (g) -0; osteoblastoma (h) -1+; inflammatory granulation tissue (i) -0

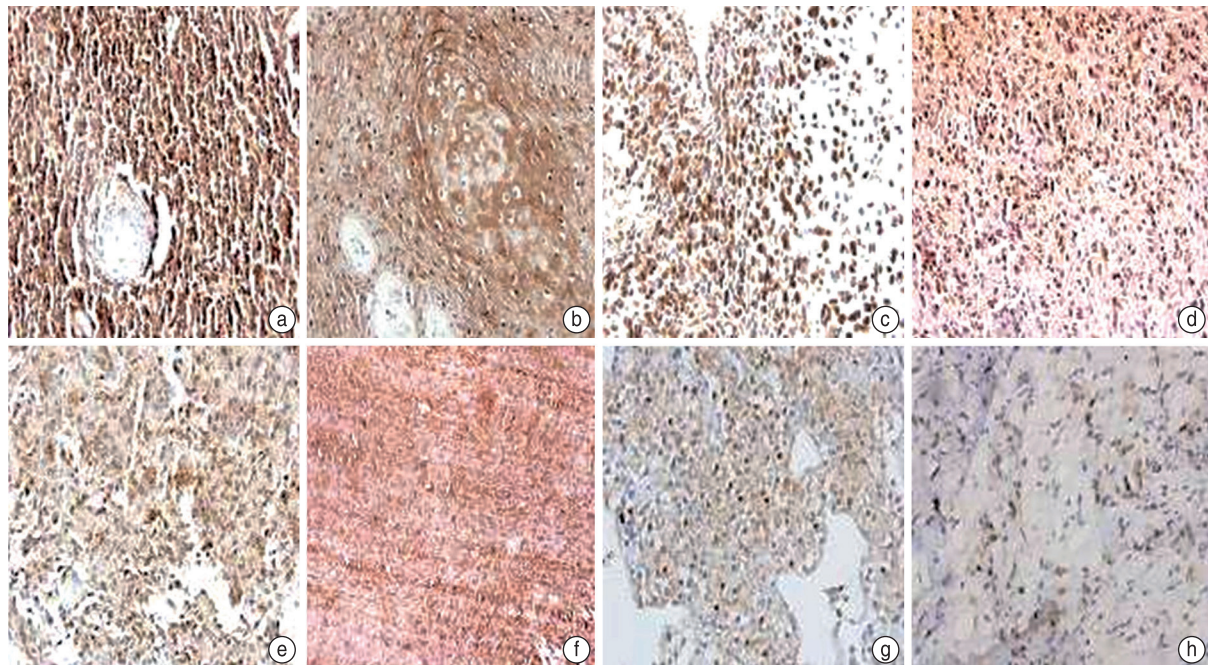


Fig. 2 Immunohistochemical staining for HERG in malignant bone tumors. Detection of HERG in the 34 selected cases of malignant tumors: Ewing sarcoma (a) -4; squamous cell carcinoma (b) -4; osteosarcoma (c) -4; malignant fibrous tissue sarcoma (d) -4; giant cell tumor II level (e) -3+; malignant peripheral nerve sheath tumor (f) -4; alveolar soft tissue sarcoma (g) -3+; sacral chordoma (h) -2+

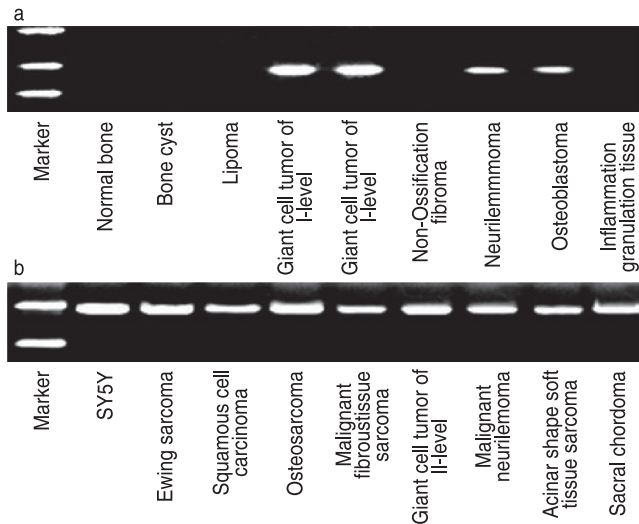


Fig. 3 The expression differences of HERG in common orthopedic tumors. Samples were divided into a benign group and a malignant group. Normal human bone tissue was used as a negative control (a, lane 1) and human neuron tumor cell line SY5Y was used as a positive control (b, lane 1)

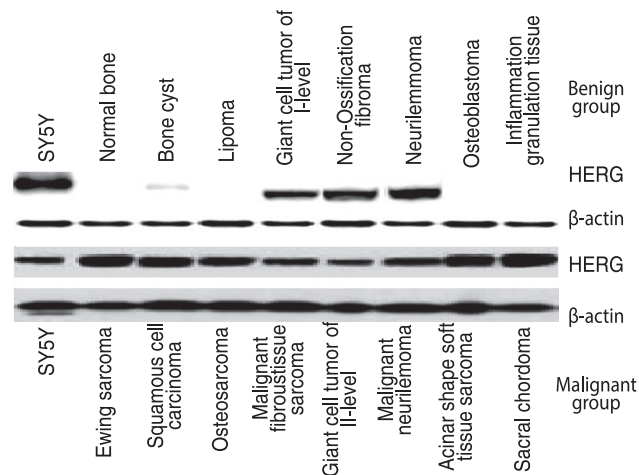


Fig. 4 HERG different expression levels in different bone tumors by western blot analysis. Specimens were divided into a benign and a malignant group. Normal human bone tissue was used as a negative control (a, lane 1) and human neuroblastoma cell line SY5Y was used as a positive control (b, lane 1)

statistical significance was found ($P > 0.05$). However, a significant difference was found with the non-specific Kv channel inhibitor 4-AP on cell proliferation at concentrations 3 mmol and 5 mmol (Fig. 6) ($P < 0.01$).

Discussion

Originally detected in fibroblast cell tumors, HERG is responsible for controlling cell membrane resting potential [10-13]. Potassium ion channels can regulate the proliferation of arterial pulsation and vascular smooth

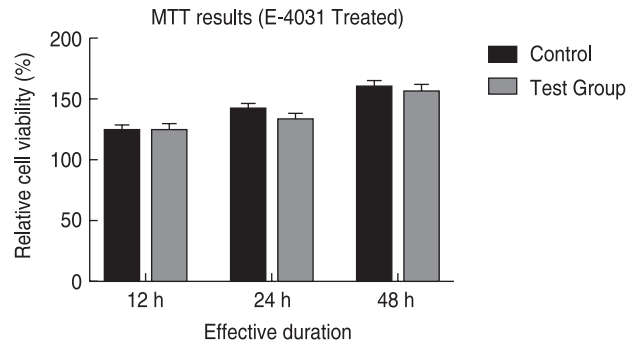


Fig. 5 Inhibition of three osteosarcoma cell lines with HERG inhibitor E-4031

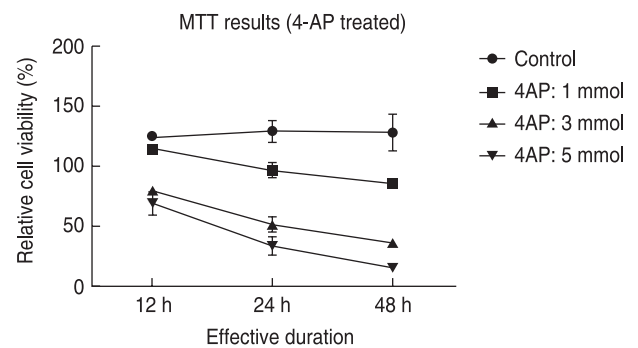


Fig. 6 Inhibition of three osteosarcoma cell lines with different concentrations of 4-AP

muscle cells [14]. Potassium ion channels have also been associated with playing an important role in gastric cancer [15]. A variety of the potassium ion channels are expressed in melanoma tumors and potassium ion channel inhibitors have the ability to inhibit the proliferation of melanoma cells [15] as well breast cancer cells [16]. Further, it was reported that blockers of potassium ion channels could effectively inhibit the proliferation of human colon cancer cell lines including SW1116, LoVo, Colo320DM, and LS174t [17]. Our study results are compatible with such previous reports. It has been well established that potassium ion channels are differentially expressed *in vitro* within multiple tissue types. However, the mechanism underpinning the involvement of potassium ion channels in the occurrence and development of tumor cells and their proliferation and differentiation remains unclear. To date, the expression of HERG in common orthopedic tumors has not been reported. In this study, which involved all common bone tumor types, 60 clinical cases were useful in observing HERG expression in bone tumors. These specimens also exposed differences between HERG expression in malignant tumors and normal bone tissue. The results showed that there is a distinct HERG expression pattern in benign

lesions and malignant orthopedic lesions. The hypothesis was consistent with the experimental results.

Using RT-PCR and western blot, the expression of the HERG gene was detected at both RNA and protein levels. As in previous clinical studies, an association between HERG expression, a potassium ion channel with electrophysiological properties, and tumor proliferation was found in osteosarcoma samples. Sample classification was differentiated according to previous research. Significant statistical differences were shown in HERG expression in different origin tissues of the tumors.

Based on the results above, it can be concluded that: (1) potassium ion channels play an important role in the progression of the cell cycle in cancer cells; (2) potassium ion channels that are involved in the progression of the cell cycle of different tumors belonging to different subtypes. For example, Kv channels are more important in oligodendrocyte progenitor cells, KCa channels may be more important in breast cancer cells, and KATP channels may be critical for human bladder tumor cancer cells^[33].

HERG has attracted attention from those interested in the study of potassium ion channels. HERG may play a role in the diagnosis of bone cancer and an understanding of its mechanism of action and subsequent blockade could prevent the development of tumor cells with the potential to become a novel treatment and guide new directions of research. Further study is required into the mechanism of HERG and its applications.

Techniques such as patch-clamp, RT-PCR, and immunohistochemistry have highlighted the prevalence of Kv1.1 channels in human breast cancer cell line MCF-7 by Ouadid-Ahidouch *et al*^[18]. Currently, potassium ion channels can be completely blocked by TEA, a non-specific inhibitor of Kv channels. Cell proliferation can be inhibited by Kv1.1 potassium channel blocker α -specific toxins. Preussat *et al*^[19] found that Kv1.3 and Kv1.5 channels were differentially expressed in a variety of different types of glioma tissues. Sukuzi *et al*^[20] found that Kv2.1 channels and HERG are strongly expressed in some cervical cancer cell lines. To some extent, cervical cancer cell proliferation was inhibited by Hanatoxin-1, which inhibits the Kv2.1 channel, but had no effect on the proliferation of cervical cancer cells that did not express the Kv2.1 channel.

HERG is differentially expressed in different species such as mice, cows, and humans^[21]. In humans, EAG and ERG channels are known as the Human ether-a-go-go gene (HEAG and HERG, respectively). Further study has shown that the HERG potassium channel has a special status in the family and a close relationship with tumor development. It is worth noting that HERG is expressed in the early stages of embryonic development. To study different HERG expression patterns in tumors, 60 patient samples were collected. Bone tumors (particularly the

malignant bone tumor osteosarcoma specimens) showed altered proliferation when their potassium ion channels were blocked, as expected. Using the HERG channel inhibitor E-4031, tumor cell proliferation inhibition was confirmed with MTT, although the results were not statistically different ($P>0.05$). However, the non-specific Kv channel inhibitor 4-AP had a significant effect on cell proliferation at concentrations of 3 mmol and 5 mmol with statistically significant differences ($P<0.01$). This study reveals that HERG is highly expressed in common tumors such as malignant bone tumor osteosarcoma. Other research has studied the physiological properties and biological behavior of HERG^[22,23]. Newer technologies such as microRNA and RNAi have been used in these studies^[24,25]. Currently, work is ongoing to understand the mechanism underpinning HERG and other mediators interact with it. It is hoped that future pharmacological developments using HERG will provide a reliable target to control various types of cancer including osteosarcomas.

Conflicts of interest

The authors declare no potential conflicts of interest.

References

- Hage-Sleiman R, Hamze AB, El-Hed AF, *et al*. Ceramide inhibits PKC θ by regulating its phosphorylation and translocation to lipid rafts in Jurkat cells. *Immunol Res*, 2016, 64: 869–886.
- Iorio J, Meattini I, Bianchi S, *et al*. hERG1 channel expression associates with molecular subtypes and prognosis in breast cancer. *Cancer Cell Int*, 2018, 18: 93.
- Hsu PH, Ma YT, Fang YC. Cullin 7 mediates proteasomal and lysosomal degradations of rat Eag1 potassium channels. *Sci Rep*, 2017, 7: 40825.
- Li H, Guo D, Zheng F, *et al*. HERG1 K⁺ channels on the leukemic cells mediated angiogenesis *in vitro*. *Wuhan Univ J Nat Sci*, 2014, 19: 178–184.
- Zhang S, Yang L, Zhang K, *et al*. ZC88, a novel N-type calcium channel blocker from 4-amino-piperidine derivatives state-dependent inhibits Cav2.2 calcium channels. *Brain Res*, 2015, 1605: 12–21.
- Izadi-Mood N, Sarmadi S, Rostamnasl B. Alteration of the k-ras gene expression in atypical and nonatypical hyperplastic endometrium. *Iran J Cancer Prev*, 2013, 6: 209–213.
- Cui G, Shu W, Wu Q, *et al*. Effect of Gambogic acid on the regulation of hERG channel in K562 cells *in vitro*. *J Huazhong Univ Sci Technolog Med Sci*, 2009, 29: 540–545.
- Hernandez L, Park KH, Cai SQ, *et al*. The antiproliferative role of ERG K⁺ channels in rat osteoblastic cells. *Cell Biochem Biophys*, 2007, 47: 199–208.
- Cambien B, Rezzonico R, Vitale S, *et al*. Silencing of hSlo potassium channels in human osteosarcoma cells promotes tumorigenesis. *Int J Cancer*, 2008, 123: 365–371.
- Pancrazio JJ, Ma W, Grant GM, *et al*. A role for inwardly rectifying K⁺ channels in differentiation of NG108–15 neuroblastoma x glioma cells. *J Neurobiol*, 1999, 38: 466–474.
- Wang R, Fu FH, Wang B. Precision medicine for diagnosis and treatment of osteosarcoma. *Oncol Transl Med*, 2016, 2: 49–54.

12. Lin Z, Santos S, Padilla K, *et al.* Biophysical and pharmacological characterization of Nav1.9 voltage dependent sodium channels stably expressed in HEK-293 cells. *PLoS One*, 2016, 11: e0161450.
13. Wei X, Sun H, Yan H, *et al.* ZC88, a novel 4-amino piperidine analog, inhibits the growth of neuroblastoma cells through blocking hERG potassium channel. *Cancer Biol Ther*, 2013, 14: 450–457.
14. Yu X, Xu M. Influence of neoadjuvant chemotherapy on proliferation, apoptosis and multi-drug resistance in osteosarcoma cells. *Oncol Transl Med*, 2006, 5: 354–357.
15. D'mello SA, Joseph WR, Green TN, *et al.* Selected GRIN2A mutations in melanoma cause oncogenic effects that can be modulated by extracellular glutamate. *Cell Calcium*, 2016, 60: 384–395.
16. Laniado ME, Fraser SP, Djamgoz MB. Voltage-gated K(+) channel activity in human prostate cancer cell lines of markedly different metastatic potential: distinguishing characteristics of PC-3 and LNCaP cells. *Prostate*, 2001, 46: 262–274.
17. Abdul M, Hoosein N. Voltage-gated potassium ion channels in colon cancer. *Oncol Rep*, 2002, 9: 961–964.
18. Bauer CK, Schwarz JR. Physiology of EAG K+ channels. *J Membr Biol*, 2001; 182: 1–15.
19. Preussat K, Beetz C, Schrey M, *et al.* Expression of voltage-gated potassium channels Kv1.3 and Kv1.5 in human gliomas. *Neurosci Lett*, 2003; 346 : 33–36.
20. Suzuki T, Takimoto K. Selective expression of HERG and Kv2 channels influences proliferation of uterine cancer cells. *Int J Oncol* 2004, 25: 153–159.
21. Han B, Tokay T, Zhang G, *et al.* Eag1 K⁺ channel: endogenous regulation and functions in nervous system. *Oxid Med Cell Longev*, 2017, 2017: 7371010.
22. Hsu PH, Ma YT, Fang YC, *et al.* Cullin 7 mediates proteasomal and lysosomal degradations of rat Eag1 potassium channels. *Sci Rep*, 2017, 7: 40825.
23. He T, Wang C, Zhang M, *et al.* Epigenetic regulation of voltage-gated potassium ion channel molecule Kv1.3 in mechanisms of colorectal cancer. *Discov Med*, 2017, 23: 155–162.
24. Abdul M, Hoosein N. Voltage-gated sodium ion channels in prostate cancer: expression and activity. *Anticancer Res*, 2002, 22: 1727–1730.
25. Jiang LH, Gamper N, Beech DJ. Properties and therapeutic potential of transient receptor potential channels with putative roles in adversity: focus on TRPC5, TRPM2 and TRPA1. *Current Drug Targets*, 2011, 12: 724–736.

DOI 10.1007/s10330-019-0376-6

Cite this article as: Gan L, Li M, Yang TT, *et al.* Expression of HERG in musculoskeletal tumors with different degrees of malignancy. *Oncol Transl Med*, 2019, 5: 242–248.



Call For Papers

Oncology and Translational Medicine

(CN 42-1865/R, ISSN 2095-9621)

Dear Authors,

Oncology and Translational Medicine (OTM), a peer-reviewed open-access journal, is very interested in your study. If you have unpublished papers in hand and have the idea of making our journal a vehicle for your research interests, please feel free to submit your manuscripts to us via the Paper Submission System.

Aims & Scope

- Lung Cancer
- Liver Cancer
- Pancreatic Cancer
- Gastrointestinal Tumors
- Breast Cancer
- Thyroid Cancer
- Bone Tumors
- Genitourinary Tumors
- Brain Tumor
- Blood Diseases
- Gynecologic Oncology
- ENT Tumors
- Skin Cancer
- Cancer Translational Medicine
- Cancer Imageology
- Cancer Chemotherapy
- Radiotherapy
- Tumors Psychology
- Other Tumor-related Contents

Contact Us

Editorial office of Oncology and
Translational Medicine
Tongji Hospital
Tongji Medical College
Huazhong University of Science
and Technology
Jie Fang Da Dao 1095
430030 Wuhan, China
Tel.: 86-27-69378388
Email: dmedizin@tjh.tjmu.edu.cn;
dmedizin@sina.com

Oncology and Translational Medicine (OTM) is sponsored by Tongji Hospital, Tongji Medical College, Huazhong University of Science and Technology, China (English, bimonthly).

OTM mainly publishes original and review articles on oncology and translational medicine. We are working with the commitment to bring the highest quality research to the widest possible audience and share the research work in a timely fashion.

Manuscripts considered for publication include regular scientific papers, original research, brief reports and case reports. Review articles, commentaries and letters are welcome.

About Us

- Peer-reviewed
- Rapid publication
- Online first
- Open access
- Both print and online versions

For more information about us, please visit:

<http://otm.tjh.com.cn>



Editors-in-Chief

Prof. Anmin Chen (Tongji Hospital, Wuhan, China)
Prof. Shiyong Yu (Tongji Hospital, Wuhan, China)